Fakultät für Medizin

Institut für Zellbiologie des Nervensystems

Cytoskeletal rearrangement during developmental motor axon remodeling

Athanasia Marahori

Vollständiger Abdruck der von der Fakultät für Medizin der Technischen Universität München zur Erlangung des akademischen Grades eines

Doktors der Medizin (Dr. med.)

genehmigten Dissertation.

Vorsitzende/-r: Prof. Dr. Jürgen Schlegel

Prüfende/-r der Dissertation:

1. Prof. Dr. Thomas Misgeld
2. Prof. Dr. Martin Kerschensteiner

Die Dissertation wurde am 30.04.2020 bei der Technischen Universität München eingereicht und durch die Fakultät für Medizin am 06.10.2020 angenommen.

To my family, especially my parents

ZUSAMMENFASSUNG

Während der Entwicklung des Nervensystems entstehen zunächst überzählige Synapsen und Axonäste, welche postnatal wieder abgebaut werden, ohne dass dabei das Neuron stirbt. Dieser Abbauprozess ähnelt dem von Axonen bei Erkrankungen oder Verletzungen des Nervensystems. Tatsächlich weist der Abbau von Axonen unter pathologischen Bedingungen mit dem entwicklungsbedingten Abbau viele Gemeinsamkeiten auf. Beispielsweise sind in beiden Fällen Veränderungen des neuronalen Zytoskeletts zu beobachten. Ziel meiner Doktorarbeit war es, Veränderungen des Zytoskeletts während der entwicklungsbedingten Synapsenelimination von Motorneuronen zu charakterisieren. Als Modell verwendete ich ein Nerv-Muskel-Explantat, in dem einzelne Axone von Motorneuronen beobachtet werden können. Während der Synapsenelimination innervieren zunächst konkurrierende terminale Axonäste verschiedener Motorneurone eine Synapse, von denen nach der zweiten postnatalen Woche ein einziges „Gewinner"-Axon übrig bleibt, während alle anderen Äste abgebaut werden. Hierbei werden in den „Verlierer"-Ästen Mikrotubuli abgebaut, woraufhin sich diese Äste zurückbilden. In einem knockout (KO)-Mausmodell des Mikrotubuli-schneidenden Enzyms Spastin konnte ich zeigen, dass der Abbau von „Verlierer"-Ästen verzögert stattfindet, da Mikrotubuli weniger geschnitten und dadurch stabilisiert werden. Des Weiteren überprüfte ich, ob verschiedene Methoden zur Manipulation von Mikrotubulistabilität den Transport von Organellen verändern. Insbesondere verwendete ich hierbei genetische (Spastin-KO) und pharmakologische (Epothilon B) Methoden. Im Spastin-KO konnte ich beispielsweise entgegen unserer Erwartungen keinen signifikant erhöhten Transport finden. Der Grund für die relativ schwache Veränderung könnte in chronischen Kompensationsmechanismen liegen. Daher verwendete ich zusätzlich Epothilon B zur Stabilisierung von Mikrotubuli. Epothilon B wird auf Grund seiner neuroprotektiven Eigenschaften derzeit zur Behandlung des spinalen Traumas erforscht. Ich konnte hierbei

zeigen, dass der mitochondriale Transport in sich zurückziehenden Axonästen spezifisch erhöht war. Insgesamt zeigen diese Ergebnisse, dass der Abbau von Mikrotubuli den verringerten axonalen Transport in sich zurückziehenden Ästen bedingt. Des Weiteren stellen die Ergebnisse eine neue Parallele zwischen entwicklungsbedingtem und neurodegenerativem Axonabbau durch Spastin auf, dessen Mutation zu Spastischer Hereditärer Paraplegie führt.

SUMMARY

Most axonal branches and synapses in the developing nervous system are generated in excessive amounts, but disassemble soon after birth without the neuron as a whole dying. This degradative process resembles axon loss following disease or injury in the adult animal. Both pathological and physiological axon loss share some common cell biological mechanisms, such as changes in the neuronal cytoskeleton. The aim of my thesis was to characterize how alterations to the cytoskeleton, especially microtubules, affect loss of terminal axon branches at the developing neuromuscular junction ('synapse elimination'). To this end, I imaged developing motor neurons on the scale of individual axon branches using a nerve-muscle-explant over time. During synapse elimination, multiple terminal branches innervate a myocyte, one of which ultimately remains as the 'winner' branch, while the others disassemble. The specific disassembly of the 'loser' branches coincides with locally reduced microtubule content, and I could show that a knock-out (KO) of the microtubule-severing enzyme spastin slows down axon loss of terminal branches during synapse elimination. Furthermore, I checked whether microtubule-based transport of organelles was altered under different conditions altering microtubule stability. Specifically, I used genetic (spastin-KO) and pharmacological means (epothilone B) to achieve this. For instance, the spastin-KO showed no significant change in transport, which might be due to chronic compensatory mechanisms. Therefore, I stabilized microtubules acutely by injecting the drug epothilone B, which is currently being explored for its neuroprotective properties during spinal cord injury. Epothilone B specifically increased the transport of mitochondria in dying axon branches when compared to winning branches. Overall, my results suggest that microtubule degradation causes impaired axonal transport in dying axon branches. Furthermore, the results show a new parallel between developmental and neurodegenerative axon loss mediated by the

microtubule-cutting enzyme spastin, whose mutation is also known to cause spastic hereditary paraplegia.

TABLE OF CONTENTS

1. INTRODUCTION

Loss of axons and synapses occurs early on in most neurodegenerative diseases (Adalbert & Coleman, 2013) and may underlie some of the functional impairments observed in circuit activity (Zott, Busche, Sperling, & Konnerth, 2018). Our understanding of the cellular and molecular events that orchestrate axon loss is still incomplete, yet in recent years, a few principles emerged. For example, shared molecular '*self-destruction pathways*' exist, which disassemble axons under diverse pathological settings (Coleman, 2005; J. T. Wang, Medress, & Barres, 2012). Also, axon degeneration uses some of the molecular pathways that are employed during developmental axonal remodeling (L. Luo & O'Leary, 2005; Misgeld, 2005; Nikolaev, McLaughlin, O'Leary, & Tessier-Lavigne, 2009; Raff, Whitmore, & Finn, 2002; Riccomagno & Kolodkin, 2015). In fact, insights gathered from studies on developmental axon loss ('*pruning*') have complemented our understanding of pathological axon death in the past (Schuldiner & Yaron, 2015).

Many axonal self-destruction pathways culminate in increased axonal calcium, microtubule disruption and decreased axonal transport (Cartelli et al., 2013; Coleman, 2005; J. T. Wang et al., 2012). Microtubules are part of the neuronal cytoskeleton, which provides structural support but also guides transport of intracellular resources to nourish the neuronal periphery (Kapitein & Hoogenraad, 2015). An example of a common mechanism of microtubule breakdown is activation of the ubiquitin-proteasome system and Ca^{2+}-mediated activation of calpain, which occurs during both fragmentation-like pruning of dendritic arborization neurons in the fly (Kanamori et al., 2013; C. T. Kuo, Jan, & Jan, 2005) and after acute axonal transection ('Wallerian degeneration') (George, Glass, &

Griffin, 1995; Zhai et al., 2003). Fragmentation-like pruning is a distinct form of pruning, which involves long sections of neurites. The axonal section to be removed is affected synchronously and has a sudden time course that is completed within hours (Saxena & Caroni, 2007). In contrast, the pruning of short, terminal branches initiates at the axon terminals and slowly propagates proximally, where it resembles the die-back pathology of many neurodegenerative diseases (Saxena & Caroni, 2007).

The pruning of short terminal branches is closely associated with a process called 'synapse elimination', since many of the terminal branches have already formed synapses before their removal (Riccomagno & Kolodkin, 2015). During embryonic development, most synapses that are initially formed are removed later as the circuit matures (Schuldiner & Yaron, 2015). Elimination of synapses is important for the proper maturation of neuronal circuits (Lichtman & Colman, 2000), and the balance between synapse elimination and formation may actually be altered in diseases such as schizophrenia or autism spectrum disorders, where synapse number is typically found decreased or increased, respectively (Penzes, Cahill, Jones, VanLeeuwen, & Woolfrey, 2011).

Synapse elimination has been studied most extensively at the murine neuromuscular junction (Bianchi, 2018). Here, several branches of an axon innervate multiple targets, of which some establish long-term innervation, while others shrink and retract toward the parent axon (Keller-Peck et al., 2001). In search of the underlying cell biological mechanisms, one study found destabilization of microtubules to be present in the dying branch (Bishop, Misgeld, Walsh, Gan, & Lichtman, 2004). The authors speculated that local microtubule disruption could influence the amount of resources transported into terminal branches and render them at a competitive disadvantage, but how neuronal

2

resources are specifically distributed among different branches was also unknown at the time (Bishop et al., 2004).

In my thesis, I tested whether stabilizing microtubules using different pharmacological and genetic manipulations affects developmental axon loss and axonal transport at the murine neuromuscular junction. In the following paragraphs, I will begin with an introduction into neuronal microtubules, axonal transport, and synapse elimination, before detailing my findings.

1.1. Neuronal microtubules

Neuronal processes are both stably maintained over long distances but also dynamically remodeled during circuit formation and plasticity (Song & Brady, 2014). Achieving the balance between stability and dynamicity depends on a neuronal cytoskeleton that reflects these versatile properties (Song & Brady, 2014). Microtubules are filamentous polymers that belong to the neuronal cytoskeleton just like actin and neurofilament (Hesketh & Pryme, 1995). They provide 'rails' for intracellular cargo transport (Hirokawa, Niwa, & Tanaka, 2010; Kapitein & Hoogenraad, 2015) and direct cargo to specific locations (Akhmanova & Steinmetz, 2008; Kapitein & Hoogenraad, 2015). Furthermore, microtubule reorganization drives the assembly of the mitotic spindle (Walczak & Heald, 2008) and generates the mechanical forces needed during neuronal development (Kapitein & Hoogenraad, 2015), in particular for neuronal migration, axon growth, synapse formation and establishing neuronal polarity (Conde & Caceres, 2009; Kapitein & Hoogenraad, 2015; Witte & Bradke, 2008). Microtubule dynamics are also implicated in synaptic plasticity and memory formation, potentially by affecting spine morphology and synaptic transmission (Fanara et al., 2010; Jaworski et al., 2009; Shumyatsky et al., 2005; Uchida et al., 2014). Not surprisingly, a variety of neurodegenerative diseases are associated with cytoskeletal dysfunction (McMurray, 2000; Sadleir et al., 2016; Sudo & Baas, 2011), and some neurological disorders are caused by microtubule-related mutations (**Table 1**) (Kapitein & Hoogenraad, 2015; Maday, Twelvetrees, Moughamian, & Holzbaur, 2014).

Disease	Mutated human gene	Protein	Reference
Hereditary spastic paraplegia	*SPG4*	Spastin	Hazan et al. (1999)
	SPG10	KIF5A	Reid et al. (2002)
	SPG30	KIF1A	Erlich et al. (2011); Klebe et al. (2012)
Pick's disease	*MAPT*	tau	Hutton et al. (1998)
Lissencephaly	*DCX*	Doublecortin	Gleeson et al. (1998)
	TUBA1A	α-tubulin	Poirier et al. (2007)
	PAFAH1B1	Lis-1	Reiner et al. (1993)
Perry syndrome	*DCTN1*	dynactin	Farrer et al. (2009)
Familial amyotrophic lateral sclerosis 22	*TUBA4A*	α-tubulin	Smith et al. (2014)

Table 1 | Neurodevelopmental and neurodegenerative diseases caused by selected mutations in tubulin or microtubule-interacting proteins.
Assembled by the author from Maday et al. (2014) and the search function in www.genecards.org (retrieved on 01. January 2020).

1.1.1. Structure and dynamics of microtubules

Microtubules are hollow tube-like polymers which assemble from α- and β-tubulin heterodimers (**Figure 1.1**) (Luduena, Shooter, & Wilson, 1977). They are about 25 nm in outer diameter and have variable length of a few μm and ascending (Baas, Rao, Matamoros, & Leo, 2016; Hawkins, Mirigian, Selcuk Yasar, & Ross, 2010; Yogev, Cooper, Fetter, Horowitz, & Shen, 2016). Both tubulin subunits are bound to a guanosine triphosphate (GTP) molecule, which can be exchanged with GDP on β-tubulin, but not on α-tubulin (Downing & Nogales, 1998b).

Being assembled of αβ-heterodimers in the described manner, microtubules are intrinsically polarized with β-tubulin facing the 'plus end' and α-tubulin the 'minus end' (**Figure 1.1**) (Baas et al., 2016). While microtubules are uniformly oriented in axons with

> 90 % of plus ends pointing towards the axon terminals, they have about 50 / 50 % mixed

polarity in vertebrate dendrites (Baas, Deitch, Black, & Banker, 1988; Kleele et al., 2014;

Stepanova et al., 2003). This difference in polarity is important for guiding cargo transport

(Kapitein & Hoogenraad, 2011) and differentiating neurites during development

(Neukirchen & Bradke, 2011; Stiess & Bradke, 2011).
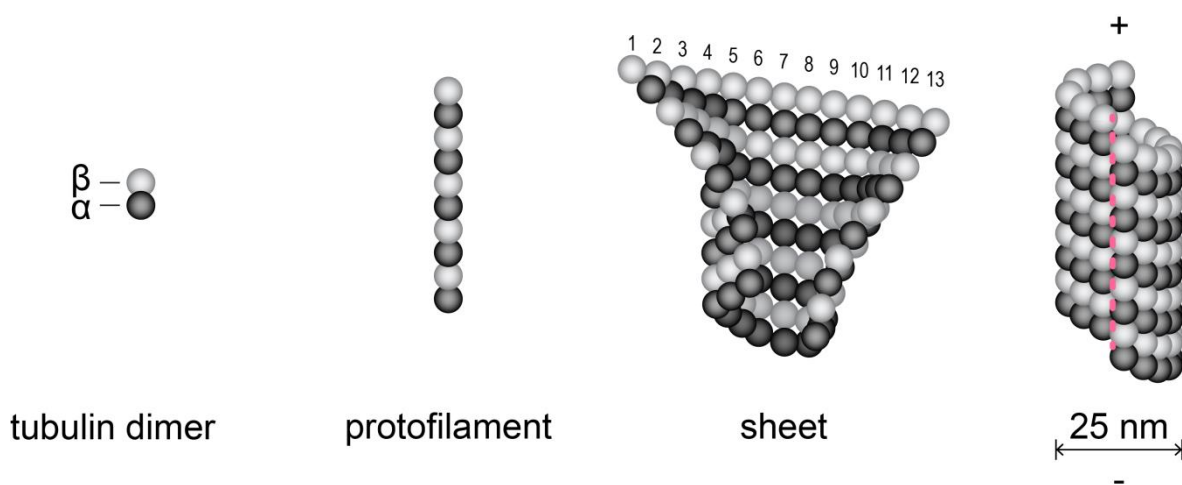
Figure 1.1 | Microtubule structure.
Microtubules are assembled from α- and β-tubulin heterodimers, which form linear
protofilaments in a head-to-tail fashion. In mammalian cells, 13 protofilaments align in
parallel to form a sheet, which winds into a 25 nm wide tube (Downing & Nogales, 1998a).
At the closing site, a discontinuity appears (the 'lattice seam', magenta line), where α- and
β-tubulin interact laterally. Modified from Akhmanova and Steinmetz (2008)

Microtubules are very dynamic and continually undergo periods of growth and

shortening, with rapid switches from shrinkage to growth ('rescue') and switches from

growth to shrinkage ('catastrophe') (Akhmanova & Steinmetz, 2008). Stochastic switches

between growth and depolymerization are known as 'dynamic instability' (**Figure 1.2**)

(Mitchison & Kirschner, 1984) and enable microtubules to rapidly explore the surrounding

intracellular space. Dynamic instability is typical for the microtubule plus end, which

grows and dismantles relatively fast, while the minus end is stabilized by proteins such as
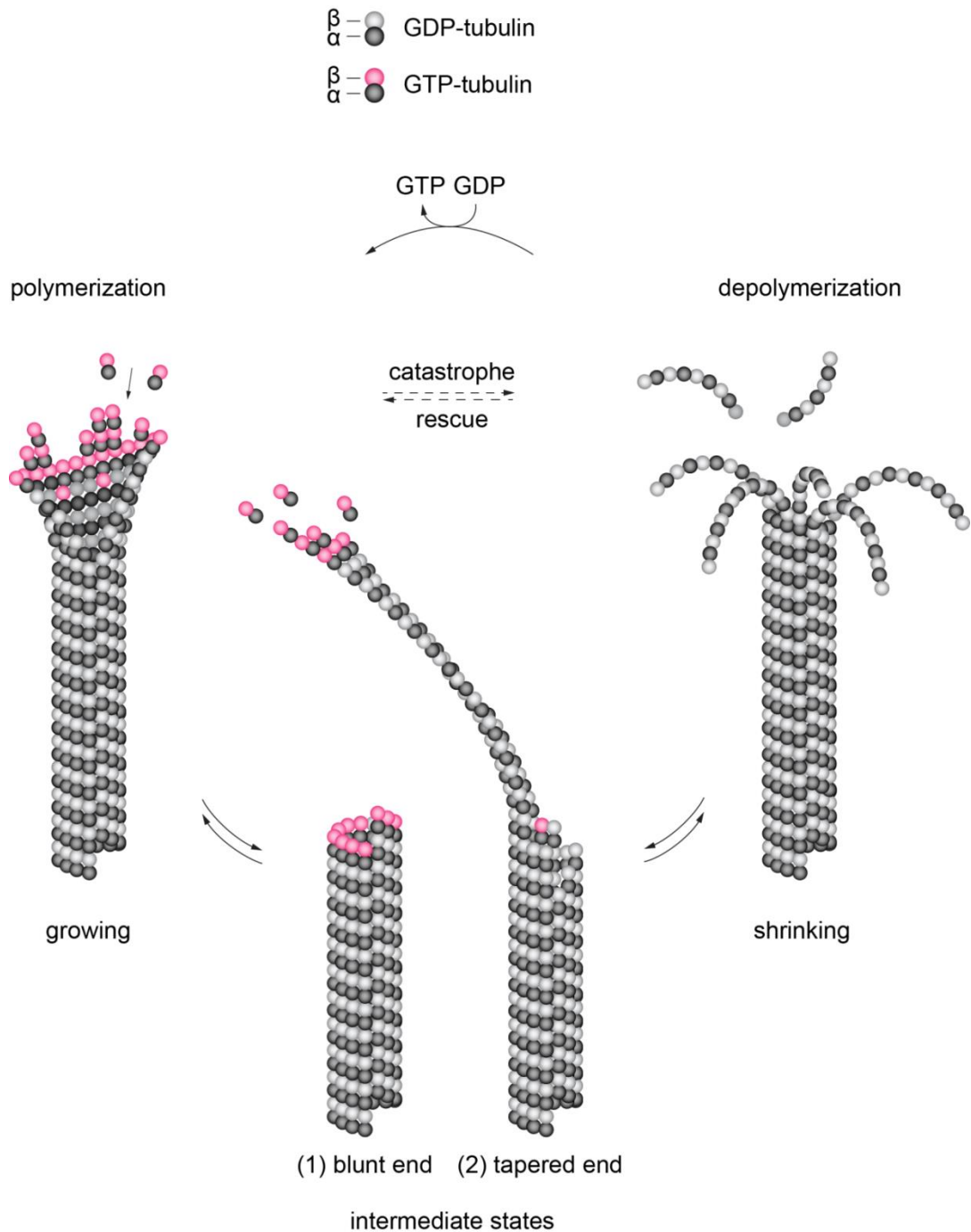
Figure 1.2 | Dynamic instability.
Microtubules continuously undergo cycles of growth and shrinkage. Newly added tubulin dimers contain GTP which is hydrolyzed to GDP after binding to the microtubule lattice. Typically, growing microtubules contain at least one layer of GTP on the (+) end, which stabilizes the microtubule. After losing the GTP cap, the microtubule tip is rapidly disassembled. Modified from Akhmanova and Steinmetz (2008) and Aher and Akhmanova (2018)

7

by γ-tubulin and CAMSAPs (Akhmanova & Hoogenraad, 2005, 2015). Microtubules ends grow by adding new tubulin dimers, which contain GTP that undergoes hydrolysis shortly after integration. Thus, the growing plus end has at least one layer of GTP-tubulin, whereas most of the stem microtubule contains GDP-tubulin (Baas et al., 2016). This so-called 'GTP-cap' stabilizes microtubules at their plus end (Caplow & Shanks, 1996), and the microtubules undergo rapid catastrophe after losing it (Baas et al., 2016) (**Figure 1.2**).

1.1.2. *Posttranslational microtubule modifications*

Despite their uniform and conserved basic architecture, microtubules specialize to fulfil diverse functions which are closely linked to their organization and dynamics (Janke, 2014; McNally & Roll-Mecak, 2018). Functional diversity is established by extensive modifications of the microtubules, known as the 'tubulin code'; it includes (1) combinations of different tubulin isoforms and (2) posttranslational modifications (PTMs) (Janke, 2014; Panda, Miller, Banerjee, Luduena, & Wilson, 1994; Vemu, Atherton, Spector, Moores, & Roll-Mecak, 2017). Many PTMs are recognition tags for extrinsic regulators and microtubule-interacting proteins, such as motor proteins, microtubule-associated proteins (MAPs), kinases, and microtubule-severing enzymes (Akhmanova & Hoogenraad, 2005; Akhmanova & Steinmetz, 2008; Conde & Caceres, 2009; Janke, 2014).

In neurons, some microtubules are stabilized and undergo dynamics less frequently than others (Baas et al., 2016). Stable microtubules passively accumulate specific collections of posttranslational tubulin modifications over time (Baas et al., 2016; Janke, 2014). Some

PTMs also provide a positive or negative feedback loop by affecting microtubule dynamics and stability on their own (Aher & Akhmanova, 2018). Microtubule domains can be divided into three groups, which are characterized by particular PTMs: (1) *labile* domains that are highly dynamic, lack acetylation and glutamylation, but are rich in tyrosination; (2) *stable* domains that undergo dynamics more slowly, and are rich in detyrosination, acetylation, and polyglutamylation; and (3) *cold-stable* domains that are highly polyaminated and remain intact even under severe stress, such as cold temperature or the addition of microtubule-destabilizing factors (Baas et al., 2016; Song et al., 2013). Since detyrosination, polyglutamylation, and acetylation are the most abundant PTMs on axonal microtubules (I. Yu, Garnham, & Roll-Mecak, 2015) they will be described in more detail in the following paragraphs.

Detyrosination/tyrosination: Detyrosination/tyrosination is a posttranslational modification that occurs exclusively on the C-terminal tyrosine residue of α-tubulin tubulin, and not on other proteins (Janke, 2014). *Detyrosination* is catalyzed by vasohibins (Aillaud et al., 2017; Nieuwenhuis et al., 2017) and *tyrosination* is mediated by a tubulin tyrosine ligase (TTL) (**Figure 1.3, A**) (Argarana, Barra, & Caputto, 1978; Hallak, Rodriguez, Barra, & Caputto, 1977; Janke, 2014). Detyrosination promotes microtubule stability by inhibiting microtubule destabilizing factors such as kinesin-13 proteins (Peris et al., 2009) and tyrosination supports microtubule growth by recruiting plus-end tracking proteins (Bieling et al., 2008). Following detyrosination, two glutamate residues are exposed, which can be further removed by members of the cytosolic carboxypeptidase family (CCPs) (Berezniuk et al., 2012; Kalinina et al., 2007), thus making detyrosination irreversible (called Δ2 and Δ3 tubulin, respectively) (**Figure 1.3, A**) (Janke, 2014; Paturle-Lafanechere et al., 1994).

A

Detyrosination   Δ2-tubulin

B   C

Polyglutamylation   Acetylation
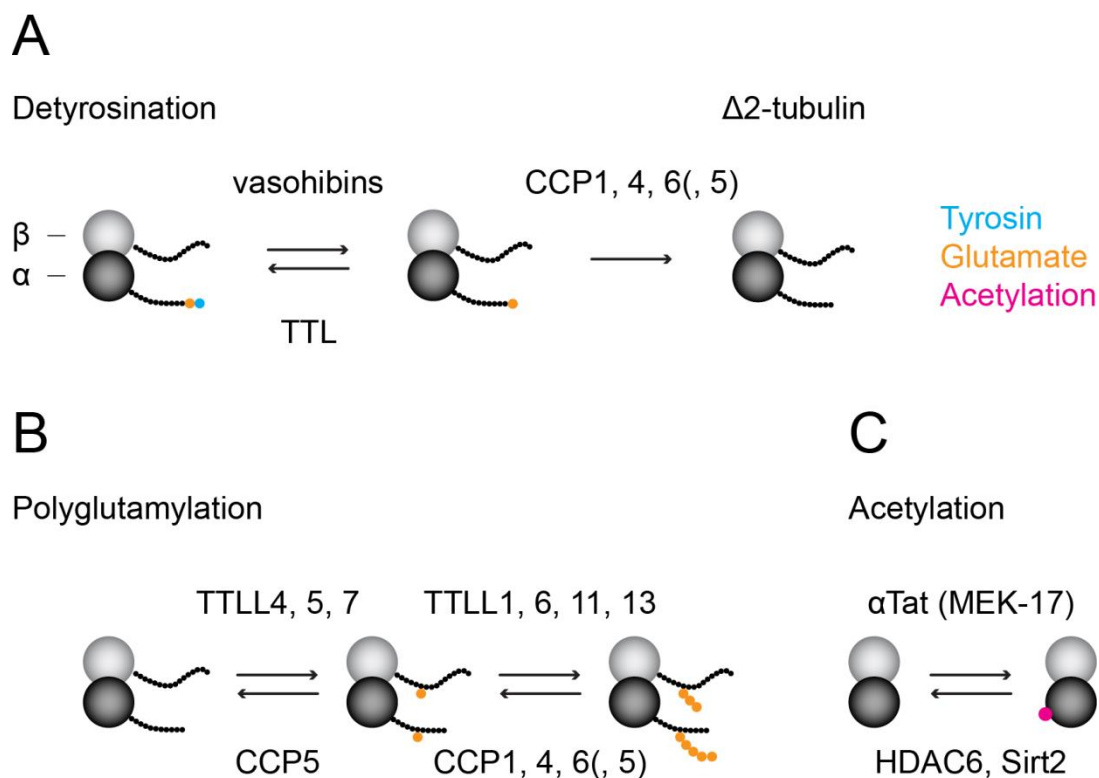
Figure 1.3 | Posttranslational modifications on axonal microtubules.
(A) Detyrosination on the C-terminal unstructured domain ('tail') of α-tubulin has indirect effects on microtubule stability and longevity. **(B)** Polyglutamylation can occur on both α/β-tubulin C-terminal tails and modifies microtubule function by recruiting microtubule-severing- or cargo transport proteins. **(C)** Acetylation occurs on the inner side of K40 and contributes to microtubule stability by making microtubules more flexible during bending. Enzymes are explained in the main text and for full names refer to "6. List of Abbreviations". Modified from (Janke, 2014).

Polyglutamylation/deglutamylation: During polyglutamylation, glutamate side chains are formed on the C-terminal unstructured domains ('tails') of either α- or β-tubulin (**Figure 1.3, B**) (Alexander et al., 1991; Edde et al., 1990). Enzymes of the TTL-like family (TTLL) catalyze *polyglutamylation* on microtubules (Janke et al., 2005), and members of the CCP family catalyze *deglutamylation* (**Figure 1.3, B**) (Kimura et al., 2010). Both enzymes are unspecific and target other proteins than tubulin as well (Rogowski et al., 2010; van Dijk et al., 2008). Polyglutamylation serves as a molecular interface by which various proteins recognize microtubules. For example, kinesin-1 and -3

mediated transport is affected by polyglutamylation (Ikegami et al., 2007; Maas et al., 2009; Sirajuddin, Rice, & Vale, 2014), and spastin and katanin, two microtubule-severing enzymes, preferentially bind to polyglutamylated microtubules (Roll-Mecak, 2018).

Acetylation: Tubulin acetylation occurs mostly on lysine 40 (K40) of α-tubulin (**Figure 1.3, C**) (L'Hernault & Rosenbaum, 1985; LeDizet & Piperno, 1987). K40 is found on the inner side of microtubules (Soppina, Herbstman, Skiniotis, & Verhey, 2012), making acetylation unlikely to interact with proteins on the outer lattice side, such as motor proteins (Janke, 2014). K40 deacetylation is catalyzed by HDAC6 (Hubbert et al., 2002) and Sirt2 (North, Marshall, Borra, Denu, & Verdin, 2003), whereas acetylation is catalyzed by αTAT1 (a.k.a. MEK-17; Akella et al. (2010)). Recently is has been shown that K40 acetylation 'softens' the microtubule lattice and protects it from breakage during bending (Xu et al., 2017).

1.1.3. *Microtubule-associated proteins*

Dynamic instability of microtubules is also regulated by microtubule-associated proteins (MAPs) (Akhmanova & Steinmetz, 2008; Mandelkow & Mandelkow, 1995). MAPs can bind to different targets on a microtubule – such as free tubulin dimers, along the lattice or on the microtubule ends – and affect microtubule stability by either promoting growth, by depolymerizing, or by providing structural support (Akhmanova & Steinmetz, 2008; de Forges, Bouissou, & Perez, 2012).

A subclass of MAPs are plus-end binding proteins (+TIPs), which associate with the growing plus end and promote polymerization (Akhmanova & Steinmetz, 2008).

Prominent examples are end-binding proteins (EB) 1, 2 and 3, which recognize the GTP-cap structure on microtubule ends, where up to a few hundred EB molecules form comet-like accumulations (Akhmanova & Steinmetz, 2011, 2015). In recent years, fluorescent imaging techniques have been developed to label the growing microtubule ends which are capped by EB's, thereby revealing the extensive dynamicity of neuronal microtubules both in culture and *in vivo* (Kleele et al., 2014; Stepanova et al., 2003; Stone, Roegiers, & Rolls, 2008). Combined with normalization over total tubulin content, EB-comet density can be used as an indirect estimate of microtubule length, although this measurement is also confounded by the ratio between the labile and stable microtubule populations (Brill et al., 2016).

1.1.4. *The microtubule-severing enzyme spastin*

Microtubule ends are highly dynamic structures, but (de)polymerization from the tip is not the only way by which microtubules (dis)assemble. Microtubule-severing enzymes can bind along the microtubule lattice and break it into smaller parts (Roll-Mecak & McNally, 2010). If the newly cut microtubule ends are stable, they will grow out, leading to an overall increase in microtubule number and mass (Y. W. Kuo, Trottier, Mahamdeh, & Howard, 2019; Roll-Mecak & Vale, 2006). However, if the newly cut microtubule ends are labile, then severing will have the opposite effect and microtubules will decrease in mass due to depolymerization (McNally & Roll-Mecak, 2018; Ribbeck & Mitchison, 2006). Both scenarios have been observed in neurons in different settings (**Table 2**) (Kapitein & Hoogenraad, 2015; Sherwood, Sun, Xue, Zhang, & Zinn, 2004; W. Yu et al., 2008).

Spastin manipulation	Model	Effect on microtubules (MT's)	Reference
Overexpression	Rat hippocampal neurons	more, shorter MT's	W. Yu et al. (2008)
Overexpression	*Drosophila* larva, muscle	fewer MT's	Sherwood et al. (2004)
Overexpression	*Drosophila* larva, NMJ	fewer MT's	Trotta, Orso, Rossetto, Daga, and Broadie (2004)
Overexpression	*Drosophila* larva, class IV da neurons	destroys stable MT's	Stewart, Tsubouchi, Rolls, Tracey, and Sherwood (2012)
Null mutant	*Drosophila* larva, NMJ	fewer MT's	Sherwood et al. (2004)
Knockdown	*Drosophila* larva, NMJ	accumulation of acetylated, dense MT's	Trotta et al. (2004)
Loss of function mutant	*Drosophila* larva, class IV da neurons	no effect on MT's	Stewart et al. (2012)
Morpholino	Zebrafish	short, malformed MT's	Wood et al. (2006)

Table 2 | The ambivalent effect of the microtubule-severing enzyme spastin.
Spastin can both amplify and disassemble microtubules in different settings (table assembled by the author from primary literature)

Spastin is one of three known microtubule-severing enzymes – the others being katanin and fidgetin (McNally & Vale, 1993; Mukherjee et al., 2012; Roll-Mecak & Vale, 2005). All three are AAA enzymes that use ATP hydrolysis for microtubule breakdown (Roll-Mecak & McNally, 2010). Spastin forms hexamers, which contain a pore at the center through which it pulls out tubulin subunits by the C-terminal tail (Roll-Mecak & McNally, 2010; Roll-Mecak & Vale, 2008). Spastin binds preferentially to polyglutamylated tubulin and its enzyme activity depends on the number of glutamate residues (Lacroix et al., 2010; Valenstein & Roll-Mecak, 2016).

For some time, it has been unclear how the GDP-tubulin lattice exposed by cutting would have to be stabilized in order to grow (Vemu et al., 2018). A recent study showed that shortly after tubulin-extraction by spastin new GTP-dimers are introduced into the

lattice to stabilize the exposed parts (Vemu et al., 2018). However, if severing activity were to outpace GTP-tubulin incorporation the microtubule would rather undergo catastrophe. Cells probably regulate severing activity by MAPs and PTMs to switch between the two fates (Vemu et al., 2018).

Spastin plays an important role during developmental remodeling to create the dense and structured microtubule arrays typically seen in neurites (Roll-Mecak & McNally, 2010). For example, spastin localizes to branch points (Errico, Claudiani, D'Addio, & Rugarli, 2004; W. Yu et al., 2008), where it provides new microtubule seeds for axonal and dendritic branch formation (Conde & Caceres, 2009; Roll-Mecak & Vale, 2006). Disruption of spastin reduces neurite outgrowth and branching (Havlicek et al., 2014; Jinushi-Nakao et al., 2007; Qiang, Yu, Liu, Solowska, & Baas, 2010; Wood et al., 2006) whereas overexpression leads to excessive branching (Sherwood et al., 2004; W. Yu et al., 2008). In addition, spastin organizes synaptic microtubules during *Drosophila* NMJ formation (Sherwood et al., 2004; Trotta et al., 2004).

Spastin likely also has homeostatic functions that exceed the developmental period, as it remains widely expressed throughout the mammalian nervous system (D. L. Ma et al., 2006). In humans, a spastin mutation is the most common cause of hereditary spastic paraplegia (HSP; Hazan et al., 1999; Schule et al., 2016), a group of inherited disorders with lower extremity weakness, spasticity and gait impairment that can manifest at any age (Fink, 2013). Core pathological findings are dying-back degeneration of particularly long axonal tracts, in particular the lateral corticospinal tracts and *fasciculus gracilis,* but also sensorimotor peripheral neuropathy and amyotrophy have been in observed (Fink, 2013). A few of the observed pathologies might also be developmental in nature (Fink, 2013).

The cellular mechanisms that link spastin malfunction to axon degeneration are largely unknown. Two spastin mutation mouse models with motor phenotypes have been generated to understand this in more detail (Kasher et al., 2009; Tarrade et al., 2006). Both studies reported axonal swellings and accumulation of organelles such as mitochondria in the spinal cord, but not the sciatic nerve. *In vitro* measurements in hippocampal slices of these mice further showed that axonal transport was altered, putatively due to microtubule fragmentation (Kasher et al., 2009). Indeed, patients with spastin mutations may have a sparser cytoskeleton in histological sections of their spinal cord (Wharton et al., 2003).

Comparing this pathology to a relevant model of developmental axon loss, such as postnatal synapse elimination at the neuromuscular junction, where axons atrophy and retract in a 'dying-back'-like pattern, might be a useful tool to understand the role spastin plays during the disassembly of axons (a study on Drosophila precluded a role of spastin during fragmentation-like pruning of dendrites; Lee, Jan, & Jan, 2009). Whether or not axonal transport deficits are present *in vivo*, and how other functions of spastin are affected is unclear. In neurons, spastin is enriched on the ER (D. L. Ma et al., 2006), interacts with the ER-protein REEP1 (Park, Zhu, Parker, & Blackstone, 2010) and interacts with the early secretory pathway (Allison et al., 2017; Connell, Lindon, Luzio, & Reid, 2009; Reid et al., 2005). In terminal branches and synapses, which are subjected to high Ca^{2+} influx partially buffered by the ER, these mechanics might play an important role in homeostasis of the terminal.

1.1.5.   Pharmacological microtubule stabilization

Drugs such as paclitaxel and epothilones stabilize microtubules by attaching to a specific binding site on β-tubulin ('taxane site'), through which they strengthen lateral tubulin contacts (Prota et al., 2013). Originally, microtubule-stabilizing drugs had been developed in the context of anti-cancer therapy, as they hamper mitosis (Baas & Ahmad, 2013; Varidaki, Hong, & Coffey, 2018). As outlined earlier, many neurological and psychiatric diseases are associated with defects in microtubule dynamics and stability (Maday et al., 2014; Varidaki et al., 2018), an apparent converging point of axon death, therefore making microtubule-stabilizing drugs attractive as neuroprotective agents (Baas & Ahmad, 2013). Indeed, microtubule stabilization using paclitaxel or epothilones enhanced axon regeneration after spinal cord injury in rodents (Fellner et al., 2002; Ruschel et al., 2015; Sandner et al., 2018) and improved disease symptoms in a mouse model of Alzheimer's disease (B. Zhang et al., 2012). Another study has been performed in experimental Parkinsonism, where epothilone D improved axonal transport and attenuated neuronal degeneration (Cartelli et al., 2013). A major advantage of epothilone is that it can cross the blood-brain barrier, unlike paclitaxel (Brunden et al., 2011). Although promising, it remains to be evaluated whether the side effects of these drugs will allow their use for neurological indications in the future (Baas & Ahmad, 2013).

1.2. Axonal transport

Microtubules serve as intracellular tracks for cargo transport in neurons, whose extended and highly branched morphology create a challenging environment to properly distribute various resources (Hirokawa et al., 2010; MacAskill & Kittler, 2010; Maday et al., 2014; Misgeld & Schwarz, 2017; Nicholls & Ferguson, 2013; Sheng, 2014). The existence of some form of axonal transport – for driving trophic support by the soma – was already suspected by Santiago Ramón y Cajal, but only many years later experimental evidence emerged when Weiss and Hiscoe (1948) demonstrated that constriction of a nerve site led to axonal swellings with accumulated axoplasm proximally of the constriction site (Grafstein & Forman, 1980). Later, experiments using radioactive tracers and video-enhanced differential interference contrast microscopy revealed that fast axonal transport occurs in two directions and is an actively driven process (Allen, Metuzals, Tasaki, Brady, & Gilbert, 1982; Brady, Lasek, & Allen, 1982; Grafstein & Forman, 1980; Hirokawa, 1998; Ochs & Burger, 1958). Neurons use a sophisticated molecular machinery (Hirokawa, 1982, 1998), which is regulated by different intracellular factors and thereby responds to the alternating supply demands of a neuron over time (Lin & Sheng, 2015; Maday et al., 2014). Kinesin and dynein motors drive long-ranged axonal transport on microtubule tracks using ATP hydrolysis (Schnapp, Vale, Sheetz, & Reese, 1985; Vale, Reese, & Sheetz, 1985), in contrast to myosin motors, which drive short-ranged transport on actin filaments (Chada & Hollenbeck, 2004; Pathak, Sepp, & Hollenbeck, 2010; Sheng, 2014). The precise molecular mechanism of transport is distinct for each cargo (Maday et al., 2014). Particularly well studied is the transport of mitochondria, whose local ATP production and Ca^{2+}-buffering capabilities are required for normal neurotransmission and synaptic plasticity (Guo et al., 2005; Kang et al., 2008; Levy, Faas, Saggau, Craigen, &

Sweatt, 2003; H. Ma, Cai, Lu, Sheng, & Mochida, 2009; Rangaraju, Calloway, & Ryan, 2014; Tang & Zucker, 1997; Verstreken et al., 2005). Not surprisingly, mutations in the axonal transport machinery typically lead to neurodegeneration (Hafezparast et al., 2003; Maday et al., 2014), and disrupted mitochondrial transport in particular is a shared theme found in many neurodegenerative diseases (De Vos, Grierson, Ackerley, & Miller, 2008; Mariano, Dominguez-Iturza, Neukomm, & Bagni, 2018) and acute axon damage (Misgeld, Kerschensteiner, Bareyre, Burgess, & Lichtman, 2007) – but it is still debated to what extent transport deficits are causative for a disease (Marinkovic et al., 2012).

1.2.1. *Axonal transport machinery*

Anterograde axonal transport toward synaptic terminals uses kinesin motors (Hurd & Saxton, 1996; Vale, Reese, et al., 1985; Vale, Schnapp, et al., 1985), which move toward the microtubule plus end (Baas et al., 2016; Vale, Schnapp, et al., 1985), while retrograde transport toward the soma mostly uses dynein motors (Hirokawa et al., 2010; Pilling, Horiuchi, Lively, & Saxton, 2006), which move toward the microtubule minus end (**Figure 1.4**) (Schroer, Steuer, & Sheetz, 1989). Both protein families will be described in more detail below.

Kinesin: The kinesin superfamily (KIF) includes 45 genes (Miki, Setou, Kaneshiro, & Hirokawa, 2001), of which mainly KIF5 (kinesin-1) but also KIF1Bα are responsible for mitochondrial transport in mammalian neurons (Hirokawa et al., 2010; Nangaku et al., 1994; Tanaka et al., 1998). Kinesin-1 is a dimer of two heavy chains (KHCs) (Hirokawa, 1998), which are encoded by the genes *KIF5A*, *KIF5B*, and *KIF5C* (Nakagawa et al., 1997). Two kinesin light chains are often associated (Hirokawa, 1998); they do not possess

any motor activity, but rather enhance the motility of KHC (Glater, Megeath, Stowers, & Schwarz, 2006; Sun, Zhu, Dixit, & Cavalli, 2011). Single kinesin-1 molecules are relatively strong among motor proteins, exerting a stall force of 5-6 pN (Svoboda & Block, 1994).
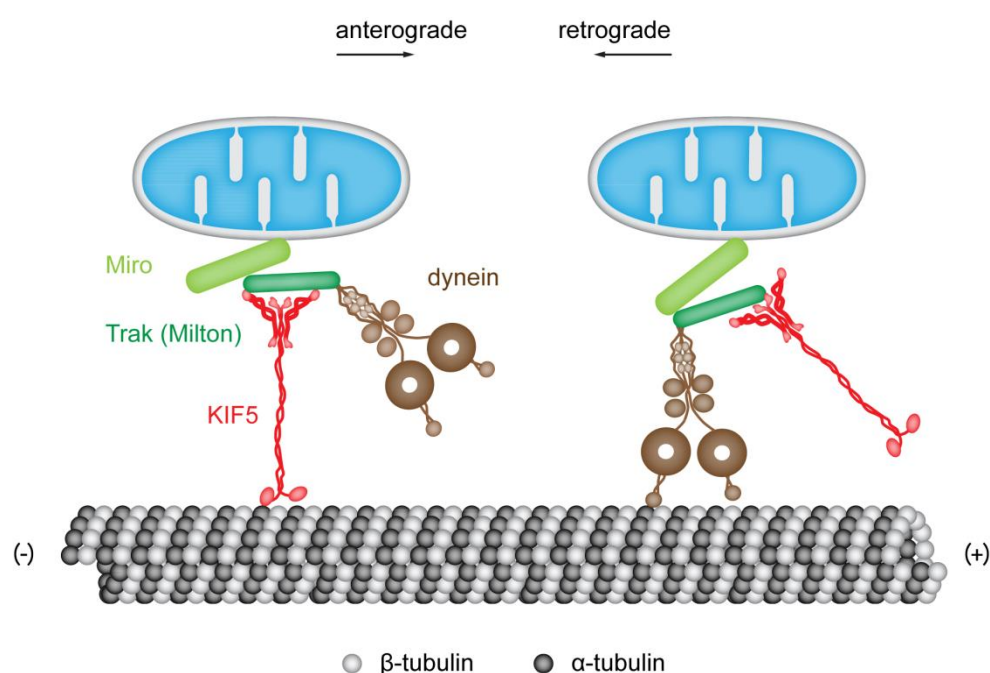

Figure 1.4 | Mitochondrial transport machinery.
Modified from Sheng (2014), kinesin and dynein structures from Vale (2003)

Dynein: From the large family of dyneins, only *cytoplasmic dynein 1* acts in minus-end directed transport (Roberts, Kon, Knight, Sutoh, & Burgess, 2013; henceforth, cytoplasmic dynein 1 will be abbreviated as 'dynein' for simplicity). Dynein belongs to the family of AAA ATPases and has a ring of six AAA+ domains, which partially form the dynein heavy chain that generates the motile force (Roberts et al., 2013). Dynein also associates with dynactin (Gill et al., 1991), a complex of multiple proteins that amplify the binding of dynein to cargo and microtubule (Schroer, 2004) to enhance the processivity of dynein

19

(King & Schroer, 2000). Dynein is relatively weak in comparison to kinesin-1; the stall force of individual molecules is assumed to be approximately 1 pN (Maday et al., 2014).

1.2.2. *Regulation of mitochondrial transport*

Apart from the biophysical properties of the individual motor proteins, several intracellular factors modulate mitochondrial movement patterns and velocity. Mitochondria cycle between short bursts of irregular movement ('runs') and temporary stops ('pauses'), as well as occasional changes in directionality, which overall leads to a saltatory moving behavior (Devireddy, Liu, Lampe, & Hollenbeck, 2015; Hollenbeck, 1996; Sheng & Cai, 2012). Average velocity of mitochondria has been reported quite variably between 0.05 – 1.4 µm/s *in vivo* (Misgeld & Schwarz, 2017). Some of this variability might be due to biological reasons (such as different relative time spent running vs. pausing) but could also be technical in nature (Misgeld & Schwarz, 2017). Several factors that regulate mitochondrial moving/stopping behavior are outlined below.

Motor protein number and distribution: Previous work showed that cargo is typically attached to multiple kinesin and dynein motor proteins at the same time (Encalada, Szpankowski, Xia, & Goldstein, 2011; Hendricks et al., 2010; Hirokawa, Sato-Yoshitake, Yoshida, & Kawashima, 1990; Maday, Wallace, & Holzbaur, 2012; Pilling et al., 2006). A popular model suggests that ultimate direction is determined in a 'tug of war' between competing motors (Derr et al., 2012), but a coupling of motor activity (Sheng & Cai, 2012) or selective manipulation of motors by scaffolding proteins (Maday et al., 2014) have also been suggested. In addition to that, motors cluster into cooperative microdomains to generate stronger forces on the microtubule, so the size and distribution of these clusters

will determine how cargo moves (Leopold, McDowall, Pfister, Bloom, & Brady, 1992; Martz, Lasek, Brady, & Allen, 1984; A. Rai et al., 2016; A. K. Rai, Rai, Ramaiya, Jha, & Mallik, 2013).

Intracellular Ca2+ and synaptic activity: Recruiting mitochondria to sites of high Ca^{2+} ion concentrations (which typically also happen to be sites of high energy demand) is important since mitochondria buffer Ca^{2+} ions and serve as intracellular stores. The proteins Miro and Milton are crucial in regulating mitochondrial transport by intracellular Ca^{2+} levels (Lin & Sheng, 2015). Together, they form the motor/adaptor complex by which kinesin-1 and dynein attach to mitochondria (**Figure 1.4**) (Brickley & Stephenson, 2011; Glater et al., 2006; Guo et al., 2005; Stowers, Megeath, Gorska-Andrzejak, Meinertzhagen, & Schwarz, 2002). Miro contains two regulatory EF-hand Ca^{2+}-binding domains (Fransson, Ruusala, & Aspenstrom, 2003), which cause mitochondria to stop in areas of high Ca^{2+} concentration such as synapses (Macaskill et al., 2009; Saotome et al., 2008). Syntaphilin, an axon-specific docking molecule (Kang et al., 2008), binds kinesin-1 motors and mitochondria onto microtubules in a Miro-Ca^{2+}-dependent manner and thus transfers mitochondria into the stationary pool on synapses (Y. Chen & Sheng, 2013).

Neuronal activity: Neuronal mitochondria are enriched at high energy consuming sites such as synapses to drive local ATP synthesis (Hollenbeck, 1996; Peters, Palay, & Webster, 1991; Rangaraju et al., 2014), and recruitment to synaptic sites is mediated by the calcium sensitivity of the Miro adaptor (see above). Less well understood remains, how neurons modulate overall mitochondrial density to match their activity level *in vivo*, as was shown by staining against cytochrome oxidase under different activity-conditions (M. Wong-Riley & Carroll, 1984; M. T. Wong-Riley & Welt, 1980) or correlations of firing

rates to mitochondrial density in neurites from 3D-EM reconstructions (Dorkenwald et al., 2017). Theoretically, such activity-dependent regulation of mitochondrial density could be a consequence of either altered mitochondrial transport or turnover (or both). So far, attempts to find acute effects of activity of mitochondrial transport showed conflicting results *in vivo* (Faits, Zhang, Soto, & Kerschensteiner, 2016; Sajic et al., 2013; Smit-Rigter et al., 2016; C. L. Zhang, Ho, Kintner, Sun, & Chiu, 2010), and the effects of chronic changes in activity remain poorly understood (Misgeld & Schwarz, 2017).

Microtubule architecture and stability: Microtubule organization and dynamics are important regulators of organelle transport in axons (Kapitein & Hoogenraad, 2015; Yogev et al., 2016). In neurons, individual microtubules do not span the entire axon, but are bundled in arrays of short filaments (Maday et al., 2014). Some cargoes pause at the end of a polymer before transferring to another, and have run-lengths that are limited by polymer length (Yogev et al., 2016). In addition, cargoes pause where microtubules intersect (Balint, Verdeny Vilanova, Sandoval Alvarez, & Lakadamyali, 2013; Zajac, Goldman, Holzbaur, & Ostap, 2013) and where they need to circumvent obstacles (Ross, Wallace, Shuman, Goldman, & Holzbaur, 2006; Verdeny-Vilanova et al., 2017). In principle, any proteins that organize or stabilize microtubules could therefore impact axonal transport. Some posttranslational modifications of microtubules such as detyrosination and polyglutamylation, which accumulate on stable microtubules, also directly regulate motor protein binding (Janke & Bulinski, 2011). For example, kinesin-1 favors moving on detyrosinated microtubules and has enhanced processivity (Dunn et al., 2008; Kaul, Soppina, & Verhey, 2014; Konishi & Setou, 2009; Kreitzer, Liao, & Gundersen, 1999; Liao & Gundersen, 1998), while tyrosinated tubulin recruits dynein to initiate retrograde transport (McKenney, Huynh, Vale, & Sirajuddin, 2016; Nirschl, Magiera, Lazarus, Janke,

& Holzbaur, 2016). Polyglutamylation enhances the motility of kinesin-1 in single-molecule assays (Sirajuddin et al., 2014), but decreases kinesin-1-mediated transport in hippocampal cultures (Maas et al., 2009), which is in agreement with the fact that polyglutamylation activates microtubule-severing enzymes like spastin (Lacroix et al., 2010).

1.3.   Developmental synapse elimination

Many of the synapses that are formed during embryonic development are later pruned as the nervous system matures (Schuldiner & Yaron, 2015). For example, humans reach maximal synaptic density within the first two years of age, which later declines until the end of puberty (Huttenlocher, 1979), and a study in macaque visual cortex estimated that about 5000 synapses/sec are lost during puberty (Bourgeois & Rakic, 1993). Thus, early synaptic wiring contains many connections which are later not used in circuits of adult animals (Lichtman & Colman, 2000).

It seems counterintuitive that organisms generate synapses only to discard most of them later (Schuldiner & Yaron, 2015). Since pruning accompanies a period of learning and mental development, many have interpreted this process as a means to refine the neuronal circuitry while the animal explores its surroundings (Lichtman & Colman, 2000). An initial "overshoot" could guarantee that each cell had abundant inputs to choose from, even if some were misguided along the way or damaged during development (Schuldiner & Yaron, 2015; Turney & Lichtman, 2012). In addition, it is easier from a cellular perspective to encode a few "general" developmental programs, instead of defining innumerous axon guidance programs for every particular connection (Schuldiner & Yaron,

2015). These possibilities are mainly speculative, but in any case, developmental pruning is a crucial neurobiological process. Abnormally excessive pruning during adolescence is suspected to be linked to schizophrenia (Riccomagno & Kolodkin, 2015; Sellgren et al., 2019), and pruning deficits potentially lead to the hyperconnectivity observed in autism spectrum disorders (Penzes et al., 2011).

There are many forms of developmental pruning, and synapse elimination describes a process where multiple inputs initially co-innervate a target and subsequently undergo competition for occupancy on the postsynapse, until all but a few inputs withdraw (Schuldiner & Yaron, 2015). Synapse elimination has been observed e.g. in thalamic reticulogeniculate synapses (C. Chen & Regehr, 2000), climbing fiber-Purkinje cell synapses of the cerebellum (Lohof, Delhaye-Bouchaud, & Mariani, 1996), autonomic ganglia (Lichtman, 1977), synapses of the cochlear nerve (Jackson & Parks, 1982), and the mammalian neuromuscular junction (NMJ). So far, synapse elimination has been studied most extensively at the NMJ (Bianchi, 2018).

1.3.1. The neuromuscular junction as a model for synapse development

The neuromuscular junction (NMJ), which connects motor neurons to muscle cells, has been a model system for almost a century, since acetylcholine was discovered as the first neurotransmitter (Tansey, 2006) and the quantal nature of neurotransmission was revealed by studies on nerve-muscle preparations (Del Castillo & Katz, 1954). NMJs show a number of similarities to central nervous system synapses when one considers their basic structure, function, and development (Sanes & Lichtman, 1999, 2001). Even today, NMJs remain the best characterized synapses (Bianchi, 2018), partly due to their *in situ* accessibility and size (300 µm² when compared to 1 µm² of CNS synapses; Kleele et al., 2014; Sanes & Lichtman, 2001).

Before describing synaptic development – in particular synapse elimination – I will briefly explain the anatomy of peripheral motor neurons (**Figure 1.5**). The mammalian NMJ is a tripartite structure consisting of a motor axon terminal, muscle cell, and terminal Schwann cell (see Fig. description: **Figure 1.5**) (Rubenstein & Rakic, 2013; Sanes & Lichtman, 1999). Motor axons arise from the ventral horn of the spinal cord and arrange their NMJs in a spread-out pattern in so-called "end-plate bands" in the center of muscles (Sanes & Lichtman, 1999). Here, each neuron's axons fan out laterally to connect to many muscle cells, which are excited together (a so-called motor unit) (Sanes & Lichtman, 1999). Average motor unit size (the number of muscle cells that a neuron innervates) determines how precisely a muscle can be moved, for example smaller motor units allow smaller force variations.
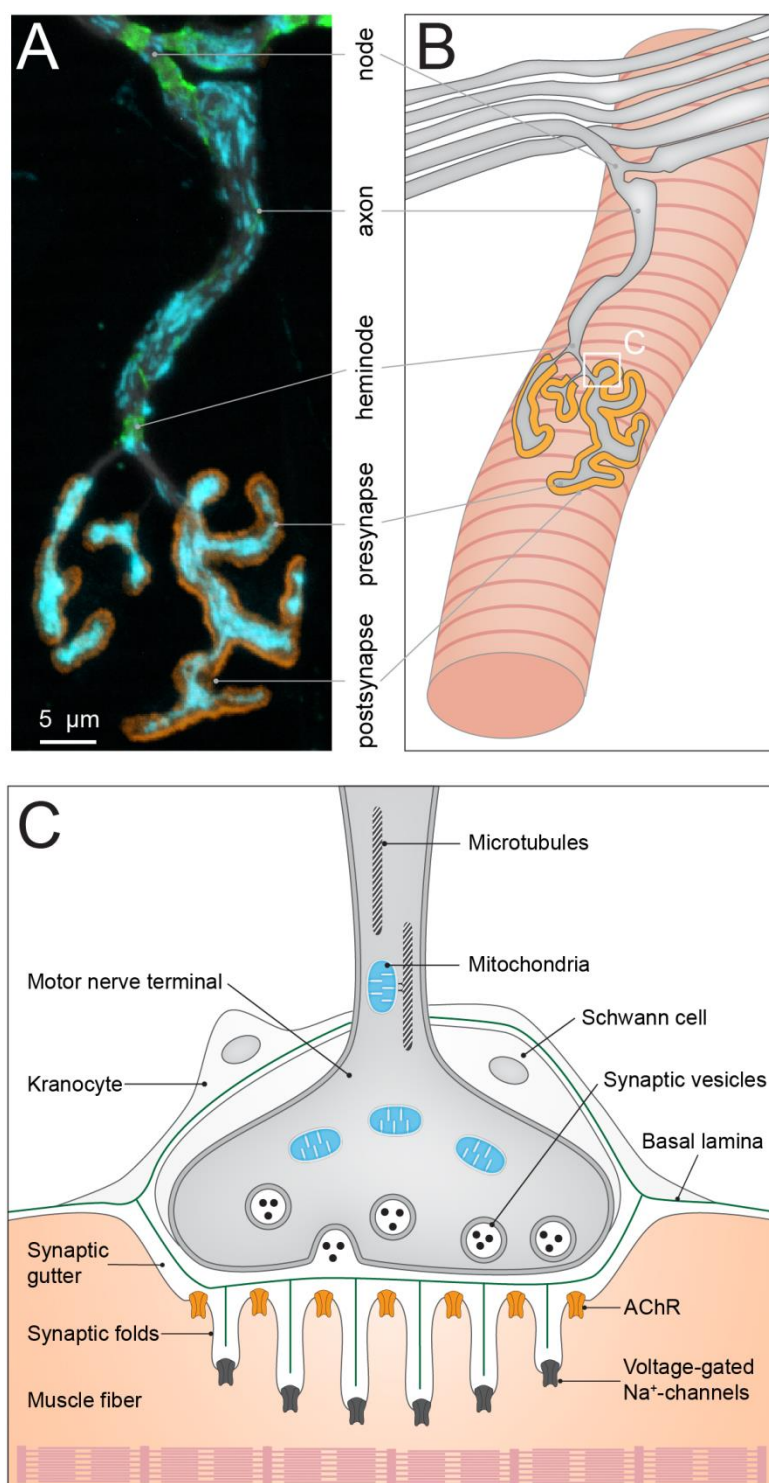
Figure 1.5 | Anatomy of the murine neuromuscular junction.
(**A**): Components of the neuromuscular junction visualized by fluorescence microscopy. Neuron-specific beta-III-tubulin is labelled with a conjugated antibody (***grey***), postsynaptic AChR are labelled with conjugated alpha-bungarotoxin (***orange***), paranodal loops of Schwann cells are labelled with an antibody against Caspr (***green***), and neuronal mitochondria are transgenically labelled with CFP (***cyan***) (Image acquired by the author in the lab of T. Misgeld).
(**B**): Schematic representing a terminal motor axon branch innervating an adult muscle fiber. Each axon terminal forms branched arrays of presynaptic boutons that are synchronously active and
(**C**) contain numerous vesicles that are filled with acetylcholine (ACh) and (Colman & Lichtman, 1993). The presynaptic terminal lies in a groove of highly folded sarcolemma that contains nicotinic ACh-receptors (AChR) and voltage-dependent sodium channels. Mitochondria are exceptionally dense at the presynapse; compare (A). Inspired by Rubenstein and Rakic (2013)

26

1.3.2. Developmental competition at neuromuscular junctions

In adult mammals, each skeletal muscle fiber is innervated by a single motor axon, whereas during early postnatal development, each fiber is innervated by multiple axons from different parent neurons (Bagust, Lewis, & Westerman, 1973; Bennett & Pettigrew, 1974; Brown, Jansen, & Van Essen, 1976; G. Luo et al., 2013; Redfern, 1970; Teriakidis, Willshaw, & Ribchester, 2012). The apparent loss of connections occurs by withdrawing exuberant inputs from the junction, then leaving a single input to be maintained and grow for most of the animal's remaining life (Balice-Gordon & Lichtman, 1990; Sanes & Lichtman, 1999). This combination of many inputs converging on one muscle cell, and each motor neuron input diverging onto many muscle cells leads to an overlapping and redundant circuit (Lichtman & Colman, 2000); but as the elimination of inputs progresses, motor unit size decreases and the circuitry becomes more refined (Sanes & Lichtman, 1999).

The mechanism of synaptic input elimination has been extensively studied in the past. Muscle fibers are rarely left denervated after pruning is done, and always end up innervated by exactly one axon, arguing that synapse elimination is a highly regulated and not random process, which involves active competition (Lichtman & Colman, 2000; Personius & Balice-Gordon, 2002). Indeed, the changes seen at junctions occur gradually as time goes by. Initially, as many as ten axons intermingle and share almost equal territory on a junction (Balice-Gordon, Chua, Nelson, & Lichtman, 1993; Balice-Gordon & Lichtman, 1993; Gan & Lichtman, 1998; Tapia et al., 2012). Between postnatal days 0-14 in mice, one axon (the 'winner') then progressively takes over regions formerly occupied by its competitors ('losers'), until the latter's branches withdraw completely (Balice-

Gordon et al., 1993; Walsh & Lichtman, 2003). Similarly, synaptic strength gradually increases in the input about to win, but decreases in the other inputs (Colman, Nabekura, & Lichtman, 1997). Both factors influence each other (larger synaptic territory increases synaptic strength, but synaptic activity also positively regulates synaptic territory), but which factor precedes the other and initiates this cycle is not known (Wyatt & Balice-Gordon, 2003).

Synaptic occupancy and axon caliber can be used to predict whether an input is more likely to win or lose competition in the future (Keller-Peck et al., 2001; Walsh & Lichtman, 2003). One study used sparse labeling of neurons with fluorescent proteins to optically measure synaptic occupancy (similar to the schematic in **Figure 1.6**) and showed that synapse elimination plays out asynchronously on the different branches of a neuron: while some terminals still undergo competition, others might have won or lost competition already (**Figure 1.6**) (Keller-Peck et al., 2001). After a terminal has lost competition, it slowly retracts from the junction until the next branch point of the parent axon is met (Bishop et al., 2004). Altogether, those results suggest that axon dismantling is executed locally within the last branch of an axon and that local cues determine the outcome of competition.

Several factors, such as synaptic activity and intracellular resource distribution, are known to influence the ability of terminals to win competition (so-called 'competitive vigor'), and will be outlined in the following.
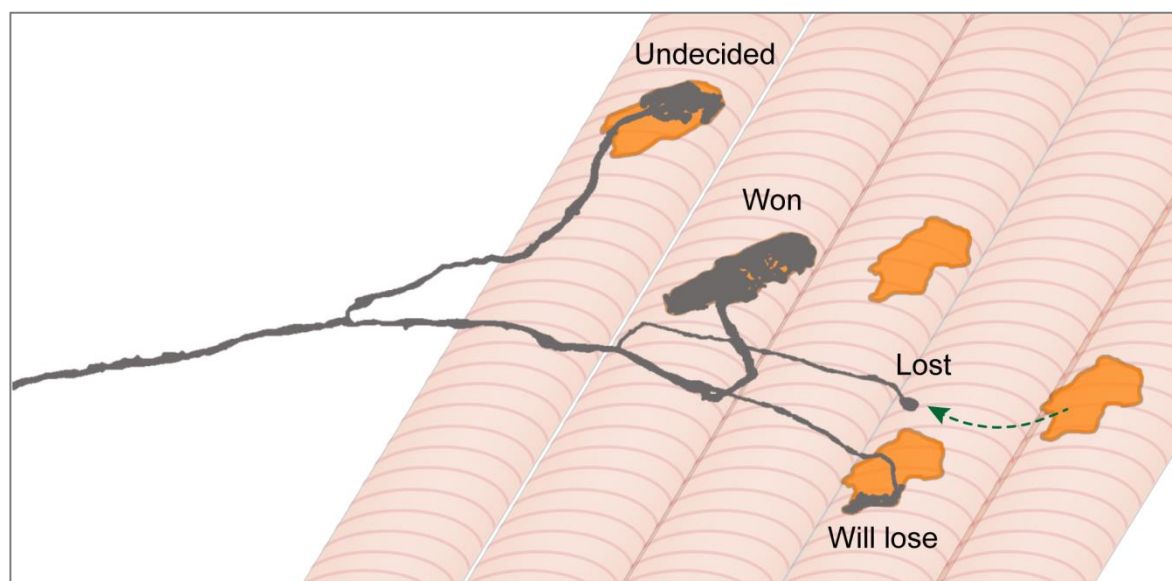
Figure 1.6 | Neuromuscular synapse elimination plays out asynchronously between different branches of the same neuron.
Schematic showing a sparse labeling of one axon and its terminal branches (grey) during the final phase of synapse elimination, the transition from double-innervation to single-innervation. One *doubly innervated NMJ* has roughly 50 % of its territory occupied by this axon branch ('undecided'), another ~20 % ('will lose'). One branch occupies the entire postsynaptic territory (*singly innervated NMJ*, 'won'); yet another branch has formed a *retraction bulb* at its tip and will retract until it reaches the branch point of the parent axon ('lost'). Modified with permission from Brill et al. (2016), design inspired by Lichtman and Colman (2000)

1.3.3. *Activity-dependence of synapse elimination*

The overall amount of activity affects the rate of synapse elimination; for example, nerve stimulation accelerates competition (Busetto, Buffelli, Tognana, Bellico, & Cangiano, 2000; Ridge & Betz, 1984; Thompson, 1983) and nerve block delays competition (Duxson, 1982; Ribchester, 1993; Thompson, Kuffler, & Jansen, 1979). However, some conflicting results were also published (Barber & Lichtman, 1999; Callaway, Soha, & Van Essen, 1987; Costanzo, Barry, & Ribchester, 2000; Hata, Tsumoto, & Stryker, 1999). Over the years, it became clear that synapse elimination is controlled by

the relative, and not the absolute, strengths of synaptic inputs (Barber & Lichtman, 1999; Buffelli et al., 2003; Busetto et al., 2000). For example, *in vivo* experiments showed that when part of the junction was blocked by the snake toxin α-bungarotoxin, the overlying input was inevitably eliminated, but when the whole junction was blocked, none of the inputs retracted (Balice-Gordon & Lichtman, 1994). Thus, it was postulated that uncorrelated activity between two inputs triggers synapse elimination (Balice-Gordon & Lichtman, 1994; Busetto et al., 2000; Personius & Balice-Gordon, 2001), which underscored the competitive nature of synapse elimination.

Those experiments suggested the existence of different 'punishing' and 'protective' signals at the synapse (Bianchi, 2018; Je et al., 2013; F. Yang et al., 2009). One such 'punishing' signal is the activity-dependent release of pro-BDNF from the muscle, which is cleaved to 'protective' BDNF by proteases secreted at active presynapses (Je et al., 2013; F. Yang et al., 2009). A consequence of this model would be that after removal of the 'punishing' signal, the 'losing' input would gain strength and potentially territory. Indeed, such an outcome has been observed after laser ablation of 'winning' inputs with more territory, where the seemingly 'losing' inputs with smaller territory took over the entire postsynaptic territory within a matter of hours (Turney & Lichtman, 2012). Similar signaling mechanisms have been described in other neurons (Cao et al., 2007; Singh et al., 2008) and many different axon growth and guidance factors have been recognized in other systems to control neurite pruning (Schuldiner & Yaron, 2015).

1.3.4. *Resource distribution in developing terminal axon branches*

In the quest to understand which properties of neurons pitch them at a competitive advantage, a study by Kasthuri and Lichtman (2003) found that whenever two neurons co-innervate different targets, the winner branches stem from the same parent neuron, which was usually also the neuron with the smaller axonal arbor. Thus at a given time point, there appeared to be a 'hierarchy' among neurons, which was based on a global property that determined synapse elimination outcome (Kasthuri & Lichtman, 2003). Global distribution of an intracellular resource might be such a property that depends on the complexity and size of the axonal arbor (Buffelli et al., 2003). Such resources could be synaptic vesicle components (Buffelli et al., 2003), organelles such as mitochondria, RNAs or signaling molecules. The availability of these resources could be regulated by local alterations of microtubule-based axonal transport. An early clue came from a study that looked at the neuronal cytoskeleton in losing input branches ('retraction bulbs'), which were devoid of microtubules, indicating that axonal transport might be downregulated in these branches (Bishop et al., 2004).

However, the idea that axonal transport is selectively hampered in retraction bulbs was not entirely undisputed. Riley (1981) suggested an initial phase of cytoplasm 'evacuation'. He speculated that these branches retreated by manner of their cytoplasm being retrogradely 'absorbed' into the parent axon. Such a mechanism would imply a relative increase in retrograde axonal transport when compared to 'winning' terminal branches. (Riley, 1981) In Liu, Chen, Wang, Wang, and Zhang (2010) retrograde axonal transport were required for synapse elimination at the NMJ of Drosophila, suggesting that the 'evacuation model' indeed was true at least in some settings.

1.3.5.   Ground work by others on the project

The project first set out to answer two questions, namely whether losing axon branches undergo a period of 'evacuation' by axonal transport, and whether there is a local cytoskeletal regulation that alternates axonal transport (Brill et al., 2016). Using transgenic mice that express fluorescent proteins under a neuronal *Thy1*-promotor in various organelles, such as mitochondria (Misgeld et al., 2007) and peroxisomes (Sorbara et al., 2014), axonal transport was time-lapse imaged in *M. triangularis sterni* thorax explants (see Materials and Methods) at terminal axon branches undergoing various 'stages' of competition. Using sequential photo-bleaching, the synaptic territory occupied by a branch was measured to infer the 'stage' of competition, which was classified into five categories, namely losers/retraction bulbs (0% territory), losing branches (1-40%), undecided branches (41-60%), winning branches (61-99%), and winners/singly-innervating branches (100%, i.e. those which have won competition). (Brill et al., 2016)

In Brill et al. (2016) they found that organelle net transport was virtually absent in branches that occupied 40 % or less synaptic territory ('losing' axons and retraction bulbs), unlike in branches with more than 60 % synaptic territory ('winning' axons and singly-innervating branches), which rather received a surplus amount of organelles. Those findings disputed an 'evacuation' model for the developing mouse NMJ and suggested that the other possibility was true, namely a breakdown of axonal transport caused by branch-specific microtubule-disruptions in dismantling axons. (Brill et al., 2016)

In order to test the latter, I used various pharmacological (epothilone B) and genetic tools (spastin-KO) to stabilize microtubules and study their effect on axonal transport. Further, I tried to understand how an upstream regulator of spastin, namely microtubule

polyglutamylation, affects axonal transport using a CCP1 and CCP6-double-KO ('CCP1/6-

dKO') mouse.

2. MATERIALS AND METHODS

2.1. Animals

Thy1-YFP-16-mice or *Thy1*-CFP5 (cytoplasmic YFP or CFP-expression in all motor neurons; Jackson Laboratory #003709, Tg(Thy1-YFP)16Jrs/J; Feng et al., 2000) were crossed to spastin-KO mice to assess retraction speed of retraction bulbs (controls were spastin-WT × *Thy1*-YFP-16 or -CFP5 littermates). Spastin-KO mice were previously generated in the lab (Brill et al., 2016). Mitochondrial transport was measured in spastin-KO × *Thy1*-mitoCFP^K and spastin-WT × *Thy1*-mitoCFP^K littermate controls (express CFP selectively in neuronal mitochondria; Misgeld et al., 2007). Epothilone B and PEG-control injections were performed in *Thy1*-YFP-16 × *Thy1*-mitoCFP^K mice to measure mitochondrial transport and tracking parameters. CCP1$^{fl/fl}$ and CCP6$^{fl/fl}$ mice were gifts from C. Janke, Paris (Magiera et al., 2018), and crossed to ChatCre mice (Jackson, Stock# 006410) to selectively knock-out these proteins in cholinergic neurons (controls were CCP1 x CCP6 x ChatCre$^-$ littermates). Experiments were performed during postnatal days (P) 7 – 13 (except for experiments involving mitoKeima, which were performed between 1 – 6 months of age) and with the approval of the Government of Upper Bavaria.

2.2. PCR

Animals were genotyped from tail biopsies by PCR before and after the experiments, weaning animals were marked on the paws by tattooing beforehand. PCR and

electrophoresis were performed by K. Wullimann, P. Krüger, and A. Gavoci, who had

isolated the DNA using the following standard protocol:

Tail lysis			
Reagent	*Quantity*	*Source*	*PCR program*
Gitocher	15 µL	See below	
10 % Triton	7.5 µL	Roth	55 °C 5 h
β-Mercaptoethanol	1.5 µL	Sigma-Aldrich, M6250	95 °C 5 min
Proteinase K	0.75 µL	Sigma-Aldrich, P2308	4 °C ∞
H_2O	125.25 µL		
Total volume 150 µL / Tube.			

The following primers and protocols (amount per reaction) were used to genotype for

the expression of fluorescent proteins or spastin:

YFP (GFP 379bp)			
Reagent	*Quantity*	*Source*	*PCR program*
GoTaq	10 µL	Promega Ref.-No. M7421	95 °C for 3 min
GFP-F (10 pmol / µL)	1 µL	Metabion	95 °C 10 sec
GFP-R (10 pmol / µL)	1 µL	Metabion	58 °C 10 sec 30x
DNA	1 µL		72 °C 10 sec
H_2O	7 µL		4 °C ∞
Total volume 20 µL. GFP-F: 5´-CACATGAAGCAGCACGACTT-3´; GFP-R: 5´-TGCTCAGGTAGTGGTTGTCG-3´			

Mito (181bp)			
Reagent	*Quantity*	*Source*	*PCR program*
GoTaq	10 µL	Promega Ref.-No. M7421	95 °C for 3 min
Mito-F (10 pmol / µL)	1 µL	Metabion	95 °C 10 sec
EYFP-R (10 pmol / µL)	1 µL	Metabion	58 °C 10 sec 30x
DNA	1 µL		72 °C 10 sec
H_2O	7 µL		4 °C ∞
Total volume 20 µL. Mito-F: 5´-CGC CAA GAT CCA TTC GTT-3´; EYFP-R: 5´-GAA CTT CAG GGT CAG CTT GC-3´			

Spastin (wt: 223bp, ko: 432bp)			
Reagent	*Quantity*	*Source*	*PCR program*
GoTaq	10 μL	Promega Ref.-No. M7421	95 °C for 2 min
Spas 41 –F (10 pmol / μL)	1 μL	Metabion	95 °C 15 sec
Spas 89 –F (10 pmol / μL)	1 μL	Metabion	60 °C 30 sec 32x
Spas 169 –C (10 pmol / μL)	1 μL	Metabion	72 °C 15 sec
DNA	1 μL		72 °C 5 min
H$_2$O	7 μL		4 °C ∞
Total volume 20 μL. Spas 41: 5'-AAGTCATGGCAGTCTTTCTGGCT-3'; Spas 89: 5'-CACATGGTGGCTCATAACCATTTA-3'; Spas 169: 5'-ATTTGCAAAAACTACTTGCTATTAAATTCC-3'			

CCP1 (wt: 296bp, flox: 405bp)			
Reagent	*Quantity*	*Source*	*PCR program*
GoTaq	10 μL	Promega Ref.-No. M7421	95 °C for 2 min
CCP1 - 1 (10 pmol / μL)	1 μL	Metabion	95 °C 15 sec
CCP1 - 2 (10 pmol / μL)	1 μL	Metabion	60 °C 30 sec 32x
			72 °C 15 sec
DNA	1 μL		72 °C 5 min
H$_2$O	7 μL		4 °C ∞
Total volume 20 μL. CCP1-1: 5'-TTAAGCAGTGGCTGCCGGAGTGC-3'; CCP1 -2: 5'-GTCTACAGCCACGTGCTCAGCAAAGG -3'			

CCP6 (wt: 202bp, flox: 337bp)			
Reagent	*Quantity*	*Source*	*PCR program*
GoTaq	10 μL	Promega Ref.-No. M7421	95 °C for 2 min
CCP6 - 1 (10 pmol / μL)	1 μL	Metabion	95 °C 15 sec
CCP6 - 2 (10 pmol / μL)	1 μL	Metabion	60 °C 30 sec 32x
			72 °C 15 sec
DNA	1 μL		72 °C 5 min
H$_2$O	7 μL		4 °C ∞
Total volume 20 μL. CCP6-1: 5'-GAATGGCAATGAGATCACCACTCTCCAGC-3'; CCP6 -2: 5'-CTGTTGGGTGTCTGAGGCAAACACTTCC -3'			

ChatCre (wt: 200bp, mut: 148bp)			
Reagent	*Quantity*	*Source*	*PCR program*
GoTaq	7 µL	Promega Ref.-No. M7421	94 °C for 2 min
ChatCre C-R (10 pmol / µL)	1 µL	Metabion	94 °C 20 sec, 65°C 15 sec (-0.5°C per cycle decrease), 68°C 10 sec (repeat these steps 10x, touchdown)
ChatCre wt-F (10 pmol / µL)	10 µL	Metabion	94 °C 15 sec, 60 °C 15 sec, 72°C 10 sec (repeat these steps 28x)
ChatCre mut-F (10 pmol / µL)	1 µL	Metabion	
DNA	1 µL		72 °C 2 min
H$_2$O	1 µL		4 °C ∞
Total volume 20 µL. WT-forward: 5'-GTTTGCAGAAGCGGTGGG-3'; mut-forward: 5'-CCTTCTATCGCCTTCTTGACG -3', common-reverse: 5'-AGATAGATAATGAGAGGCTC-3'			

DNA electrophoresis was performed on agarose (Sigma, A9539) in a gel chamber (DNA Pocket Block-UV, Biozym Diagnostik). The agarose gel was loaded with 15 µL of the PCR reaction mix and 2 µL 6x loading buffer (Millipore; 69046-3); in addition, 8 µl of a 1K ladder (New England Biolabs, N0468L) as loaded on the first well. Electrophoresis was performed under 90 mV in TAE buffer (Carl Roth, CL86.1), DNA bands recorded under 312 nm light (Genoplex system, VWR).

2.3. Acute explants of the triangularis sterni muscle-nerve tissue

To image synaptic pruning and mitochondrial transport in neuromuscular junctions, a modified protocol to prepare acute explants of the triangularis sterni muscle was used (**Figure 2.1**) (Kerschensteiner, Reuter, Lichtman, & Misgeld, 2008). The triangularis sterni muscle is a thin muscle on the inner side of the thorax where neuromuscular junctions and parts of the intercostal nerves lie superficially on the muscle and are therefore readily

accessible for imaging. In brief, infant mice were decapitated with a large scissors (#14101-14, FST). Animals were sprayed with 80 % ethanol to prevent fur from contaminating the underlying tissue. The thorax was exposed by removing skin and pectoral muscles and released from the surrounding tissue by severing the ribs close to the spinal column (#2 forceps, 11223-20, FST). After transferring the explant to a dish with cooled Ringer's solution on ice, the remaining thymus and loose connective tissue were removed from the inner side of the thorax. The explant was pinned on a Sylgard-coated 3.5 cm petri dish with minute insect pins (Fine Science Tools) with the inner side facing up. During imaging, the explant was continually perfused with warmed Ringer's solution (bubbled with 95 % O_2 / 5 % CO_2) at a speed of 1.5 – 2.5 mL / min and kept at a temperature between 33 - 36 °C on a heated stage.
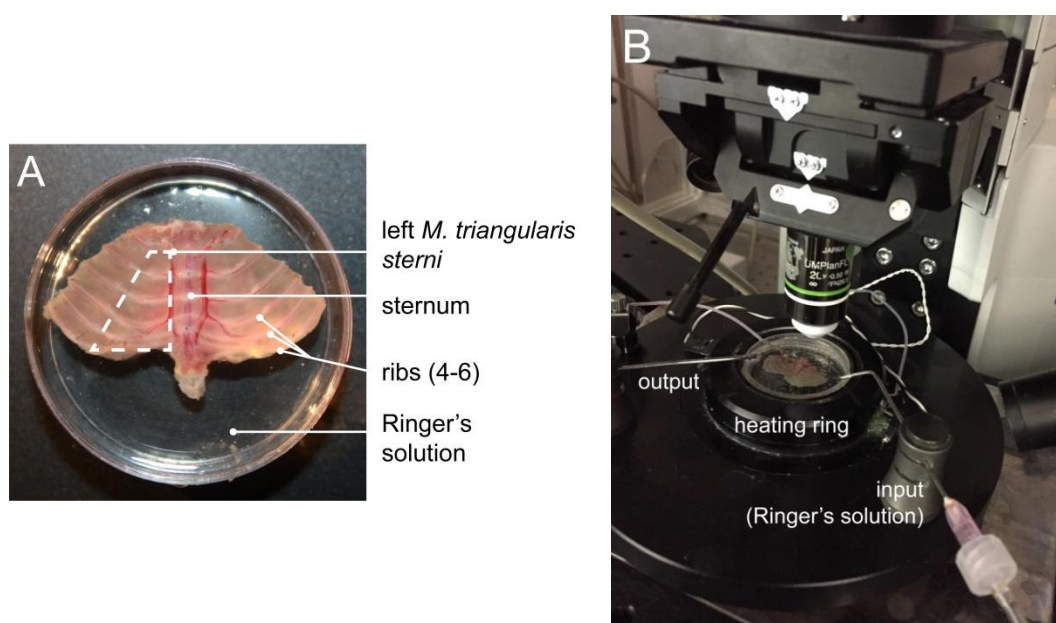

Figure 2.1 | Perfusion and microscopy setup for live imaging of acute thorax explants
(**A**) Murine thorax explant, freshly prepared in oxygenated Ringer's solution and pinned onto a Sylgard dish with the inner side including the *M. triangularis sterni* facing up (image with permission from M. Brill). (**B**) Imaging setup at an upright widefield setup (image by the author). The explant is placed in a heating chamber and continually perfused with oxygenated, warmed Ringer's solution during the experiment.

2.4. Imaging of mitochondrial transport

Mitochondrial transport in neuromuscular junctions and intercostal nerves was time-lapsed on an upright wide-field microscope (Olympus BX51WI) equipped with 20x / 0.5 N.A. and 100x / 1.0 N.A. water-immersion objectives, an automated filter wheel (Sutter), a mercury arc lamp and a CCD camera (Retiga EXi by Qimaging). Images were acquired using μManager software (NIH). For imaging *Thy1*-mitoCFP-K x *Thy1*-YFP-16, a CFP or YFP filter cube was used (F36-544, F36-528; AHF), additionally, neutral density filters (5, 10, or 25 %; AHF) were used to minimize photo-bleaching. Time-lapse movies were acquired at 0.5 - 1 Hz for 60 min with an exposure time of 300 - 400 ms.

2.5. Epothilone injections

Epothilone subcutaneous injections were performed by Dr. M. Brill. Mice were injected with 15 μL epothilone B (Selleckchem, 0.5 μg / μL in vehicle) or 15 μL vehicle using a 30G insulin needle. Litters (including experimental and control pups) were returned to the mother in the home cage and acute thorax explants were prepared for mitochondrial transport imaging at 3-5 days after injection.

2.6. Confocal imaging

To observe axon branch retraction, two image stacks spanning a time window of 2.5 – 4.5 h were acquired in explants from *Thy1*-YFP-16 or *Thy1*-CFP-5 mice on a confocal microscope (Olympus FV1000 equipped with a 100x / 1.0 N.A. water-immersion objective and 440 / 488 nm lasers). During the experiment, explants were heated on a stage to 33 –

36 ° C and continually perfused with 1.5 – 2.5 mL / min of carbogen-bubbled Ringer's solution.

2.7. Transport of Keima particles

For labelling of mitochondria and mitolysosomes with Keima, mice were injected on P3 with an AAV9-ds-hSyn-mitoKeima virus (kindly provided by a collaboration with P. Avramopoulos and S. Engelhardt, TUM/DZKH). Briefly, pups were anaesthetized with isoflurane and injected with 3 µL of the virus (titer: $6x10^{13} – 1x10^{14}$ vg/mL) into the 3rd brain ventricle using a nanoliter injector attached to a fine glass pipette. The injection was guided by ultrasound (Visualsonics, Vevo® 2100). Movies of adult mice were acquired as described in **sections 2.3** and **2.4** using a Keima filter cube (AHF, #F76-504) and with a 0.75 - 0.9 Hz frame rate.

2.8. Image processing and analysis

Microscopic images were processed using the software Fiji (Schindelin et al., 2012) and mitochondrial transport movies were aligned using the *StackReg* algorithm (Thevenaz, Ruttimann, & Unser, 1998). Mitochondrial transport rate was measured by counting the number of mitochondria moving over an axonal cross section per time interval.

Mitochondria were tracked with the *Manual Tracking* plugin in Fiji. Average speed was calculated as the total distance travelled divided through the observation time; average running speed was calculated accordingly after excluding the time spent pausing. A stop was defined as a previously motile mitochondrion that moved less than 0.091 µm/s; stops

were excluded if they were open-ended toward the end of the movie. Run length was defined as the distance travelled between stops. A script to calculate those parameters from tracking coordinates of the *Manual Tracking* .csv files was written in *Python*.

To determine the speed of axon branch shortening, maximum intensity projections of the two-time-point stacks of retraction bulbs were generated in *Fiji*. The images were manually aligned and the distance between the two positions of the retraction bulb was measured. The images were re-analyzed by Dr. M. Wang in a blinded fashion to exclude observer bias.

2.9. Statistics

Statistical analysis was performed using Prism 8 (GraphPad Software). Data were tested for normal distribution using the D'Agostino-Pearson normality test. In datasets which passed this test, significance was determined by a two-sided *t*-test; in datasets which failed the test, significance was determined using a Mann-Whitney-U test. *p*-values < 0.05 were considered as significant. In graphs, *p*-values < 0.05 are indicated by *, < 0.01 by **, and < 0.001 by ***. Bar plots show mean ± s.e.m. Boxplot are shown as Tukey plots, where the median is annotated by a black horizontal line, the interquartile range (IQR) by a bar, points within 1.5 times of the IQR by whiskers, and outliers by dots. In violin plots, a black horizontal line shows the median and two dotted lines the quartiles. Sample size calculations were performed using an online calculator (Boston-University-Research-Support, Retrieved on 31.03.2020 from https: // www .bu.edu/ researchsupport/ compliance/ animal-care/ working-with-animals/ research/ sample-size-calculations-

iacuc/). At least three animals were included in each condition or group of an experiment,

except in **Figure 3.8**, which shows a preliminary analysis with one animal per group.

2.10. Buffers and solutions

Ringer's solution			
Reagent	*Quantity*	*Concentration*	*Source*
1M $CaCl_2$	2 mL	2 mM	Sigma-Aldrich, C1016
1M $MgCl_2$	1 mL	1 mM	
H_2O	900 mL		
10x Ringer's solution	100 mL	20 mM	see below
Glucose	3.6 g		Sigma-Aldrich, 16301
Total volume 1 L. Stored at 4 °C. *Ringer's was bubbled with carbogen gas (95 % O_2, 5 % CO_2) at least 20 min before use.*			

10x Ringer's solution			
Reagent	*Quantity*	*Concentration*	*Source*
$NaHCO_3$	21.84 g	260 mM	Sigma-Aldrich, S6297
$NaH_2PO_4 * H_2O$	1.72 g	12.5 mM	Riedel de Haen, 04270
KCl	1.86 g	25 mM	
NaCl	73.05 g	1.2 mM	
H_2O	up to 1 L		
Total volume 1 L. Stored at 4 °C.			

Agarose gel		
Reagent	*Quantity*	*Source*
1x TAE buffer	50 mL	Carl Roth, CL86.1
Agarose	0.5 g	Sigma, A9539
Gel Red nucleic acid stain	5 µL	VWR International,730-2957
Total volume 50 mL.		

Gitocher buffer			
Reagent	*Quantity*	*Concentration*	*Source*
Tris	15 µL	1.43 mol/L	Roth, 4855.1
$(NH_4)_2SO_4$	5 mL	1.66 mol/L	Sigma-Aldrich, M3148
$MgCl_2$	5 mL	0.65 mol/L	
Gelatine	0.05 g		Roth, 4275.3
H_2O	15 mL		
Total volume 50 mL.			

3. RESULTS

The experiments described in this section were partly published in:

Brill, Kleele, Ruschkies, Wang, Marahori, Reuter, Hausrat, Weigand, Fisher, Ahles, Engelhardt, Bishop, Kneussel, Misgeld (2016). Branch-Specific Microtubule Destabilization Mediates Axon Branch Loss during Neuromuscular Synapse Elimination. *Neuron*, 92(4):845-856.

The work detailed here was performed by N. Marahori in the laboratory of T. Misgeld

(TUM, Munich, Germany), unless specified otherwise (contributions to collaborative

datasets have been detailed in the corresponding figure legends).
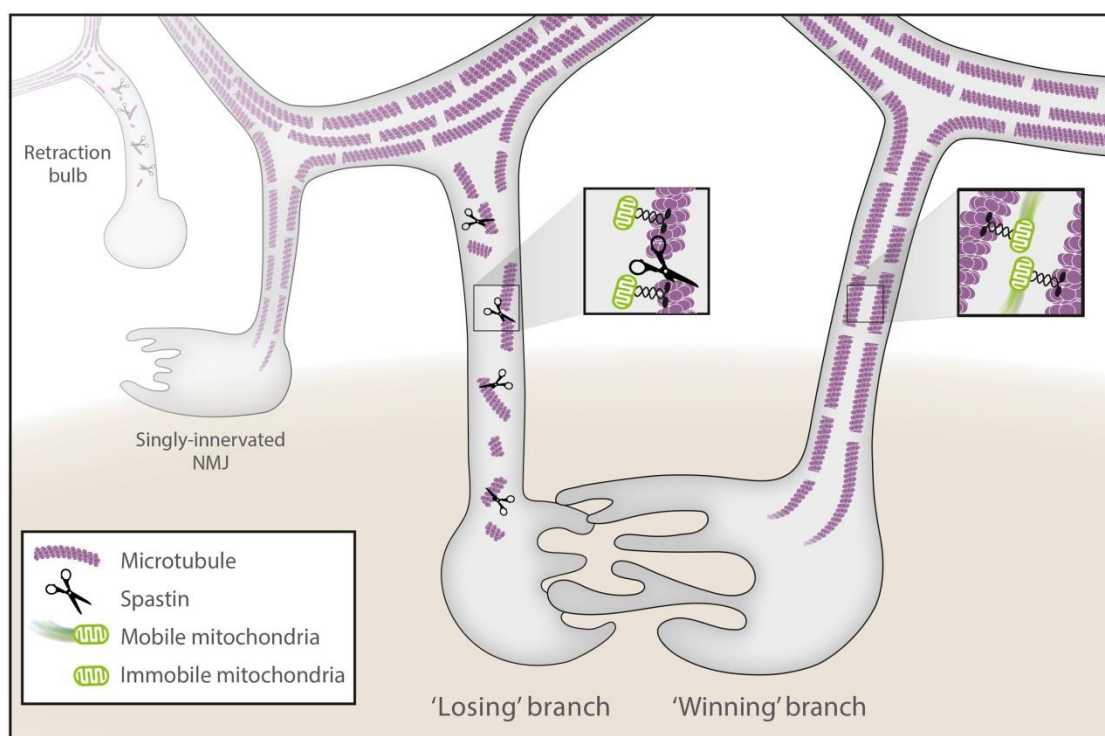
Figure 3.1 | Spastin mediates microtubule destabilization and axon branch dismantling. (Figure from the journal preview of the article Meltzer and Schuldiner (2016))

3.1. Pharmacological microtubule stabilization restores mitochondrial transport in dismantled axon branches

The previous results suggested that microtubule disassembly and reduced organelle supply are important elements of motor axon pruning (Brill et al., 2016). In fact, pharmacological microtubule stabilization using epothilone B (see Material and Methods) delayed synapse elimination significantly (Brill et al., 2016). To test the causal relationship between microtubule disassembly and organelle transport, $Thy1$-mitoCFP^K pups, where the neuronal $Thy1$-promotor drives expression of cytosolic CFP in mitochondria, were injected subcutaneously with a single dose of 7.5 µg epothilone B on postnatal day (P) 5 and were then sacrificed between P 8-10 for live imaging (**Figure 3.2**, **A**). For controls, littermates were injected with the same volume of vehicle (PEG, see Material and Methods).

Mitochondrial transport was then measured in *M. triangularis sterni* explants (Kerschensteiner et al., 2008) at different locations of the axonal arbor, namely singly innervating terminal branches ('winners'), retraction bulbs ('losers'), and stem axons (intercostal nerve) (**Figure 3.2**, **B-C**). Our hypothesis was that in retraction bulbs with disassembled microtubules epothilone B would stabilize and thus increase mitochondrial transport rates. Indeed, in retraction bulbs treatment with epothilone B increased anterograde mitochondrial transport 10.8-fold compared to PEG-injected littermate controls (**Figure 3.2**, **D**; 'rebu', Ctr: 0.06 ± 0.06 mitochondria (mito)/h; Epo: 0.65 ± 0.24 mito/h). Similarly, retrograde transport increased significantly in retraction bulbs of epothilone B-treated animals (**Figure 3.2**, **E**; 'rebu', Ctr: 0.00 ± 0.00 mito/h; Epo: 0.66 ± 0.29 mito/h). In comparison, mitochondrial transport was only slightly changed in singly innervating terminal branches (~1.3-fold; 'sin') and the (unbranched) stem axons (**Figure**

3.2, **D-E**; sin/ant: Ctr: 3.83± 0.43 / h; Epo: 5.10 ± 0.49 /h; sin/ret: Ctr: 2.46 ± 0.38 /h; Epo:

3.26 ± 0.44 /h; stem axons/ant: Ctr: 5.1 ± 0.3 /min; Epo: 6.1 ± 0.4 /min; stem axons/ret:

Ctr: 3.1 ± 0.3 /min; Epo: 2.7 ± 0.3 /min). Thus, the relatively strong ~63-fold difference

between retraction bulbs and singly innervating inputs was substantially decreased to ~8-

fold in epothilone-injected mice (numbers for anterograde transport, **Figure 3.2**, **D**).
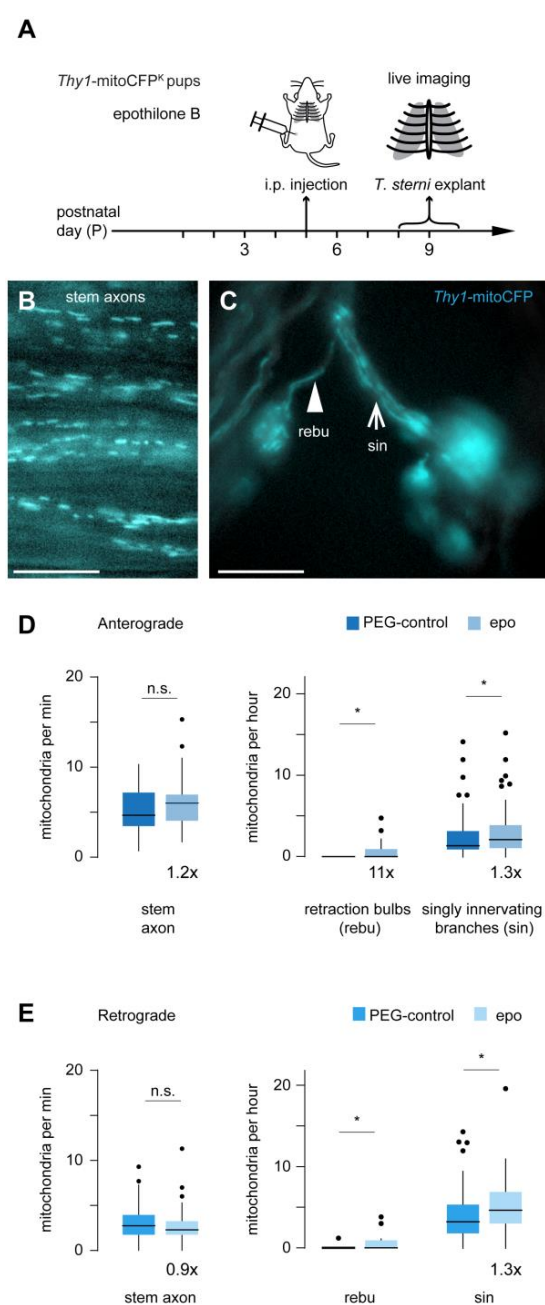
Figure 3.2 | Epothilone B treatment partially restores mitochondrial transport.
(**A**) Experimental timeline. *Thy1*-mitoCFP[K] pups were injected intraperitoneally with a single dose of epothilone B on P5 and imaged between P8-10 on Triangularis sterni explants. (**B, C**) Widefield image of recorded axons in (**B**) an intercostal nerve, as well as (**C**) a singly innervating axon ('sin') and a retraction bulb ('rebu'). (**D, E**) Mitochondrial transport in anterograde (**D**) and retrograde (**E**) direction (stem axon; n ≥ 51 axons, ≥ 5 mice), as well as retraction bulbs ('rebu'; n ≥ 20 axon branches, ≥ 18 mice) or singly innervating terminal branches ('sin'; n ≥ 51 axons, ≥ 22 mice). Boxplots are Tukey plots (see Material and Methods for detailed description). Fold-increases (below epo-data) are calculated from means. Mann-Whitney test was used to determine significance in D, E: * p < 0.05; n.s. p ≥ 0.05. Scale bars in B, C are 10 µm. The entire dataset on stem axons (103 data points) was acquired and analyzed by the author; on rebus and sins it was acquired together with M. Brill (14 of 151 data points by the author). Figure and text were modified from Brill et al. (2016).

Overall, the results show that stabilizing microtubules using epothilone B partially restores organelle transport in retraction bulbs. Further, they hint that in a situation where transport rates are more similar between inputs, competition plays out more slowly – which is in line with the fact that epothilone B injection delays synapse elimination (Azzouz et al., 1997; Brill et al., 2016).

3.2.   Mitochondrial tracking parameters in epothilone B-injected mice

To better understand how mitochondrial movements are affected by developmental microtubule disassembly, I tracked individual moving mitochondria in retraction bulbs ('losers') and singly-innervating terminal branches ('winner') (**Figure 3.3, A-D**; analysis was performed on the experiments from **section 3.1**). Due to the low transport rates in retraction bulbs, PEG-injected controls were pooled with uninjected controls acquired by M. Brill). I then calculated the average speed (total distance travelled divided by the observation time), running speed (speed during 'runs', i.e. excluding pauses), average pause duration and pause rate (see Materials and Methods for more details).

In the control, the average speed of mitochondria was significantly lower in retraction bulbs than in singly innervating inputs (**Figure 3.3, E**; rebu: 0.06 ± 0.02 μm/s; sin: 0.20 ± 0.03 μm/s). This difference in average speed was mainly influenced by two parameters, namely decreased running speed (i.e., the speed during 'runs' (excluding pauses), **Figure 3.3, E**; rebu: 0.23 ± 0.03 μm/s; sin: 0.40 ± 0.02 μm/s) and increased average pause duration (rebu: 38.6 ± 13.0 sec; sin: 13.1 ± 2.2 sec). Epothilone B treatment rescued all three parameters in retraction bulbs to the normal levels of singly innervating inputs (**Figure 3.3, E**). Interestingly, epothilone B treatment did not change mitochondrial movement

parameters significantly in singly innervating inputs (**Figure 3.3, E**; see discussion). The

pause rates were not significantly changed between all groups (**Figure 3.3, E**). Some of

these parameters might be differentially affected in anterograde or retrograde direction but

due to the low number of mitochondria that could be tracked in retraction bulbs (n = 6), I

did not perform more detailed analyses.
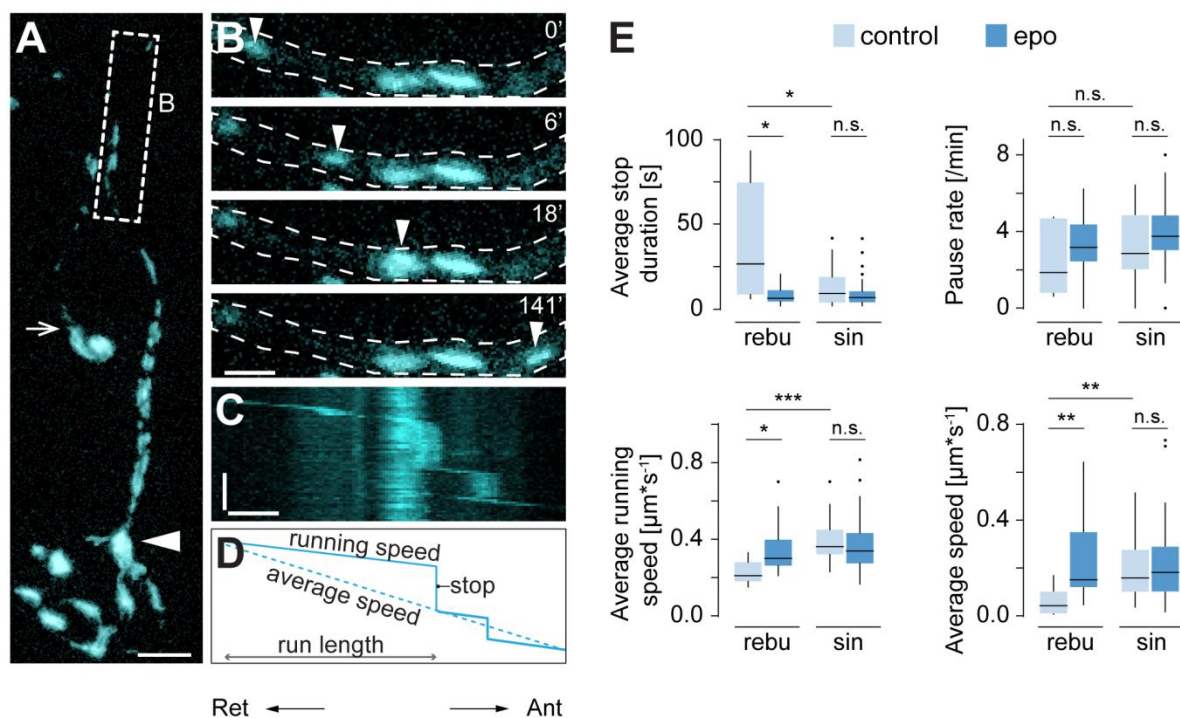
Figure 3.3 | Epothilone B differentially affects mitochondrial movement parameters in terminal axon branches.
(**A**) Widefield image of recorded axons in an axon from a singly innervated junction (filled arrow; closed arrow: shows a neighboring retraction bulb; here, a widefield stack was background-subtracted and maximum-projected) of *Thy1*-mitoCFP^K pups. (**B**) Blowup of the axon outlined in a box in **A,** dotted lines indicate the axon outline. The images show selected frames from a time-lapse of a moving mitochondrion (arrow). (**C**) Kymograph of the axon shown in **B**. (**D**) Illustration of the movement parameters extracted from the mitochondrion tracked in (**B, C**), namely average speed, moving speed, stopping, and run length. (**E**) Quantification of different movement parameters from mitochondria tracked in retraction bulbs ('rebu') and singly innervating branches ('sin') of epothilone-injected ('epo') mice and controls. For controls, data from PEG-injected littermates were pooled with a data from uninjected mice, due to the extremely low amount of transport in retraction bulbs (Rebus: n ≥ 6 mitochondria from ≥ 3 mice per group; Sins: n ≥ 27 mitochondria from ≥ 5 mice). Scale bar in **A** is 5 µm, in **B** 2 µm. In **C** horizontal scale bar is

⟶

2 µm and vertical is 15 sec. Boxplots are Tukey plots (see Material and Methods for description). Mann-Whitney test was used in **E** to determine significance: *** P < 0.001; ** P < 0.01; * P < 0.05; n.s. P ≥ 0.05. Data were acquired in collaboration with M. Brill (10 of 112 mitochondria were acquired by the author), particle tracking and analysis (112 of 112 mitochondria) was performed by the author.

Overall, these results support the idea that selective microtubule destabilization in dismantling branches causes the changes observed in transport parameters. Further, the finding that pause durations and speed are altered supports the idea that microtubule content decreases due to microtubule disruption in dismantling branches, as earlier work has pointed out that some organelles pause at microtubule ends and that pause durations negatively correlate with microtubule density (Yogev et al., 2016).

3.3. Spastin mediates axon dismantling during synapse elimination

Considering the profound effects of pharmacological microtubule stabilization in dismantling axons, we next asked which mechanisms mediate microtubule disassembly in our setting. Among the proteins which affect microtubule length and stability, microtubule-severing enzymes such as spastin and katanin have been implicated in sculpting neuronal morphology during development (Roll-Mecak & McNally, 2010). Microtubule-severing enzymes cut microtubules along their long axis to increase the number of microtubules and dynamic plus-end tips (Baas et al., 2016; McNally & Roll-Mecak, 2018). The generated fragments can either grow (increase in mass) or shrink (decrease in mass) (McNally & Roll-Mecak, 2018). In our setting, shorter, less dense microtubules with an overall increase in dynamic plus-end tips were observed in retraction bulbs and losing inputs (experiments by M. Brill and T. Kleele; Brill et al., 2016). Taken together, these observations indicated to us that microtubule severing enzymes might play a role in axon branch stabilization.

49

To test whether spastin mediates synapse elimination, a new spastin knockout (KO) mouse was generated (a katanin-KO had no detectable effect on synapse elimination, Monika Brill, personal communication, on 15. January 2020) (Kneussel lab; Brill et al., 2016). Spastin deletion significantly delayed synapse elimination when compared to wild type littermate controls (experiments by M. Brill and T. Kleele; Brill et al., 2016). Here, the speed of transition from the poly-innervated to singly innervated state was measured by quantifying the relative amount of poly-innervated NMJs at a given time point. However, synapse elimination is a multi-step process (Sanes & Lichtman, 1999), and it was important to understand precisely whether axon withdrawal played out more slowly upon genetic spastin deletion. Ideally, one would therefore perform live imaging to observe the speed at which terminal branches lose synaptic territory and retract. To make this experiment feasible within the time constraints of the nerve-muscle explant, I limited my observations to the final step of synapse elimination, retraction (Bishop et al., 2004) and acquired confocal stacks spanning a time interval of ~3 hours from retraction bulbs in *Thy1*-YFP-16 x spastin$^{ko/ko}$ or spastin$^{wt/wt}$ littermate controls (**Figure 3.4, A**). As expected, retraction speed was reduced by half in spastin-KO mice compared to wild type littermates (**Figure 3.4, B**; spastin$^{wt/wt}$: 1.2 ± 0.2 µm/h; spastin$^{ko/ko}$: 0.6 ± 0.1 µm/h) and the distribution of retraction speeds shifted to lower speeds (**Figure 3.4, C**).
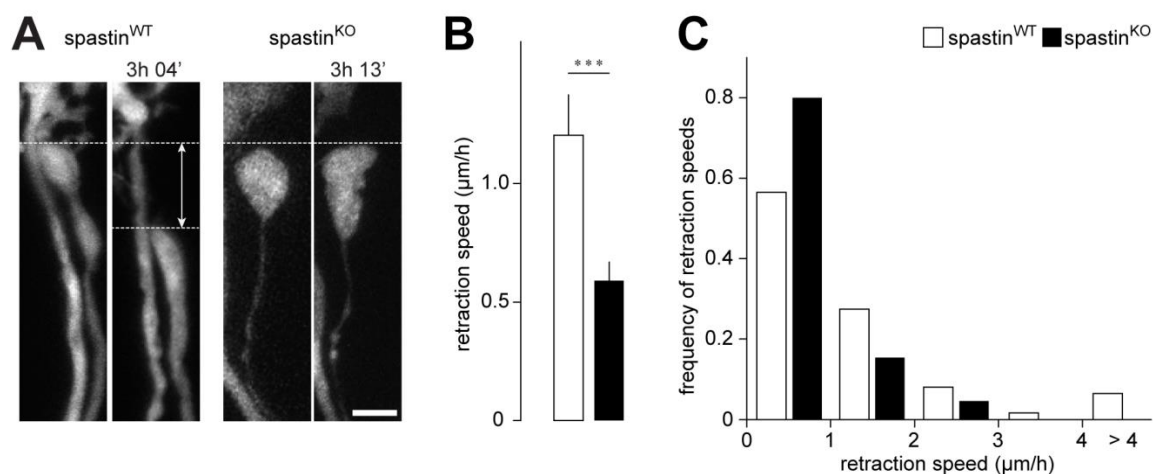
Figure 3.4 | Genetic stabilization of microtubules delays retraction of 'loser' branches.
(**A**) Confocal images spanning a time interval of ~3 hours were taken in explants from spastin[wt/wt] (left) and spastin[ko/ko] (right) pups crossed to *Thy1*-YFP-16 or *Thy1*-CFP-5 (between P8-10). (**B**) Average retraction speed (**C**) and histogram of individual recordings (KO: n ≥ 65 axons from 7 mice; WT: n ≥ 62 axons from 7 mice). Figure and text were modified from (Brill et al., 2016). Scale bar 3 μm. Data are mean + SEM. Mann-Whitney test was used to determine significance in (B): *** p < 0.001. The entire dataset was acquired and analyzed by the author (127 of 127 axons).

In summary, these results indicate that the enzyme spastin mediates synapse elimination. One further set of experiments to test whether the microtubule-severing activity of spastin also affects resource distribution was to measure axonal transport in these mice.

3.4. Mitochondrial transport in axons from spastin-KO mice

To test whether microtubule stabilization by spastin-KO restores mitochondrial transport in losing branches, a dataset on mitochondrial transport rates (n ≥ 9 axons) in developing axons of *M. triangularis sterni* explants from *Thy1*-mitoCFP[K] x spastin-KO pups was also acquired (**Figure 3.5**). Neither of the three locations (stem axons, 'sin', or 'rebu') had significantly altered transport in spastin[ko/ko] mice compared to littermate

controls (spastin$^{wt/wt}$) (**Figure 3.5, A-B;** numbers for 'rebu': ant: 0.0 ± 0.0 mito/h in WT,

0.2 ± 0.2 mito/h in KO; ret: 0.1 ± 0.1 mito/h in WT, 0.4 ± 0.3 mito/h in KO). Performing a

sample size calculation (see Material and Methods) showed that with n ≥ 9 retraction bulb

axons per group one could already attain statistical significance of p < 0.05 with an 80 %

probability (statistical power), although to reject the hypothesis with more power one

would have to acquire more axons. On overall, this leads to the conclusion that spastin-KO

most likely does not affect transport significantly (see Discussion).
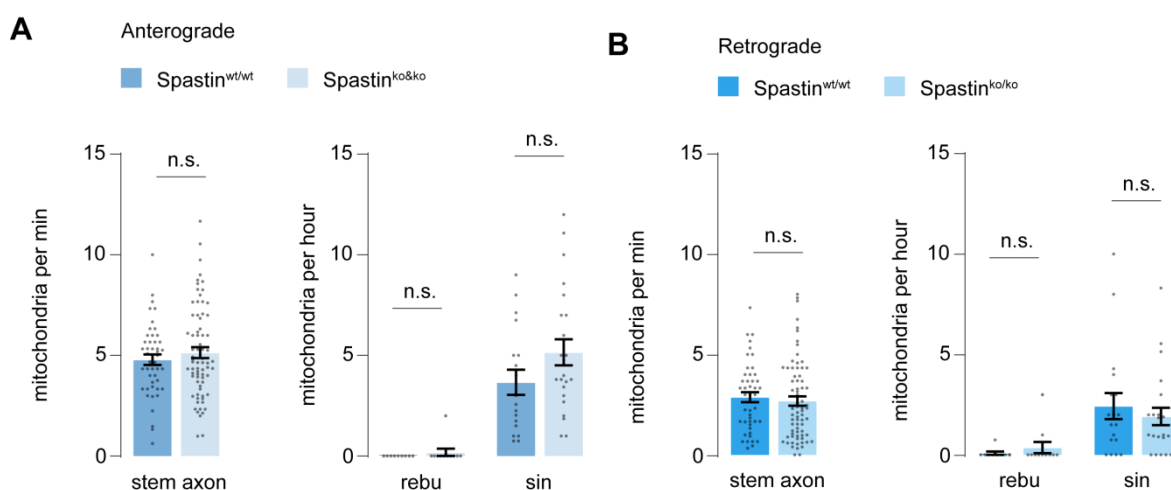
Figure 3.5 | Effect on mitochondrial transport by genetic stabilization of microtubules.
Anterograde (**A**) and retrograde (**B**) mitochondrial transport rates in axons of intercostal nerves ('stem axon'; n ≥ 47 axons, n ≥ 6 pups), as well as retraction bulbs ('rebu'; n ≥ 9 axon branches, n ≥ 9 mice) or singly-innervating terminal branches ('sin'; n ≥ 18 axons, ≥ 11 mice) in spastin$^{ko/ko}$ x *Thy1*-mitoCFP^K mice. Bar graphs are mean ± s.e.m. Mann-Whitney-U test was used to determine significance; n.s.: p ≥ 0.05. Dataset was acquired together with M. Brill (32 of 62 data points were acquired and analyzed by the author).

3.5. Decreased transport of mitolysosomes in CCP1/6 double-KO mice

Spastin is recruited to microtubules by polyglutamylation, which can be removed by the enzymes CCP (cytosolic carboxypeptidase) 1 and CCP6, amongst other enzymes. Thus, a CCP1 and CCP 6 double-knockout ('CCP1/6-dKO') would enhance the generation of glutamate side chains on microtubules (as was initially reported in cerebral cortex and hippocampus of these mice; Magiera et al., 2018) and therefore promote the microtubule-severing activity of spastin, potentially also leading to decreased axonal transport. Since CCP1 was also reported to interact with Parkin, a mitophagy mediator, (Gilmore-Hall et al., 2019) we decided to use a tool which would allow us to measure axonal transport of both mitochondria and mitolysosomes concurrently (COXVIII (mito)-Keima under a human synapsin promotor, see Material and Methods; experiments were performed in collaboration with A. Gavoci and Dr. M. Wang). Keima has an excitation spectrum that depends on pH, meaning that in a neutral environment (such as is present in a healthy mitochondrion or a mitophagosome) it has an excitation optimum at shorter wavelengths (440 nm, Keima-'green') than in an acidic environment (586 nm, such as is present in a mitolysosome, i.e. a lysosome with mitochondrial material inside, 'Keima-red') (**Figure 3.6, A, B**) (Katayama, Kogure, Mizushima, Yoshimori, & Miyawaki, 2011).
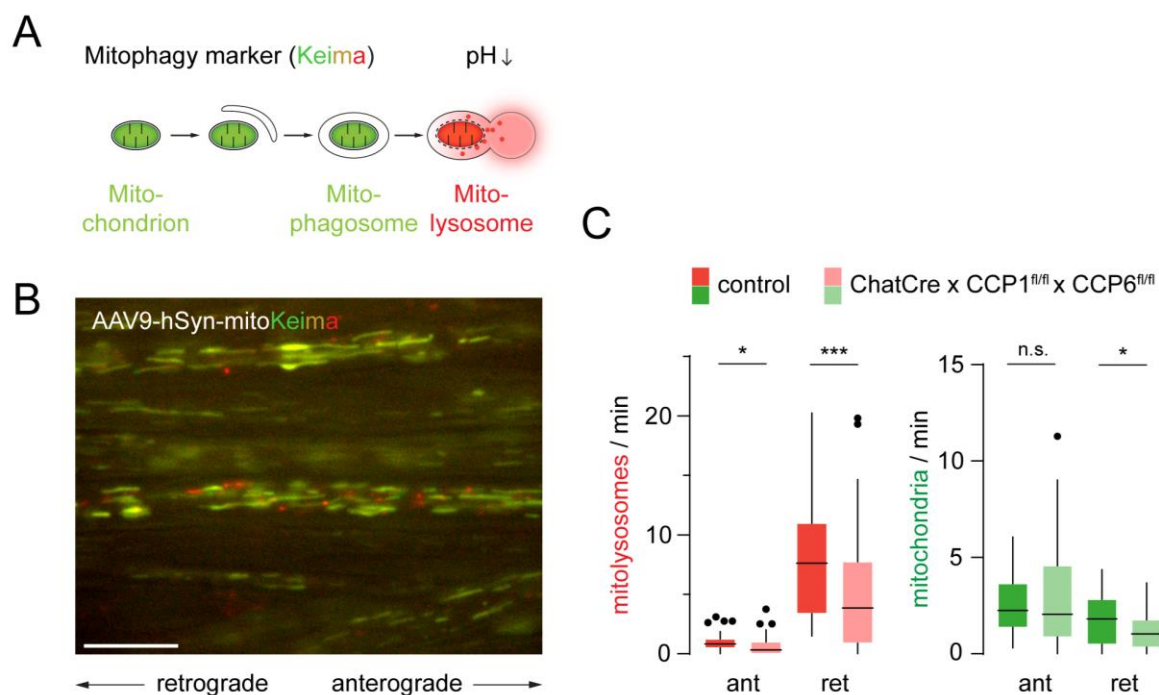
Figure 3.6 | Transport of mitolysosomes in a CCP1 and CCP6 double-knockout.

(**A**) Keima is a fluorophore that shifts its excitation optimum according to pH. Mitochondria / mitophagosomes are depicted here in green (neutral pH), mitolysosomes in red (acidic pH). (**B**) Intercostal nerve of a mouse injected with an AAV9-hSyn-mitoKeima virus. Scale bar 10 µm. (**C**) Mitolysosome (Keima-red) transport rates compared between a control (ChatCre- x CCP1 x CCP6 littermate) and a CCP1/6-dKO mouse (specifically, a ChatCre+ x CCP1$^{fl/fl}$ x CCP6$^{fl/fl}$) (n ≥ 34 axons from 3 mice per group). Mann-Whitney test; *** P < 0.001; * P < 0.05; n.s. = non-significant. Performed in collaboration with A. Gavoci (15 of 86 axons were imaged and 86 of 86 data points were analyzed by the author).

The transport rates of mitolysosomes were reduced in the CCP1/6-dKO in both anterograde and retrograde direction (**Figure 3.6, C**; ant/ctr: 0.95 ± 0.13/min; ant/ctr: 0.67 ± 0.13/min; ret/ctr: 8.41 ± 0.84/min; ret/ctr: 4.82 ± 0.70/min). In contrast, transport of mitochondria (Keima-green) was less strongly affected, with only retrograde transport rates being significantly decreased (ant/ctr: 2.45 ± 0.25/min; ant/ctr: 2.77 ± 0.38/min; ret/ctr: 1.81 ± 0.21/min; ret/ctr: 1.18 ± 0.14/min).

Similarly, the movement parameters of mitolysosomes were profoundly altered – mitolysosomes had both slower running speeds and paused longer and more often in the CCP1/6-dKO (preliminary analysis, **Figure 3.7**). Conversely, run length was not significantly different in the CCP1/6-dKO (preliminary analysis, **Figure 3.7**).

In summary, mitolysosome transport rates are reduced in the CCP1/6-double-KO, these organelles also move more slowly and pause more frequently. This effect could be a consequence of either altered microtubule stability (spastin activation) or altered PTM profile of the microtubules. Therefore, to interpret these data one must see them in conjunction with stainings that label microtubule content and PTMs (see discussion, **section 4.4**).
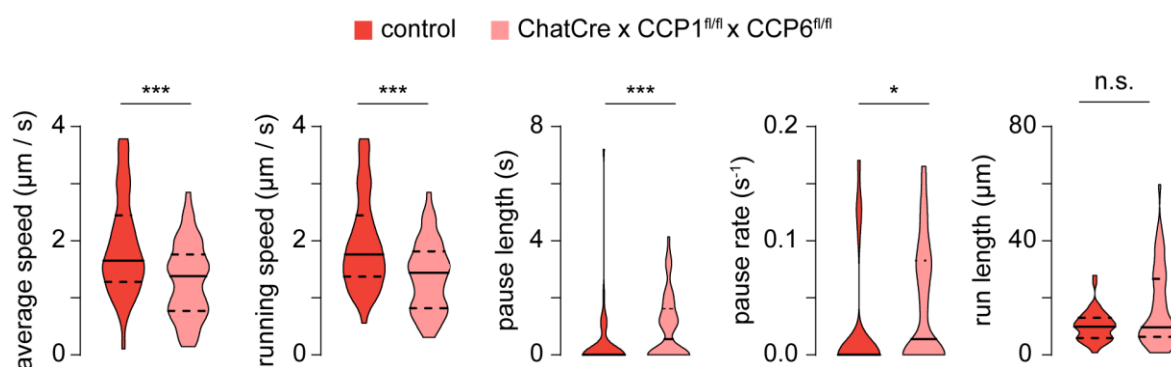

Figure 3.7 | MitoKeima-red movement parameters in intercostal nerve axons from CCP1/6 double-KO mice.
Quantification of different movement parameters from axonal mitoKeima-red puncta moving in retrograde direction (n ≥ 45 mitoKeima-red puncta from 1 mouse per group). *t*-test was used in datasets which passed the D'Agostino & Pearson normality test (average speed and running speed), otherwise a Mann-Whitney test was used to determine significance: *** $P < 0.001$; * $P < 0.05$; n.s. = non-significant. Performed in collaboration with A. Gavoci (movie files from the same experiment as in **Figure 3.6**; tracking and analysis was performed by the author).

4. DISCUSSION

During developmental synapse elimination, terminal branches of different motor axons compete for postsynaptic occupancy on the neuromuscular junction, until a 'winner' is chosen and the respective 'losers' disassemble (Sanes & Lichtman, 1999). Those 'loser' axons dismantle in a branch-specific manner, meaning that disassembly only occurs within that specific branch without affecting the parent axon (Bishop et al., 2004; Keller-Peck et al., 2001). How is this localized degradation of the axon executed on a molecular level? In the paper that I co-authored (Brill et al., 2016), it was shown for the first time that branch-specific axon removal is characterized by local microtubule disruptions that occur early on even before the 'losing' branches retract. It was further shown that microtubule disassembly is mediated by the disease-associated enzyme spastin (Brill et al., 2016). To understand the consequences of microtubule disassembly for the axon, I used various pharmacological and genetic tools to stabilize microtubules and study how microtubule stability affects axon retraction and axonal transport. Using live imaging in nerve muscle explants, I obtained the following results: (1) microtubule disassembly causes diminished transport of mitochondria in retraction bulbs (epothilone B experiment), (2) spastin mediates the retraction speed of dying branches, but probably lacks an effect on axonal transport, and (3) a knock-out of two deglutamylation enzymes (CCP1 and 6), which presumably would lead to spastin activation and microtubule disassembly, negatively regulates axonal transport.

4.1. Microtubule destabilization and organelle transport during synapse elimination

In Brill et al. (2016), my colleagues M. Brill and M. Reuter found that mitochondrial transport inversely correlates with relative occupancy on the postsynapse. Specifically, branches that occupied 40 % or less synaptic territory ('losing' axons and retraction bulbs; Walsh & Lichtman, 2003) largely lacked transport, unlike branches with more than 60 % synaptic territory ('winning' axons and singly-innervating branches; Walsh & Lichtman, 2003). Those disruptions in transport affected both directions (anterograde and retrograde), thereby suggesting they might be caused by branch-specific disruption of the cytoskeleton, which provides the routes for intracellular transport (Hirokawa, 1998). An earlier study (Bishop et al., 2004) found that microtubules were absent in 'loser' branches that were beginning to retract (retraction bulbs), however, it was unclear if these changes were a late phenomenon or whether they had an early, instructive role. My colleague M. Brill showed that branches which were more likely to lose (1 – 40 % territory) had significantly decreased tubulin content compared to branches which were more likely to win competition (61 – 99 % territory), arguing that microtubule disruptions occur early on even before the branch starts to retract. (Brill et al., 2016)

Combined together, these results showed that disruption in the microtubule skeleton and axonal transport occur in parallel, but they did not prove a causal relationship between the two. Mitochondria can also traverse small distances on actin (Chada & Hollenbeck, 2004) (the possibility that actin rearrangement is involved in synapse elimination is currently being explored by A. Gavoci and M. Brill through efforts to generate a reporter mouse line). Further, synaptic activity and the action of a neurotrophin (BDNF) positively regulate the outcome of competition (Je et al., 2013; Personius & Balice-Gordon, 2002; F.

Yang et al., 2009) and both can recruit mitochondria to synapses by interaction with the mitochondrial transport machinery (Lin & Sheng, 2015; Su, Ji, Sun, Liu, & Chen, 2014; Yoshii & Constantine-Paton, 2010).

In my experiments using the microtubule-stabilizing drug epothilone B, I observed that mitochondrial transport was partially restored in retraction bulbs (by 10.8-fold in anterograde direction, **Figure 3.2**). Mitochondrial transport also increased in singly-innervating branches, but the effect was less pronounced (1.3-fold, **Figure 3.2**). Those results imply that microtubule disassembly is partially responsible for the breakdown of transport observed in retraction bulbs.

This dataset further showed that while in the normal (control) situation, mitochondrial transport rates were extremely different between retraction bulbs and singly innervating branches (63-fold, **Figure 3.2**), this difference was not as pronounced after epothilone B treatment (8-fold, numbers for anterograde transport, **Figure 3.2**). Other publications looking at synaptic activity have shown that rather than depending on absolute electrical signals, synapse elimination is controlled by the relative difference between inputs (Balice-Gordon & Lichtman, 1994). My results suggest that synapse elimination also slows down in a situation where axonal transport is more similar between inputs. One could test this idea, e.g. by locally depolymerizing microtubules of either one or both inputs with photo-switchable drugs to affect transport rate, and then observing the outcome or rate of synapse elimination.

Those experiments did not, however, answer which vital resource it is that might affect competitive vigor. Microtubule disruption probably not only affects mitochondrial transport, but also transport of other organelles, RNAs, proteins or vesicles. At least

peroxisomal transport appeared decreased in retraction bulbs (Brill et al., 2016). Since many cargoes are transported by specific anterograde machinery (Hirokawa et al., 2010; Maday et al., 2014), manipulating specific motor(/adaptor) proteins would give further insight into which cargo transport influences synapse elimination.

Further, mitochondrial transport rates in retraction bulbs were not 'rescued' by epothilone B to match the levels observed in singly innervating branches (**Figure 3.2**). Why is that so? The absolute amount of mitochondria that traverses an axonal branch would depend on several factors, one of which is the amount of 'tracks' available. Experiments by M. Brill showed that tubulin content was not completely restored (Brill et al., 2016), which would explain why transport was only partially affected. A complete recovery was also not expected from a pharmacological intervention, which acts only during a limited time window.

4.2. Mitochondrial tracking in dismantling axon branches

The absolute transport rate (flux) of mitochondria is determined by various factors, such as the average speed of the individual organelles, but also the overall number of mitochondria present in the compartment of interest (Devireddy, Sung, Liao, Garland-Kuntz, & Hollenbeck, 2014). For example, slower mitochondria result in lower flux, but flux can also decrease if mitochondrial density is low, irrespective of average mitochondrial speed (Devireddy et al., 2014). Average speed is not constant but rather depends on how often and long mitochondria pause and how fast they are during runs (Hollenbeck, 1996), and these so-called movement parameters can be affected by alteration to the microtubule cytoskeleton (Yogev et al., 2016).

For example, a study by Yogev et al. (2016) showed that moving synaptic vesicle precursors (SVPs) paused at microtubule ends and that pause durations inversely correlated with microtubule coverage (Yogev et al., 2016). In our setting, I observed longer mitochondrial pause durations in retraction bulbs than in singly innervating axons (**Figure 3.3**), indicative of lower microtubule coverage in retraction bulbs. After stabilization of microtubules with epothilone B, average pause durations dropped in retraction bulbs (from 39 to 8 sec), suggesting that epothilone B increased microtubule content in retraction bulbs. Thus, my results are in agreement with measurements of tubulin content by immunostaining (Brill et al., 2016).

In retraction bulbs, mitochondria moved with half of their speed during 'runs' when compared to singly innervating branches (0.2 and 0.4 µm/s, respectively, **Figure 3.3**). The running speed of an organelle depends on various factors, among them motor protein processivity as well as the total number of bound motors. Processivity of a motor can be regulated by microtubule-binding proteins (e.g., tau), scaffolding proteins and posttranslational modifications (PTMs) on the microtubule (Maday et al., 2014). Kinesin-1 preferentially moves on detyrosinated (Dunn et al., 2008; Kaul et al., 2014; Konishi & Setou, 2009; Kreitzer et al., 1999; Liao & Gundersen, 1998) and polyglutamylated microtubules (Sirajuddin et al., 2014). PTMs such as polyglutamylation and detyrosination accumulate on more stable microtubules (Baas et al., 2016), as would be expected of singly-innervating branches. My results therefore indicate that decreased levels of PTMs such as polyglutamylation or detyrosination might lead to slower running speed in retraction bulbs. Indeed, immunostainings showed retraction bulbs have lower amounts of detyrosinated and polyglutamylated microtubules than singly innervating branches (Brill et

al., 2016) (the latter however was not be shown to increase transport in cells; Gilmore-Hall et al., 2019; Maas et al., 2009).

While epothilone B had profound effects in retraction bulbs, it did not affect the movement parameters in singly innervating branches, even though tubulin content increased here as well (Brill et al., 2016). For example, pause durations showed a small but non-significant decrease from 13 to 9 sec in singly-innervating branches (**Figure 3.3**). This might be due to the following reasons:

- *Imaging parameters:* It is possible that an effect on average pause duration was partially masked, since these movies were acquired with a relatively low sampling rate (0.5 Hz), which would hide small pauses < 2 s. A control using faster imaging would have to be performed. (Wehnekamp, Plucinska, Thong, Misgeld, & Lamb, 2019)

- *PTMs:* Epothilone B might affect PTMs differentially in retraction bulbs and singly-innervating branches, which would affect the processivity of motors (we have not tested this possibility by immunostaining yet).

- *Non-linear relationship between microtubule content and movement parameters:* A linear relationship between microtubule coverage and transport parameters has not been shown so far. Above a certain, physiological threshold, microtubules might even aggregate or reverse polarity and not be available for axonal transport as effectively anymore (Baas & Ahmad, 2013; Theiss & Meller, 2000). Thus, if there are no more cargoes and speed is optimized, flux will plateau – only when track availability is the limiting factor, microtubule stabilization will affect flux. In our setting, tubulin content shows a similar fold-increase in retraction bulbs and singly-

innervating branches following epothilone B application (Brill et al., 2016), but axonal transport is much more affected in retraction bulbs (**Figure 3.2**, **Figure 3.3**).

4.3.   Role of spastin during synapse elimination

In Brill et al. (2016) we showed that spastin mediates branch-specific microtubule destabilization in losing branches, which delays the time course of synapse elimination (Brill et al., 2016) and slows down the retraction of 'loser' branches (**Figure 3.4**). Even though microtubule disassembly is common in various forms of pruning in *Drosophila* (mediated for example by Kat60L and Kif2A; Lee et al., 2009; Maor-Nof et al., 2013), the implication of spastin in this setting is new. Spastin is a good candidate in mammalian neurons, since it localizes to branch points (Errico et al., 2004; W. Yu et al., 2008), and unlike katanin, remains highly expressed even after developing neurons have initially contacted their targets (Karabay, Yu, Solowska, Baird, & Baas, 2004; D. L. Ma et al., 2006). This study also elevates spastin beyond its early function in development, where it cuts microtubules to generate amplification seeds during axonal and dendritic branch formation (Conde & Caceres, 2009; Roll-Mecak & Vale, 2006). It remains to be shown if spastin also mediates postnatal pruning in the central nervous system.

To understand how spastin influences transport during synapse elimination, I also acquired a dataset on mitochondrial transport rates ($n \geq 9$ axons). Here, I saw a (non-significant) increase of mitochondrial transport in retraction bulbs (Ant: from 0 to 0.2 mito/h; Ret: from 0.1 to 0.4 mito/h; **Figure 3.5**). Overall, the difference was not as pronounced as in the epothilone B experiment (Ant: from ~ 0.2 to 0.7 mito/h; Ret: ~ 0 to 0.7 mito/h; $n \geq 20$ axons; **Figure 3.2**). It appears that the spastin-KO results in a weaker

kind of microtubule stabilization than epothilone B, since the EB3-density/tubulin content-ratio was changed less (indicative of microtubule length, see **section 1.1.3. "Microtubule-associated proteins"**) (Brill et al., 2016). Together with the fact that synapse elimination is only delayed and not completely abolished, the results suggests that other mechanisms exist which influence microtubule mass and length during synapse elimination; for example, katanin and kinesin-13 could compensate for spastin-dependent microtubule dynamics (Havlicek et al., 2014; Kurup, Yan, Goncharov, & Jin, 2015).

4.4.   Impact of microtubule glutamylation on axonal transport

Our combined results raised the question how spastin was able to act in losing braches in such a locally confined manner. Spastin recruitment to microtubules is enhanced by polyglutamylation (Lacroix et al., 2010; Valenstein & Roll-Mecak, 2016) and preliminary immunostainings showed that in the spastin-KO, polyglutamylation levels are higher in retraction bulbs than singly-innervating branches (Monika Brill, personal communication, on 15th January 2020).

My colleagues A. Gavoci and M. Brill are currently performing a follow-up study, where they investigate a CCP1 and CCP6-double-KO mouse ('CCP1/6-dKO') in the context of synapse elimination. In theory, this knockout would result in an increase of polyglutamylation on microtubules (Magiera et al., 2018) and thus increased microtubule-severing activity by spastin (Valenstein & Roll-Mecak, 2016). In the knockout, they could find that tubulin content was diminished; however, the microtubules were rather hypoglutamylated and longer (measured by EB3/tubulin ratio), presumably because those were the microtubules that were left after spastin has done its job and cut away the others

(Monika Brill and Antoneta Gavoci, personal communication on 15th January 2020). A previous study by Yogev et al. (2016) has shown that run length of cargo correlates with microtubule length; therefore, the finding that microtubules are longer could be corroborated by measuring run length of transported organelles in the CCP1/6-dKO in the future (ongoing dataset, see **Figure 3.7** for preliminary results from mitoKeima-red puncta, which correspond to lysosomes or endosome containing mitochondrial material).

Glutamylation has been described in the literature to affect axonal transport (Gilmore-Hall et al., 2019; Maas et al., 2009; Magiera et al., 2018; Sirajuddin et al., 2014), but so far no studies have been performed *in vivo* to understand the relationship. We are currently investigating how transport of different organelles is affected in the CCP1/6-dKO. My count of mitoKeima-red transport rates shows that flux is decreased in the CCP1/6-dKO (**Figure 3.6**). This indicates that either, (1) CCP1 or 6 have a function in the generation of Keima-red puncta (initial analysis of other substrates than tubulin did not imply proteins with a well-known role in lysosomal degradation, see Rogowski et al. (2010), however, a later study implied an interaction between parkin and CCP1, see Gilmore-Hall et al. (2019)), (2) in initiating transport, (3) or in promoting cargo transport while on the microtubule. Indeed, tracking revealed that Keima-red puncta have slower running speeds and pause more frequently in the CCP1/6-dKO (**Figure 3.7**). The interpretation of the data is complicated by the fact that presumably, most of the hyperglutamylated microtubules generated by this knockout would be 'cut away' by microtubule-severing enzymes. It is not clear yet what the identity of the left-over, elongated microtubules is, for example, they might correspond to the polyaminated, "cold-stable" fraction that has been shown before to exist in brain tissue (Song et al., 2013). A stable population of microtubules could

accumulate microtubule-associated factors (like tau) that hinder transport (Dixit, Ross, Goldman, & Holzbaur, 2008).

Surprisingly, the transport rates of mitoKeima-green puncta (corresponding to "normal" mitochondria and mitophagosomes) were less affected, with only the retrograde flux being slightly decreased (**Figure 3.6**). This could mean that either different motor proteins are not affected in the same manner, or that mitochondria as large cargoes might be less affected by small changes in microtubule architecture, since they are able to move on multiple microtubules simultaneously (Hirokawa, 1982).

4.5.   Lessons from developmental axon remodeling for axon pathology

Rearrangements in the cytoskeleton are increasingly being recognized as important elements of neuronal development and plasticity, but also of neuronal pathology and axon death (Cartelli et al., 2013; Coleman, 2005; Jaworski et al., 2009; L. Luo & O'Leary, 2005; J. T. Wang et al., 2012). Stabilization of microtubules is seen as an option to mitigate axon pathology, and microtubule-stabilizing drugs such as epothilones are currently being explored as potential treatments (Baas & Ahmad, 2013; Ruschel et al., 2015; Varidaki et al., 2018). For example, microtubule-stabilizing drugs prevent the formation of retraction bulbs that form on lesioned corneal nerve or CNS axons (Erturk, Hellal, Enes, & Bradke, 2007; H. Wang et al., 2018). Those retraction bulbs resemble the ones that form on pruning axons during development (Misgeld, 2005). Microtubules serve as tracks for axonal transport (Hirokawa et al., 2010), and the organization and stability of microtubules affects axonal transport (Baas & Ahmad, 2013; Kapitein & Hoogenraad, 2015; Yogev et al., 2016). Indeed, studies using epothilone treatment for different disease models such as

models of Alzheimer's disease or intracerebral hemorrhage found signs of enhanced axonal

transport accompanying better regeneration (Y. Yang et al., 2018; B. Zhang et al., 2012).

My own results from developmental pruning demonstrate that a (relatively low) dose of

epothilone B is able to increase mitochondrial transport in a way that affects 'dying'

branches the most (**Figure 3.2**). These findings also raise an interesting question, namely

whether increasing axonal transport alone could have a beneficial effect during and after

axon degeneration. Other studies specifically increased mitochondrial transport by

targeting mitochondrial anchoring or transport proteins and found that it indeed facilitated

regeneration after acute axon injury (Cartoni et al., 2016; Han, Baig, & Hammarlund,

2016; Zhou et al., 2016). Those results suggest approaches that increase (mitochondrial)

axonal transport as a promising option to protect degenerating axons and promote neuronal

repair, however, this assumption would still have to be tested for models of (chronic)

neurodegenerative disease. Further, not all forms of axon degeneration have a preceding

phase of transport disruption (Marinkovic et al., 2012), so that it remains to be better

understood how axonal transport can modulate disease in different models.

In our model of developmental remodeling at the neuromuscular junction, spastin

seemed to play a role in disassembling microtubules of 'dying' axon branches (**Figure

3.4**). Spastin mutations are the most common cause of hereditary spastic paraplegia (HSP;

Hazan et al., 1999; Schule et al., 2016), a group of disorders where patients suffer from

lower extremity weakness, spasticity and gait impairment (Fink, 2013). Spastin cuts

microtubules, which can result in either microtubule disassembly or proliferation (by

generating a higher number of microtubule 'seeds') (McNally & Roll-Mecak, 2018). It is

still unclear which of the two scenarios underlies the pathology of HSP patients with

spastin mutations, or even whether a different function of spastin (such as interaction with

the ER) (Park et al., 2010) mainly drives pathogenesis. For example, in our work on developmental disassembly of α-motoneuron axons, a spastin-KO increased tubulin density, apparently resulting in more stable microtubules (Brill et al., 2016), and delayed retraction bulb pruning (**Figure 3.4**). However, mice with a mutation in spastin show a degenerative phenotype in CNS axons, with focal swellings, microtubule disorganization and axonal transport impairment (Fassier et al., 2013; Kasher et al., 2009; Tarrade et al., 2006). Interestingly, the authors of the spastin-mutated mice found accumulations of detyrosinated tubulin, tau and Δ2-tubulin in axon swellings, indicative of longer-lived, stable microtubules (Fassier et al., 2013; Tarrade et al., 2006). Further work will need to be done in order to understand how HSP-causing spastin mutations alter the function and organization of the microtubule cytoskeleton in different neuronal populations. In addition, how spastin (mal)function affects posttranslational microtubule modifications and axonal transport will further need to be studied in appropriate human and *in vivo* mouse models to help our understanding of the underlying pathogenesis in the future.

5. ACKNOWLEDGEMENTS

fostering my early passion in biology, and most of all, my parents, without whom I would have nothing at all – my thanks to you is beyond words.

6. LIST OF ABBREVIATIONS

ACh	acetylcholine
AChR	acetylcholine receptor
ATP	adenosine triphosphate
αTAT1	α-Tubulin acetyltransferase 1
BDNF	brain-derived neurotrophic factor
Ca^{2+}	Calcium-ions
CAMSAPs	calmodulin-regulated spectrin-associated proteins
CCP	cytosolic carboxypeptidase
CFP	cyan fluorescent protein
CLIP	cytoplasmic linker protein
CNS	central nervous system
Ctr	control group
DCX	doublecortin
EB1, 2, or 3	end-binding protein 1, 2, or 3
EM	electron microscopy
Epo	epothilone B-treated group
ER	endoplasmic reticulum
GDP	guanosine diphosphate
GTP	guanosine triphosphate
HDAC6	histone deacetylase family member 6
HSP	hereditary spastic paraplegia
IQR	interquartile range
KHC	kinesin heavy chain
KIF	kinesin superfamily
KO	knockout
Lis1	lissencephaly 1 (protein)
MAP	microtubule-associated protein
mRNA	messenger ribonucleic acid
MT	microtubule

n	sample size
NMJ	neuromuscular junction
PEG	Polyethylene glycol
PTM	posttranslational modification
rebu	retraction bulb
sem	standard error of the mean
sin	singly innervating branch
Sirt2	sirtuin type 2
+TIPs	microtubule plus-end/positive-end tracking proteins
TTL	tubulin tyrosine ligase
TTLL	TTL-like protein
WT	wildtype
YFP	yellow fluorescent protein

7. LIST OF FIGURES

8. LIST OF TABLES

9. REFERENCES

Adalbert, R., & Coleman, M. P. (2013). Review: Axon pathology in age-related neurodegenerative disorders. *Neuropathol Appl Neurobiol, 39*(2), 90-108. doi:10.1111/j.1365-2990.2012.01308.x

Aher, A., & Akhmanova, A. (2018). Tipping microtubule dynamics, one protofilament at a time. *Curr Opin Cell Biol, 50*, 86-93. doi:10.1016/j.ceb.2018.02.015

Aillaud, C., Bosc, C., Peris, L., Bosson, A., Heemeryck, P., Van Dijk, J., Le Friec, J., Boulan, B., Vossier, F., Sanman, L. E., Syed, S., Amara, N., Coute, Y., Lafanechere, L., Denarier, E., Delphin, C., Pelletier, L., Humbert, S., Bogyo, M., Andrieux, A., Rogowski, K., & Moutin, M. J. (2017). Vasohibins/SVBP are tubulin carboxypeptidases (TCPs) that regulate neuron differentiation. *Science, 358*(6369), 1448-1453. doi:10.1126/science.aao4165

Akella, J. S., Wloga, D., Kim, J., Starostina, N. G., Lyons-Abbott, S., Morrissette, N. S., Dougan, S. T., Kipreos, E. T., & Gaertig, J. (2010). MEC-17 is an alpha-tubulin acetyltransferase. *Nature, 467*(7312), 218-222. doi:10.1038/nature09324

Akhmanova, A., & Hoogenraad, C. C. (2005). Microtubule plus-end-tracking proteins: mechanisms and functions. *Curr Opin Cell Biol, 17*(1), 47-54. doi:10.1016/j.ceb.2004.11.001

Akhmanova, A., & Hoogenraad, C. C. (2015). Microtubule minus-end-targeting proteins. *Curr Biol, 25*(4), R162-171. doi:10.1016/j.cub.2014.12.027

Akhmanova, A., & Steinmetz, M. O. (2008). Tracking the ends: a dynamic protein network controls the fate of microtubule tips. *Nat Rev Mol Cell Biol, 9*(4), 309-322. doi:10.1038/nrm2369

Akhmanova, A., & Steinmetz, M. O. (2011). Microtubule end binding: EBs sense the guanine nucleotide state. *Curr Biol, 21*(8), R283-285. doi:10.1016/j.cub.2011.03.023

Akhmanova, A., & Steinmetz, M. O. (2015). Control of microtubule organization and dynamics: two ends in the limelight. *Nat Rev Mol Cell Biol, 16*(12), 711-726. doi:10.1038/nrm4084

Alexander, J. E., Hunt, D. F., Lee, M. K., Shabanowitz, J., Michel, H., Berlin, S. C., MacDonald, T. L., Sundberg, R. J., Rebhun, L. I., & Frankfurter, A. (1991). Characterization of posttranslational modifications in neuron-specific class III beta-tubulin by mass spectrometry. *Proc Natl Acad Sci U S A, 88*(11), 4685-4689.

Allen, R. D., Metuzals, J., Tasaki, I., Brady, S. T., & Gilbert, S. P. (1982). Fast axonal transport in squid giant axon. *Science, 218*(4577), 1127-1129.

Allison, R., Edgar, J. R., Pearson, G., Rizo, T., Newton, T., Gunther, S., Berner, F., Hague, J., Connell, J. W., Winkler, J., Lippincott-Schwartz, J., Beetz, C., Winner, B., & Reid, E. (2017). Defects in ER-endosome contacts impact lysosome function in hereditary spastic paraplegia. *J Cell Biol, 216*(5), 1337-1355. doi:10.1083/jcb.201609033

Argarana, C. E., Barra, H. S., & Caputto, R. (1978). Release of [14C]tyrosine from tubulinyl-[14C]tyrosine by brain extract. Separation of a carboxypeptidase from tubulin-tyrosine ligase. *Mol Cell Biochem, 19*(1), 17-21.

Azzouz, M., Leclerc, N., Gurney, M., Warter, J. M., Poindron, P., & Borg, J. (1997). Progressive motor neuron impairment in an animal model of familial amyotrophic lateral sclerosis. *Muscle Nerve, 20*(1), 45-51.

Baas, P. W., & Ahmad, F. J. (2013). Beyond taxol: microtubule-based treatment of disease and injury of the nervous system. *Brain, 136*(Pt 10), 2937-2951. doi:10.1093/brain/awt153

Baas, P. W., Deitch, J. S., Black, M. M., & Banker, G. A. (1988). Polarity orientation of microtubules in hippocampal neurons: uniformity in the axon and nonuniformity in the dendrite. *Proc Natl Acad Sci U S A, 85*(21), 8335-8339.

Baas, P. W., Rao, A. N., Matamoros, A. J., & Leo, L. (2016). Stability properties of neuronal microtubules. *Cytoskeleton (Hoboken), 73*(9), 442-460. doi:10.1002/cm.21286

Bagust, J., Lewis, D. M., & Westerman, R. A. (1973). Polyneuronal innervation of kitten skeletal muscle. *J Physiol, 229*(1), 241-255.

Balice-Gordon, R. J., Chua, C. K., Nelson, C. C., & Lichtman, J. W. (1993). Gradual loss of synaptic cartels precedes axon withdrawal at developing neuromuscular junctions. *Neuron, 11*(5), 801-815.

Balice-Gordon, R. J., & Lichtman, J. W. (1990). In vivo visualization of the growth of pre- and postsynaptic elements of neuromuscular junctions in the mouse. *J Neurosci, 10*(3), 894-908.

Balice-Gordon, R. J., & Lichtman, J. W. (1993). In vivo observations of pre- and postsynaptic changes during the transition from multiple to single innervation at developing neuromuscular junctions. *J Neurosci, 13*(2), 834-855.

Balice-Gordon, R. J., & Lichtman, J. W. (1994). Long-term synapse loss induced by focal blockade of postsynaptic receptors. *Nature, 372*(6506), 519-524. doi:10.1038/372519a0

Balint, S., Verdeny Vilanova, I., Sandoval Alvarez, A., & Lakadamyali, M. (2013). Correlative live-cell and superresolution microscopy reveals cargo transport dynamics at microtubule intersections. *Proc Natl Acad Sci U S A, 110*(9), 3375-3380. doi:10.1073/pnas.1219206110

Barber, M. J., & Lichtman, J. W. (1999). Activity-driven synapse elimination leads paradoxically to domination by inactive neurons. *J Neurosci, 19*(22), 9975-9985.

Bennett, M. R., & Pettigrew, A. G. (1974). The formation of synapses in striated muscle during development. *J Physiol, 241*(2), 515-545.

Berezniuk, I., Vu, H. T., Lyons, P. J., Sironi, J. J., Xiao, H., Burd, B., Setou, M., Angeletti, R. H., Ikegami, K., & Fricker, L. D. (2012). Cytosolic carboxypeptidase 1 is involved in processing alpha- and beta-tubulin. *J Biol Chem, 287*(9), 6503-6517. doi:10.1074/jbc.M111.309138

Bianchi, L. (2018). *Developmental neurobiology*. New York, NY: Garland Science, Taylor & Francis Group, LLC.

Bieling, P., Kandels-Lewis, S., Telley, I. A., van Dijk, J., Janke, C., & Surrey, T. (2008). CLIP-170 tracks growing microtubule ends by dynamically recognizing composite EB1/tubulin-binding sites. *J Cell Biol, 183*(7), 1223-1233. doi:10.1083/jcb.200809190

Bishop, D. L., Misgeld, T., Walsh, M. K., Gan, W. B., & Lichtman, J. W. (2004). Axon branch removal at developing synapses by axosome shedding. *Neuron, 44*(4), 651-661. doi:10.1016/j.neuron.2004.10.026

Boston-University-Research-Support. (Retrieved on 31.03.2020 from https: // www .bu.edu/ researchsupport/ compliance/ animal-care/ working-with-animals/ research/ sample-size-calculations-iacuc/). Sample Size Calculations (IACUC).

Bourgeois, J. P., & Rakic, P. (1993). Changes of synaptic density in the primary visual cortex of the macaque monkey from fetal to adult stage. *J Neurosci, 13*(7), 2801-2820.

Brady, S. T., Lasek, R. J., & Allen, R. D. (1982). Fast axonal transport in extruded axoplasm from squid giant axon. *Science, 218*(4577), 1129-1131.

Brickley, K., & Stephenson, F. A. (2011). Trafficking kinesin protein (TRAK)-mediated transport of mitochondria in axons of hippocampal neurons. *J Biol Chem, 286*(20), 18079-18092. doi:10.1074/jbc.M111.236018

Brill, M. S., Kleele, T., Ruschkies, L., Wang, M., Marahori, N. A., Reuter, M. S., Hausrat, T. J., Weigand, E., Fisher, M., Ahles, A., Engelhardt, S., Bishop, D. L., Kneussel, M., & Misgeld, T. (2016). Branch-Specific Microtubule Destabilization Mediates Axon Branch Loss during Neuromuscular Synapse Elimination. *Neuron*. doi:10.1016/j.neuron.2016.09.049

Brown, M. C., Jansen, J. K., & Van Essen, D. (1976). Polyneuronal innervation of skeletal muscle in new-born rats and its elimination during maturation. *J Physiol, 261*(2), 387-422.

Brunden, K. R., Yao, Y., Potuzak, J. S., Ferrer, N. I., Ballatore, C., James, M. J., Hogan, A. M., Trojanowski, J. Q., Smith, A. B., 3rd, & Lee, V. M. (2011). The characterization of microtubule-stabilizing drugs as possible therapeutic agents for Alzheimer's disease and related tauopathies. *Pharmacol Res, 63*(4), 341-351. doi:10.1016/j.phrs.2010.12.002

Buffelli, M., Burgess, R. W., Feng, G., Lobe, C. G., Lichtman, J. W., & Sanes, J. R. (2003). Genetic evidence that relative synaptic efficacy biases the outcome of synaptic competition. *Nature, 424*(6947), 430-434. doi:10.1038/nature01844

Busetto, G., Buffelli, M., Tognana, E., Bellico, F., & Cangiano, A. (2000). Hebbian mechanisms revealed by electrical stimulation at developing rat neuromuscular junctions. *J Neurosci, 20*(2), 685-695.

Callaway, E. M., Soha, J. M., & Van Essen, D. C. (1987). Competition favouring inactive over active motor neurons during synapse elimination. *Nature, 328*(6129), 422-426. doi:10.1038/328422a0

Cao, L., Dhilla, A., Mukai, J., Blazeski, R., Lodovichi, C., Mason, C. A., & Gogos, J. A. (2007). Genetic modulation of BDNF signaling affects the outcome of axonal competition in vivo. *Curr Biol, 17*(11), 911-921. doi:10.1016/j.cub.2007.04.040

Caplow, M., & Shanks, J. (1996). Evidence that a single monolayer tubulin-GTP cap is both necessary and sufficient to stabilize microtubules. *Mol Biol Cell, 7*(4), 663-675.

Cartelli, D., Casagrande, F., Busceti, C. L., Bucci, D., Molinaro, G., Traficante, A., Passarella, D., Giavini, E., Pezzoli, G., Battaglia, G., & Cappelletti, G. (2013). Microtubule alterations occur early in experimental parkinsonism and the microtubule stabilizer epothilone D is neuroprotective. *Sci Rep, 3*, 1837. doi:10.1038/srep01837

Cartoni, R., Norsworthy, M. W., Bei, F., Wang, C., Li, S., Zhang, Y., Gabel, C. V., Schwarz, T. L., & He, Z. (2016). The Mammalian-Specific Protein Armcx1 Regulates Mitochondrial Transport during Axon Regeneration. *Neuron, 92*(6), 1294-1307. doi:10.1016/j.neuron.2016.10.060

Chada, S. R., & Hollenbeck, P. J. (2004). Nerve growth factor signaling regulates motility and docking of axonal mitochondria. *Curr Biol, 14*(14), 1272-1276. doi:10.1016/j.cub.2004.07.027

Chen, C., & Regehr, W. G. (2000). Developmental remodeling of the retinogeniculate synapse. *Neuron, 28*(3), 955-966.

Chen, Y., & Sheng, Z. H. (2013). Kinesin-1-syntaphilin coupling mediates activity-dependent regulation of axonal mitochondrial transport. *J Cell Biol, 202*(2), 351-364. doi:10.1083/jcb.201302040

Coleman, M. (2005). Axon degeneration mechanisms: commonality amid diversity. *Nat Rev Neurosci, 6*(11), 889-898. doi:10.1038/nrn1788

Colman, H., & Lichtman, J. W. (1993). Interactions between nerve and muscle: synapse elimination at the developing neuromuscular junction. *Dev Biol, 156*(1), 1-10. doi:10.1006/dbio.1993.1054

Colman, H., Nabekura, J., & Lichtman, J. W. (1997). Alterations in synaptic strength preceding axon withdrawal. *Science, 275*(5298), 356-361.

Conde, C., & Caceres, A. (2009). Microtubule assembly, organization and dynamics in axons and dendrites. *Nat Rev Neurosci, 10*(5), 319-332. doi:10.1038/nrn2631

Connell, J. W., Lindon, C., Luzio, J. P., & Reid, E. (2009). Spastin couples microtubule severing to membrane traffic in completion of cytokinesis and secretion. *Traffic, 10*(1), 42-56. doi:10.1111/j.1600-0854.2008.00847.x

Costanzo, E. M., Barry, J. A., & Ribchester, R. R. (2000). Competition at silent synapses in reinnervated skeletal muscle. *Nat Neurosci, 3*(7), 694-700. doi:10.1038/76649

de Forges, H., Bouissou, A., & Perez, F. (2012). Interplay between microtubule dynamics and intracellular organization. *Int J Biochem Cell Biol, 44*(2), 266-274. doi:10.1016/j.biocel.2011.11.009

De Vos, K. J., Grierson, A. J., Ackerley, S., & Miller, C. C. (2008). Role of axonal transport in neurodegenerative diseases. *Annu Rev Neurosci, 31*, 151-173. doi:10.1146/annurev.neuro.31.061307.090711

Del Castillo, J., & Katz, B. (1954). Quantal components of the end-plate potential. *J Physiol, 124*(3), 560-573.

Derr, N. D., Goodman, B. S., Jungmann, R., Leschziner, A. E., Shih, W. M., & Reck-Peterson, S. L. (2012). Tug-of-war in motor protein ensembles revealed with a programmable DNA origami scaffold. *Science, 338*(6107), 662-665. doi:10.1126/science.1226734

Devireddy, S., Liu, A., Lampe, T., & Hollenbeck, P. J. (2015). The Organization of Mitochondrial Quality Control and Life Cycle in the Nervous System In Vivo in the Absence of PINK1. *J Neurosci, 35*(25), 9391-9401. doi:10.1523/JNEUROSCI.1198-15.2015

Devireddy, S., Sung, H., Liao, P. C., Garland-Kuntz, E., & Hollenbeck, P. J. (2014). Analysis of mitochondrial traffic in Drosophila. *Methods Enzymol, 547*, 131-150. doi:10.1016/B978-0-12-801415-8.00008-4

Dixit, R., Ross, J. L., Goldman, Y. E., & Holzbaur, E. L. (2008). Differential regulation of dynein and kinesin motor proteins by tau. *Science, 319*(5866), 1086-1089. doi:10.1126/science.1152993

Dorkenwald, S., Schubert, P. J., Killinger, M. F., Urban, G., Mikula, S., Svara, F., & Kornfeld, J. (2017). Automated synaptic connectivity inference for volume electron microscopy. *Nat Methods, 14*(4), 435-442. doi:10.1038/nmeth.4206

Downing, K. H., & Nogales, E. (1998a). Tubulin and microtubule structure. *Curr Opin Cell Biol, 10*(1), 16-22.

Downing, K. H., & Nogales, E. (1998b). Tubulin structure: insights into microtubule properties and functions. *Curr Opin Struct Biol, 8*(6), 785-791.

Dunn, S., Morrison, E. E., Liverpool, T. B., Molina-Paris, C., Cross, R. A., Alonso, M. C., & Peckham, M. (2008). Differential trafficking of Kif5c on tyrosinated and detyrosinated microtubules in live cells. *J Cell Sci, 121*(Pt 7), 1085-1095. doi:10.1242/jcs.026492

Duxson, M. J. (1982). The effect of postsynaptic block on development of the neuromuscular junction in postnatal rats. *J Neurocytol, 11*(3), 395-408.

Edde, B., Rossier, J., Le Caer, J. P., Desbruyeres, E., Gros, F., & Denoulet, P. (1990). Posttranslational glutamylation of alpha-tubulin. *Science, 247*(4938), 83-85.

Encalada, S. E., Szpankowski, L., Xia, C. H., & Goldstein, L. S. (2011). Stable kinesin and dynein assemblies drive the axonal transport of mammalian prion protein vesicles. *Cell, 144*(4), 551-565. doi:10.1016/j.cell.2011.01.021

Erlich, Y., Edvardson, S., Hodges, E., Zenvirt, S., Thekkat, P., Shaag, A., Dor, T., Hannon, G. J., & Elpeleg, O. (2011). Exome sequencing and disease-network analysis of a single family implicate a mutation in KIF1A in hereditary spastic paraparesis. *Genome Res, 21*(5), 658-664. doi:10.1101/gr.117143.110

Errico, A., Claudiani, P., D'Addio, M., & Rugarli, E. I. (2004). Spastin interacts with the centrosomal protein NA14, and is enriched in the spindle pole, the midbody and the distal axon. *Hum Mol Genet, 13*(18), 2121-2132. doi:10.1093/hmg/ddh223

Erturk, A., Hellal, F., Enes, J., & Bradke, F. (2007). Disorganized microtubules underlie the formation of retraction bulbs and the failure of axonal regeneration. *J Neurosci, 27*(34), 9169-9180. doi:10.1523/JNEUROSCI.0612-07.2007

Faits, M. C., Zhang, C., Soto, F., & Kerschensteiner, D. (2016). Dendritic mitochondria reach stable positions during circuit development. *Elife, 5*, e11583. doi:10.7554/eLife.11583

Fanara, P., Husted, K. H., Selle, K., Wong, P. Y., Banerjee, J., Brandt, R., & Hellerstein, M. K. (2010). Changes in microtubule turnover accompany synaptic plasticity and memory formation in response to contextual fear conditioning in mice. *Neuroscience, 168*(1), 167-178. doi:10.1016/j.neuroscience.2010.03.031

Farrer, M. J., Hulihan, M. M., Kachergus, J. M., Dachsel, J. C., Stoessl, A. J., Grantier, L. L., Calne, S., Calne, D. B., Lechevalier, B., Chapon, F., Tsuboi, Y., Yamada, T., Gutmann, L., Elibol, B., Bhatia, K. P., Wider, C., Vilarino-Guell, C., Ross, O. A., Brown, L. A., Castanedes-Casey, M., Dickson, D. W., & Wszolek, Z. K. (2009). DCTN1 mutations in Perry syndrome. *Nat Genet, 41*(2), 163-165. doi:10.1038/ng.293

Fassier, C., Tarrade, A., Peris, L., Courageot, S., Mailly, P., Dalard, C., Delga, S., Roblot, N., Lefevre, J., Job, D., Hazan, J., Curmi, P. A., & Melki, J. (2013). Microtubule-targeting drugs rescue axonal swellings in cortical neurons from spastin knockout mice. *Dis Model Mech, 6*(1), 72-83. doi:10.1242/dmm.008946

Fellner, S., Bauer, B., Miller, D. S., Schaffrik, M., Fankhanel, M., Spruss, T., Bernhardt, G., Graeff, C., Farber, L., Gschaidmeier, H., Buschauer, A., & Fricker, G. (2002). Transport of paclitaxel (Taxol) across the blood-brain barrier in vitro and in vivo. *J Clin Invest, 110*(9), 1309-1318. doi:10.1172/JCI15451

Feng, G., Mellor, R. H., Bernstein, M., Keller-Peck, C., Nguyen, Q. T., Wallace, M., Nerbonne, J. M., Lichtman, J. W., & Sanes, J. R. (2000). Imaging neuronal subsets in transgenic mice expressing multiple spectral variants of GFP. *Neuron, 28*(1), 41-51.

Fink, J. K. (2013). Hereditary spastic paraplegia: clinico-pathologic features and emerging molecular mechanisms. *Acta Neuropathol, 126*(3), 307-328. doi:10.1007/s00401-013-1115-8

Fransson, A., Ruusala, A., & Aspenstrom, P. (2003). Atypical Rho GTPases have roles in mitochondrial homeostasis and apoptosis. *J Biol Chem, 278*(8), 6495-6502. doi:10.1074/jbc.M208609200

Gan, W. B., & Lichtman, J. W. (1998). Synaptic segregation at the developing neuromuscular junction. *Science, 282*(5393), 1508-1511.

George, E. B., Glass, J. D., & Griffin, J. W. (1995). Axotomy-induced axonal degeneration is mediated by calcium influx through ion-specific channels. *J Neurosci, 15*(10), 6445-6452.

Gill, S. R., Schroer, T. A., Szilak, I., Steuer, E. R., Sheetz, M. P., & Cleveland, D. W. (1991). Dynactin, a conserved, ubiquitously expressed component of an activator of vesicle motility mediated by cytoplasmic dynein. *J Cell Biol, 115*(6), 1639-1650.

Gilmore-Hall, S., Kuo, J., Ward, J. M., Zahra, R., Morrison, R. S., Perkins, G., & La Spada, A. R. (2019). CCP1 promotes mitochondrial fusion and motility to prevent Purkinje cell neuron loss in pcd mice. *J Cell Biol, 218*(1), 206-219. doi:10.1083/jcb.201709028

Glater, E. E., Megeath, L. J., Stowers, R. S., & Schwarz, T. L. (2006). Axonal transport of mitochondria requires milton to recruit kinesin heavy chain and is light chain independent. *J Cell Biol, 173*(4), 545-557. doi:10.1083/jcb.200601067

Gleeson, J. G., Allen, K. M., Fox, J. W., Lamperti, E. D., Berkovic, S., Scheffer, I., Cooper, E. C., Dobyns, W. B., Minnerath, S. R., Ross, M. E., & Walsh, C. A. (1998). Doublecortin, a brain-specific gene mutated in human X-linked lissencephaly and double cortex syndrome, encodes a putative signaling protein. *Cell, 92*(1), 63-72. doi:10.1016/s0092-8674(00)80899-5

Grafstein, B., & Forman, D. S. (1980). Intracellular transport in neurons. *Physiol Rev, 60*(4), 1167-1283. doi:10.1152/physrev.1980.60.4.1167

Guo, X., Macleod, G. T., Wellington, A., Hu, F., Panchumarthi, S., Schoenfield, M., Marin, L., Charlton, M. P., Atwood, H. L., & Zinsmaier, K. E. (2005). The GTPase dMiro is required for axonal transport of mitochondria to Drosophila synapses. *Neuron, 47*(3), 379-393. doi:10.1016/j.neuron.2005.06.027

Hafezparast, M., Klocke, R., Ruhrberg, C., Marquardt, A., Ahmad-Annuar, A., Bowen, S., Lalli, G., Witherden, A. S., Hummerich, H., Nicholson, S., Morgan, P. J., Oozageer, R., Priestley, J. V., Averill, S., King, V. R., Ball, S., Peters, J., Toda, T., Yamamoto, A., Hiraoka, Y., Augustin, M., Korthaus, D., Wattler, S., Wabnitz, P., Dickneite, C., Lampel, S., Boehme, F., Peraus, G., Popp, A., Rudelius, M., Schlegel, J., Fuchs, H., Hrabe de Angelis, M., Schiavo, G., Shima, D. T., Russ, A. P., Stumm, G., Martin, J. E., & Fisher, E. M. (2003). Mutations in dynein link motor neuron degeneration to defects in retrograde transport. *Science, 300*(5620), 808-812. doi:10.1126/science.1083129

Hallak, M. E., Rodriguez, J. A., Barra, H. S., & Caputto, R. (1977). Release of tyrosine from tyrosinated tubulin. Some common factors that affect this process and the assembly of tubulin. *FEBS Lett, 73*(2), 147-150.

Han, S. M., Baig, H. S., & Hammarlund, M. (2016). Mitochondria Localize to Injured Axons to Support Regeneration. *Neuron, 92*(6), 1308-1323. doi:10.1016/j.neuron.2016.11.025

Hata, Y., Tsumoto, T., & Stryker, M. P. (1999). Selective pruning of more active afferents when cat visual cortex is pharmacologically inhibited. *Neuron, 22*(2), 375-381.

Havlicek, S., Kohl, Z., Mishra, H. K., Prots, I., Eberhardt, E., Denguir, N., Wend, H., Plotz, S., Boyer, L., Marchetto, M. C., Aigner, S., Sticht, H., Groemer, T. W., Hehr, U., Lampert, A., Schlotzer-Schrehardt, U., Winkler, J., Gage, F. H., & Winner, B. (2014). Gene dosage-

dependent rescue of HSP neurite defects in SPG4 patients' neurons. *Hum Mol Genet, 23*(10), 2527-2541. doi:10.1093/hmg/ddt644

Hawkins, T., Mirigian, M., Selcuk Yasar, M., & Ross, J. L. (2010). Mechanics of microtubules. *J Biomech, 43*(1), 23-30. doi:10.1016/j.jbiomech.2009.09.005

Hazan, J., Fonknechten, N., Mavel, D., Paternotte, C., Samson, D., Artiguenave, F., Davoine, C. S., Cruaud, C., Durr, A., Wincker, P., Brottier, P., Cattolico, L., Barbe, V., Burgunder, J. M., Prud'homme, J. F., Brice, A., Fontaine, B., Heilig, B., & Weissenbach, J. (1999). Spastin, a new AAA protein, is altered in the most frequent form of autosomal dominant spastic paraplegia. *Nat Genet, 23*(3), 296-303. doi:10.1038/15472

Hendricks, A. G., Perlson, E., Ross, J. L., Schroeder, H. W., 3rd, Tokito, M., & Holzbaur, E. L. (2010). Motor coordination via a tug-of-war mechanism drives bidirectional vesicle transport. *Curr Biol, 20*(8), 697-702. doi:10.1016/j.cub.2010.02.058

Hesketh, J. E., & Pryme, I. F. (1995). *The cytoskeleton : a multi-volume treatise*. Greenwich, Conn.: JAI Press.

Hirokawa, N. (1982). Cross-linker system between neurofilaments, microtubules, and membranous organelles in frog axons revealed by the quick-freeze, deep-etching method. *J Cell Biol, 94*(1), 129-142.

Hirokawa, N. (1998). Kinesin and dynein superfamily proteins and the mechanism of organelle transport. *Science, 279*(5350), 519-526.

Hirokawa, N., Niwa, S., & Tanaka, Y. (2010). Molecular motors in neurons: transport mechanisms and roles in brain function, development, and disease. *Neuron, 68*(4), 610-638. doi:10.1016/j.neuron.2010.09.039

Hirokawa, N., Sato-Yoshitake, R., Yoshida, T., & Kawashima, T. (1990). Brain dynein (MAP1C) localizes on both anterogradely and retrogradely transported membranous organelles in vivo. *J Cell Biol, 111*(3), 1027-1037. doi:10.1083/jcb.111.3.1027

Hollenbeck, P. J. (1996). The pattern and mechanism of mitochondrial transport in axons. *Front Biosci, 1*, d91-102.

Hubbert, C., Guardiola, A., Shao, R., Kawaguchi, Y., Ito, A., Nixon, A., Yoshida, M., Wang, X. F., & Yao, T. P. (2002). HDAC6 is a microtubule-associated deacetylase. *Nature, 417*(6887), 455-458. doi:10.1038/417455a

Hurd, D. D., & Saxton, W. M. (1996). Kinesin mutations cause motor neuron disease phenotypes by disrupting fast axonal transport in Drosophila. *Genetics, 144*(3), 1075-1085.

Huttenlocher, P. R. (1979). Synaptic density in human frontal cortex - developmental changes and effects of aging. *Brain Res, 163*(2), 195-205.

Hutton, M., Lendon, C. L., Rizzu, P., Baker, M., Froelich, S., Houlden, H., Pickering-Brown, S., Chakraverty, S., Isaacs, A., Grover, A., Hackett, J., Adamson, J., Lincoln, S., Dickson, D., Davies, P., Petersen, R. C., Stevens, M., de Graaff, E., Wauters, E., van Baren, J., Hillebrand, M., Joosse, M., Kwon, J. M., Nowotny, P., Che, L. K., Norton, J., Morris, J. C., Reed, L. A., Trojanowski, J., Basun, H., Lannfelt, L., Neystat, M., Fahn, S., Dark, F., Tannenberg, T., Dodd, P. R., Hayward, N., Kwok, J. B., Schofield, P. R., Andreadis, A., Snowden, J., Craufurd, D., Neary, D., Owen, F., Oostra, B. A., Hardy, J., Goate, A., van Swieten, J., Mann, D., Lynch, T., & Heutink, P. (1998). Association of missense and 5'-splice-site mutations in tau with the inherited dementia FTDP-17. *Nature, 393*(6686), 702-705. doi:10.1038/31508

Ikegami, K., Heier, R. L., Taruishi, M., Takagi, H., Mukai, M., Shimma, S., Taira, S., Hatanaka, K., Morone, N., Yao, I., Campbell, P. K., Yuasa, S., Janke, C., Macgregor, G. R., & Setou, M. (2007). Loss of alpha-tubulin polyglutamylation in ROSA22 mice is associated with abnormal targeting of KIF1A and modulated synaptic function. *Proc Natl Acad Sci U S A, 104*(9), 3213-3218. doi:10.1073/pnas.0611547104

Jackson, H., & Parks, T. N. (1982). Functional synapse elimination in the developing avian cochlear nucleus with simultaneous reduction in cochlear nerve axon branching. *J Neurosci, 2*(12), 1736-1743.

Janke, C. (2014). The tubulin code: molecular components, readout mechanisms, and functions. *J Cell Biol, 206*(4), 461-472. doi:10.1083/jcb.201406055

Janke, C., & Bulinski, J. C. (2011). Post-translational regulation of the microtubule cytoskeleton: mechanisms and functions. *Nat Rev Mol Cell Biol, 12*(12), 773-786. doi:10.1038/nrm3227

Janke, C., Rogowski, K., Wloga, D., Regnard, C., Kajava, A. V., Strub, J. M., Temurak, N., van Dijk, J., Boucher, D., van Dorsselaer, A., Suryavanshi, S., Gaertig, J., & Edde, B. (2005). Tubulin polyglutamylase enzymes are members of the TTL domain protein family. *Science, 308*(5729), 1758-1762. doi:10.1126/science.1113010

Jaworski, J., Kapitein, L. C., Gouveia, S. M., Dortland, B. R., Wulf, P. S., Grigoriev, I., Camera, P., Spangler, S. A., Di Stefano, P., Demmers, J., Krugers, H., Defilippi, P., Akhmanova, A., & Hoogenraad, C. C. (2009). Dynamic microtubules regulate dendritic spine morphology and synaptic plasticity. *Neuron, 61*(1), 85-100. doi:10.1016/j.neuron.2008.11.013

Je, H. S., Yang, F., Ji, Y., Potluri, S., Fu, X. Q., Luo, Z. G., Nagappan, G., Chan, J. P., Hempstead, B., Son, Y. J., & Lu, B. (2013). ProBDNF and mature BDNF as punishment and reward signals for synapse elimination at mouse neuromuscular junctions. *J Neurosci, 33*(24), 9957-9962. doi:10.1523/JNEUROSCI.0163-13.2013

Jinushi-Nakao, S., Arvind, R., Amikura, R., Kinameri, E., Liu, A. W., & Moore, A. W. (2007). Knot/Collier and cut control different aspects of dendrite cytoskeleton and synergize to define final arbor shape. *Neuron, 56*(6), 963-978. doi:10.1016/j.neuron.2007.10.031

Kalinina, E., Biswas, R., Berezniuk, I., Hermoso, A., Aviles, F. X., & Fricker, L. D. (2007). A novel subfamily of mouse cytosolic carboxypeptidases. *FASEB J, 21*(3), 836-850. doi:10.1096/fj.06-7329com

Kanamori, T., Kanai, M. I., Dairyo, Y., Yasunaga, K., Morikawa, R. K., & Emoto, K. (2013). Compartmentalized calcium transients trigger dendrite pruning in Drosophila sensory neurons. *Science, 340*(6139), 1475-1478. doi:10.1126/science.1234879

Kang, J. S., Tian, J. H., Pan, P. Y., Zald, P., Li, C., Deng, C., & Sheng, Z. H. (2008). Docking of axonal mitochondria by syntaphilin controls their mobility and affects short-term facilitation. *Cell, 132*(1), 137-148. doi:10.1016/j.cell.2007.11.024

Kapitein, L. C., & Hoogenraad, C. C. (2011). Which way to go? Cytoskeletal organization and polarized transport in neurons. *Mol Cell Neurosci, 46*(1), 9-20. doi:10.1016/j.mcn.2010.08.015

Kapitein, L. C., & Hoogenraad, C. C. (2015). Building the Neuronal Microtubule Cytoskeleton. *Neuron, 87*(3), 492-506. doi:10.1016/j.neuron.2015.05.046

Karabay, A., Yu, W., Solowska, J. M., Baird, D. H., & Baas, P. W. (2004). Axonal growth is sensitive to the levels of katanin, a protein that severs microtubules. *J Neurosci, 24*(25), 5778-5788. doi:10.1523/JNEUROSCI.1382-04.2004

Kasher, P. R., De Vos, K. J., Wharton, S. B., Manser, C., Bennett, E. J., Bingley, M., Wood, J. D., Milner, R., McDermott, C. J., Miller, C. C., Shaw, P. J., & Grierson, A. J. (2009). Direct evidence for axonal transport defects in a novel mouse model of mutant spastin-induced hereditary spastic paraplegia (HSP) and human HSP patients. *J Neurochem, 110*(1), 34-44. doi:10.1111/j.1471-4159.2009.06104.x

Kasthuri, N., & Lichtman, J. W. (2003). The role of neuronal identity in synaptic competition. *Nature, 424*(6947), 426-430. doi:10.1038/nature01836

Katayama, H., Kogure, T., Mizushima, N., Yoshimori, T., & Miyawaki, A. (2011). A sensitive and quantitative technique for detecting autophagic events based on lysosomal delivery. *Chem Biol, 18*(8), 1042-1052. doi:10.1016/j.chembiol.2011.05.013

Kaul, N., Soppina, V., & Verhey, K. J. (2014). Effects of alpha-tubulin K40 acetylation and detyrosination on kinesin-1 motility in a purified system. *Biophys J, 106*(12), 2636-2643. doi:10.1016/j.bpj.2014.05.008

Keller-Peck, C. R., Walsh, M. K., Gan, W. B., Feng, G., Sanes, J. R., & Lichtman, J. W. (2001). Asynchronous synapse elimination in neonatal motor units: studies using GFP transgenic mice. *Neuron, 31*(3), 381-394.

Kerschensteiner, M., Reuter, M. S., Lichtman, J. W., & Misgeld, T. (2008). Ex vivo imaging of motor axon dynamics in murine triangularis sterni explants. *Nat Protoc, 3*(10), 1645-1653. doi:10.1038/nprot.2008.160

Kimura, Y., Kurabe, N., Ikegami, K., Tsutsumi, K., Konishi, Y., Kaplan, O. I., Kunitomo, H., Iino, Y., Blacque, O. E., & Setou, M. (2010). Identification of tubulin deglutamylase among Caenorhabditis elegans and mammalian cytosolic carboxypeptidases (CCPs). *J Biol Chem, 285*(30), 22936-22941. doi:10.1074/jbc.C110.128280

King, S. J., & Schroer, T. A. (2000). Dynactin increases the processivity of the cytoplasmic dynein motor. *Nat Cell Biol, 2*(1), 20-24. doi:10.1038/71338

Klebe, S., Lossos, A., Azzedine, H., Mundwiller, E., Sheffer, R., Gaussen, M., Marelli, C., Nawara, M., Carpentier, W., Meyer, V., Rastetter, A., Martin, E., Bouteiller, D., Orlando, L., Gyapay, G., El-Hachimi, K. H., Zimmerman, B., Gamliel, M., Misk, A., Lerer, I., Brice, A., Durr, A., & Stevanin, G. (2012). KIF1A missense mutations in SPG30, an autosomal recessive spastic paraplegia: distinct phenotypes according to the nature of the mutations. *Eur J Hum Genet, 20*(6), 645-649. doi:10.1038/ejhg.2011.261

Kleele, T., Marinkovic, P., Williams, P. R., Stern, S., Weigand, E. E., Engerer, P., Naumann, R., Hartmann, J., Karl, R. M., Bradke, F., Bishop, D., Herms, J., Konnerth, A., Kerschensteiner, M., Godinho, L., & Misgeld, T. (2014). An assay to image neuronal microtubule dynamics in mice. *Nat Commun, 5*, 4827. doi:10.1038/ncomms5827

Konishi, Y., & Setou, M. (2009). Tubulin tyrosination navigates the kinesin-1 motor domain to axons. *Nat Neurosci, 12*(5), 559-567. doi:10.1038/nn.2314

Kreitzer, G., Liao, G., & Gundersen, G. G. (1999). Detyrosination of tubulin regulates the interaction of intermediate filaments with microtubules in vivo via a kinesin-dependent mechanism. *Mol Biol Cell, 10*(4), 1105-1118. doi:10.1091/mbc.10.4.1105

Kuo, C. T., Jan, L. Y., & Jan, Y. N. (2005). Dendrite-specific remodeling of Drosophila sensory neurons requires matrix metalloproteases, ubiquitin-proteasome, and ecdysone signaling. *Proc Natl Acad Sci U S A, 102*(42), 15230-15235. doi:10.1073/pnas.0507393102

Kuo, Y. W., Trottier, O., Mahamdeh, M., & Howard, J. (2019). Spastin is a dual-function enzyme that severs microtubules and promotes their regrowth to increase the number and mass of

microtubules. *Proc Natl Acad Sci U S A, 116*(12), 5533-5541. doi:10.1073/pnas.1818824116

Kurup, N., Yan, D., Goncharov, A., & Jin, Y. (2015). Dynamic microtubules drive circuit rewiring in the absence of neurite remodeling. *Curr Biol, 25*(12), 1594-1605. doi:10.1016/j.cub.2015.04.061

L'Hernault, S. W., & Rosenbaum, J. L. (1985). Chlamydomonas alpha-tubulin is posttranslationally modified by acetylation on the epsilon-amino group of a lysine. *Biochemistry, 24*(2), 473-478.

Lacroix, B., van Dijk, J., Gold, N. D., Guizetti, J., Aldrian-Herrada, G., Rogowski, K., Gerlich, D. W., & Janke, C. (2010). Tubulin polyglutamylation stimulates spastin-mediated microtubule severing. *J Cell Biol, 189*(6), 945-954. doi:10.1083/jcb.201001024

LeDizet, M., & Piperno, G. (1987). Identification of an acetylation site of Chlamydomonas alpha-tubulin. *Proc Natl Acad Sci U S A, 84*(16), 5720-5724. doi:10.1073/pnas.84.16.5720

Lee, H. H., Jan, L. Y., & Jan, Y. N. (2009). Drosophila IKK-related kinase Ik2 and Katanin p60-like 1 regulate dendrite pruning of sensory neuron during metamorphosis. *Proc Natl Acad Sci U S A, 106*(15), 6363-6368. doi:10.1073/pnas.0902051106

Leopold, P. L., McDowall, A. W., Pfister, K. K., Bloom, G. S., & Brady, S. T. (1992). Association of kinesin with characterized membrane-bounded organelles. *Cell Motil Cytoskeleton, 23*(1), 19-33. doi:10.1002/cm.970230104

Levy, M., Faas, G. C., Saggau, P., Craigen, W. J., & Sweatt, J. D. (2003). Mitochondrial regulation of synaptic plasticity in the hippocampus. *J Biol Chem, 278*(20), 17727-17734. doi:10.1074/jbc.M212878200

Liao, G., & Gundersen, G. G. (1998). Kinesin is a candidate for cross-bridging microtubules and intermediate filaments. Selective binding of kinesin to detyrosinated tubulin and vimentin. *J Biol Chem, 273*(16), 9797-9803.

Lichtman, J. W. (1977). The reorganization of synaptic connexions in the rat submandibular ganglion during post-natal development. *J Physiol, 273*(1), 155-177.

Lichtman, J. W., & Colman, H. (2000). Synapse elimination and indelible memory. *Neuron, 25*(2), 269-278.

Lin, M. Y., & Sheng, Z. H. (2015). Regulation of mitochondrial transport in neurons. *Exp Cell Res, 334*(1), 35-44. doi:10.1016/j.yexcr.2015.01.004

Liu, Z., Chen, Y., Wang, D., Wang, S., & Zhang, Y. Q. (2010). Distinct presynaptic and postsynaptic dismantling processes of Drosophila neuromuscular junctions during metamorphosis. *J Neurosci, 30*(35), 11624-11634. doi:10.1523/JNEUROSCI.0410-10.2010

Lohof, A. M., Delhaye-Bouchaud, N., & Mariani, J. (1996). Synapse elimination in the central nervous system: functional significance and cellular mechanisms. *Rev Neurosci, 7*(2), 85-101.

Luduena, R. F., Shooter, E. M., & Wilson, L. (1977). Structure of the tubulin dimer. *J Biol Chem, 252*(20), 7006-7014.

Luo, G., Yi, J., Ma, C., Xiao, Y., Yi, F., Yu, T., & Zhou, J. (2013). Defective mitochondrial dynamics is an early event in skeletal muscle of an amyotrophic lateral sclerosis mouse model. *PLoS One, 8*(12), e82112. doi:10.1371/journal.pone.0082112

Luo, L., & O'Leary, D. D. (2005). Axon retraction and degeneration in development and disease. *Annu Rev Neurosci, 28*, 127-156. doi:10.1146/annurev.neuro.28.061604.135632

Ma, D. L., Chia, S. C., Tang, Y. C., Chang, M. L., Probst, A., Burgunder, J. M., & Tang, F. R. (2006). Spastin in the human and mouse central nervous system with special reference to its expression in the hippocampus of mouse pilocarpine model of status epilepticus and temporal lobe epilepsy. *Neurochem Int, 49*(7), 651-664. doi:10.1016/j.neuint.2006.05.008

Ma, H., Cai, Q., Lu, W., Sheng, Z. H., & Mochida, S. (2009). KIF5B motor adaptor syntabulin maintains synaptic transmission in sympathetic neurons. *J Neurosci, 29*(41), 13019-13029. doi:10.1523/JNEUROSCI.2517-09.2009

Maas, C., Belgardt, D., Lee, H. K., Heisler, F. F., Lappe-Siefke, C., Magiera, M. M., van Dijk, J., Hausrat, T. J., Janke, C., & Kneussel, M. (2009). Synaptic activation modifies microtubules underlying transport of postsynaptic cargo. *Proc Natl Acad Sci U S A, 106*(21), 8731-8736. doi:10.1073/pnas.0812391106

MacAskill, A. F., & Kittler, J. T. (2010). Control of mitochondrial transport and localization in neurons. *Trends Cell Biol, 20*(2), 102-112. doi:10.1016/j.tcb.2009.11.002

Macaskill, A. F., Rinholm, J. E., Twelvetrees, A. E., Arancibia-Carcamo, I. L., Muir, J., Fransson, A., Aspenstrom, P., Attwell, D., & Kittler, J. T. (2009). Miro1 is a calcium sensor for glutamate receptor-dependent localization of mitochondria at synapses. *Neuron, 61*(4), 541-555. doi:10.1016/j.neuron.2009.01.030

Maday, S., Twelvetrees, A. E., Moughamian, A. J., & Holzbaur, E. L. (2014). Axonal transport: cargo-specific mechanisms of motility and regulation. *Neuron, 84*(2), 292-309. doi:10.1016/j.neuron.2014.10.019

Maday, S., Wallace, K. E., & Holzbaur, E. L. (2012). Autophagosomes initiate distally and mature during transport toward the cell soma in primary neurons. *J Cell Biol, 196*(4), 407-417. doi:10.1083/jcb.201106120

Magiera, M. M., Bodakuntla, S., Ziak, J., Lacomme, S., Marques Sousa, P., Leboucher, S., Hausrat, T. J., Bosc, C., Andrieux, A., Kneussel, M., Landry, M., Calas, A., Balastik, M., & Janke, C. (2018). Excessive tubulin polyglutamylation causes neurodegeneration and perturbs neuronal transport. *EMBO J, 37*(23). doi:10.15252/embj.2018100440

Mandelkow, E., & Mandelkow, E. M. (1995). Microtubules and microtubule-associated proteins. *Curr Opin Cell Biol, 7*(1), 72-81.

Maor-Nof, M., Homma, N., Raanan, C., Nof, A., Hirokawa, N., & Yaron, A. (2013). Axonal pruning is actively regulated by the microtubule-destabilizing protein kinesin superfamily protein 2A. *Cell Rep, 3*(4), 971-977. doi:10.1016/j.celrep.2013.03.005

Mariano, V., Dominguez-Iturza, N., Neukomm, L. J., & Bagni, C. (2018). Maintenance mechanisms of circuit-integrated axons. *Curr Opin Neurobiol, 53*, 162-173. doi:10.1016/j.conb.2018.08.007

Marinkovic, P., Reuter, M. S., Brill, M. S., Godinho, L., Kerschensteiner, M., & Misgeld, T. (2012). Axonal transport deficits and degeneration can evolve independently in mouse models of amyotrophic lateral sclerosis. *Proc Natl Acad Sci U S A, 109*(11), 4296-4301. doi:10.1073/pnas.1200658109

Martz, D., Lasek, R. J., Brady, S. T., & Allen, R. D. (1984). Mitochondrial motility in axons: membranous organelles may interact with the force generating system through multiple surface binding sites. *Cell Motil, 4*(2), 89-101.

McKenney, R. J., Huynh, W., Vale, R. D., & Sirajuddin, M. (2016). Tyrosination of alpha-tubulin controls the initiation of processive dynein-dynactin motility. *EMBO J, 35*(11), 1175-1185. doi:10.15252/embj.201593071

McMurray, C. T. (2000). Neurodegeneration: diseases of the cytoskeleton? *Cell Death Differ, 7*(10), 861-865. doi:10.1038/sj.cdd.4400764

McNally, F. J., & Roll-Mecak, A. (2018). Microtubule-severing enzymes: From cellular functions to molecular mechanism. *J Cell Biol, 217*(12), 4057-4069. doi:10.1083/jcb.201612104

McNally, F. J., & Vale, R. D. (1993). Identification of katanin, an ATPase that severs and disassembles stable microtubules. *Cell, 75*(3), 419-429.

Meltzer, H., & Schuldiner, O. (2016). Cut Your Losses: Spastin Mediates Branch-Specific Axon Loss. *Neuron, 92*(4), 677-680. doi:10.1016/j.neuron.2016.11.004

Miki, H., Setou, M., Kaneshiro, K., & Hirokawa, N. (2001). All kinesin superfamily protein, KIF, genes in mouse and human. *Proc Natl Acad Sci U S A, 98*(13), 7004-7011. doi:10.1073/pnas.111145398

Misgeld, T. (2005). Death of an axon: studying axon loss in development and disease. *Histochem Cell Biol, 124*(3-4), 189-196. doi:10.1007/s00418-005-0036-6

Misgeld, T., Kerschensteiner, M., Bareyre, F. M., Burgess, R. W., & Lichtman, J. W. (2007). Imaging axonal transport of mitochondria in vivo. *Nat Methods, 4*(7), 559-561. doi:10.1038/nmeth1055

Misgeld, T., & Schwarz, T. L. (2017). Mitostasis in Neurons: Maintaining Mitochondria in an Extended Cellular Architecture. *Neuron, 96*(3), 651-666. doi:10.1016/j.neuron.2017.09.055

Mitchison, T., & Kirschner, M. (1984). Dynamic instability of microtubule growth. *Nature, 312*(5991), 237-242.

Mukherjee, S., Diaz Valencia, J. D., Stewman, S., Metz, J., Monnier, S., Rath, U., Asenjo, A. B., Charafeddine, R. A., Sosa, H. J., Ross, J. L., Ma, A., & Sharp, D. J. (2012). Human Fidgetin is a microtubule severing the enzyme and minus-end depolymerase that regulates mitosis. *Cell Cycle, 11*(12), 2359-2366. doi:10.4161/cc.20849

Nakagawa, T., Tanaka, Y., Matsuoka, E., Kondo, S., Okada, Y., Noda, Y., Kanai, Y., & Hirokawa, N. (1997). Identification and classification of 16 new kinesin superfamily (KIF) proteins in mouse genome. *Proc Natl Acad Sci U S A, 94*(18), 9654-9659.

Nangaku, M., Sato-Yoshitake, R., Okada, Y., Noda, Y., Takemura, R., Yamazaki, H., & Hirokawa, N. (1994). KIF1B, a novel microtubule plus end-directed monomeric motor protein for transport of mitochondria. *Cell, 79*(7), 1209-1220.

Neukirchen, D., & Bradke, F. (2011). Neuronal polarization and the cytoskeleton. *Semin Cell Dev Biol, 22*(8), 825-833. doi:10.1016/j.semcdb.2011.08.007

Nicholls, D. G., & Ferguson, S. J. (2013). *Bioenergetics* (Fourth edition / ed.). Amsterdam: Academic Press, Elsevier.

Nieuwenhuis, J., Adamopoulos, A., Bleijerveld, O. B., Mazouzi, A., Stickel, E., Celie, P., Altelaar, M., Knipscheer, P., Perrakis, A., Blomen, V. A., & Brummelkamp, T. R. (2017). Vasohibins encode tubulin detyrosinating activity. *Science, 358*(6369), 1453-1456. doi:10.1126/science.aao5676

Nikolaev, A., McLaughlin, T., O'Leary, D. D., & Tessier-Lavigne, M. (2009). APP binds DR6 to trigger axon pruning and neuron death via distinct caspases. *Nature, 457*(7232), 981-989. doi:10.1038/nature07767

Nirschl, J. J., Magiera, M. M., Lazarus, J. E., Janke, C., & Holzbaur, E. L. (2016). alpha-Tubulin Tyrosination and CLIP-170 Phosphorylation Regulate the Initiation of Dynein-Driven Transport in Neurons. *Cell Rep, 14*(11), 2637-2652. doi:10.1016/j.celrep.2016.02.046

North, B. J., Marshall, B. L., Borra, M. T., Denu, J. M., & Verdin, E. (2003). The human Sir2 ortholog, SIRT2, is an NAD+-dependent tubulin deacetylase. *Mol Cell, 11*(2), 437-444.

Ochs, S., & Burger, E. (1958). Movement of substance proximo-distally in nerve axons as studied with spinal cord injections of radioactive phosphorus. *Am J Physiol, 194*(3), 499-506. doi:10.1152/ajplegacy.1958.194.3.499

Panda, D., Miller, H. P., Banerjee, A., Luduena, R. F., & Wilson, L. (1994). Microtubule dynamics in vitro are regulated by the tubulin isotype composition. *Proc Natl Acad Sci U S A, 91*(24), 11358-11362.

Park, S. H., Zhu, P. P., Parker, R. L., & Blackstone, C. (2010). Hereditary spastic paraplegia proteins REEP1, spastin, and atlastin-1 coordinate microtubule interactions with the tubular ER network. *J Clin Invest, 120*(4), 1097-1110. doi:10.1172/JCI40979

Pathak, D., Sepp, K. J., & Hollenbeck, P. J. (2010). Evidence that myosin activity opposes microtubule-based axonal transport of mitochondria. *J Neurosci, 30*(26), 8984-8992. doi:10.1523/JNEUROSCI.1621-10.2010

Paturle-Lafanechere, L., Manier, M., Trigault, N., Pirollet, F., Mazarguil, H., & Job, D. (1994). Accumulation of delta 2-tubulin, a major tubulin variant that cannot be tyrosinated, in neuronal tissues and in stable microtubule assemblies. *J Cell Sci, 107 (Pt 6)*, 1529-1543.

Penzes, P., Cahill, M. E., Jones, K. A., VanLeeuwen, J. E., & Woolfrey, K. M. (2011). Dendritic spine pathology in neuropsychiatric disorders. *Nat Neurosci, 14*(3), 285-293. doi:10.1038/nn.2741

Peris, L., Wagenbach, M., Lafanechere, L., Brocard, J., Moore, A. T., Kozielski, F., Job, D., Wordeman, L., & Andrieux, A. (2009). Motor-dependent microtubule disassembly driven by tubulin tyrosination. *J Cell Biol, 185*(7), 1159-1166. doi:10.1083/jcb.200902142

Personius, K. E., & Balice-Gordon, R. J. (2001). Loss of correlated motor neuron activity during synaptic competition at developing neuromuscular synapses. *Neuron, 31*(3), 395-408.

Personius, K. E., & Balice-Gordon, R. J. (2002). Activity-dependent synaptic plasticity: insights from neuromuscular junctions. *Neuroscientist, 8*(5), 414-422. doi:10.1177/107385802236970

Peters, A., Palay, S. L., & Webster, H. d. (1991). *The fine structure of the nervous system : neurons and their supporting cells* (3rd ed.). New York: Oxford University Press.

Pilling, A. D., Horiuchi, D., Lively, C. M., & Saxton, W. M. (2006). Kinesin-1 and Dynein are the primary motors for fast transport of mitochondria in Drosophila motor axons. *Mol Biol Cell, 17*(4), 2057-2068. doi:10.1091/mbc.e05-06-0526

Poirier, K., Keays, D. A., Francis, F., Saillour, Y., Bahi, N., Manouvrier, S., Fallet-Bianco, C., Pasquier, L., Toutain, A., Tuy, F. P., Bienvenu, T., Joriot, S., Odent, S., Ville, D., Desguerre, I., Goldenberg, A., Moutard, M. L., Fryns, J. P., van Esch, H., Harvey, R. J., Siebold, C., Flint, J., Beldjord, C., & Chelly, J. (2007). Large spectrum of lissencephaly and pachygyria phenotypes resulting from de novo missense mutations in tubulin alpha 1A (TUBA1A). *Hum Mutat, 28*(11), 1055-1064. doi:10.1002/humu.20572

Prota, A. E., Bargsten, K., Zurwerra, D., Field, J. J., Diaz, J. F., Altmann, K. H., & Steinmetz, M. O. (2013). Molecular mechanism of action of microtubule-stabilizing anticancer agents. *Science, 339*(6119), 587-590. doi:10.1126/science.1230582

Qiang, L., Yu, W., Liu, M., Solowska, J. M., & Baas, P. W. (2010). Basic fibroblast growth factor elicits formation of interstitial axonal branches via enhanced severing of microtubules. *Mol Biol Cell, 21*(2), 334-344. doi:10.1091/mbc.E09-09-0834

Raff, M. C., Whitmore, A. V., & Finn, J. T. (2002). Axonal self-destruction and neurodegeneration. *Science, 296*(5569), 868-871. doi:10.1126/science.1068613

Rai, A., Pathak, D., Thakur, S., Singh, S., Dubey, A. K., & Mallik, R. (2016). Dynein Clusters into Lipid Microdomains on Phagosomes to Drive Rapid Transport toward Lysosomes. *Cell, 164*(4), 722-734. doi:10.1016/j.cell.2015.12.054

Rai, A. K., Rai, A., Ramaiya, A. J., Jha, R., & Mallik, R. (2013). Molecular adaptations allow dynein to generate large collective forces inside cells. *Cell, 152*(1-2), 172-182. doi:10.1016/j.cell.2012.11.044

Rangaraju, V., Calloway, N., & Ryan, T. A. (2014). Activity-driven local ATP synthesis is required for synaptic function. *Cell, 156*(4), 825-835. doi:10.1016/j.cell.2013.12.042

Redfern, P. A. (1970). Neuromuscular transmission in new-born rats. *J Physiol, 209*(3), 701-709.

Reid, E., Connell, J., Edwards, T. L., Duley, S., Brown, S. E., & Sanderson, C. M. (2005). The hereditary spastic paraplegia protein spastin interacts with the ESCRT-III complex-associated endosomal protein CHMP1B. *Hum Mol Genet, 14*(1), 19-38. doi:10.1093/hmg/ddi003

Reid, E., Kloos, M., Ashley-Koch, A., Hughes, L., Bevan, S., Svenson, I. K., Graham, F. L., Gaskell, P. C., Dearlove, A., Pericak-Vance, M. A., Rubinsztein, D. C., & Marchuk, D. A. (2002). A kinesin heavy chain (KIF5A) mutation in hereditary spastic paraplegia (SPG10). *Am J Hum Genet, 71*(5), 1189-1194. doi:10.1086/344210

Reiner, O., Carrozzo, R., Shen, Y., Wehnert, M., Faustinella, F., Dobyns, W. B., Caskey, C. T., & Ledbetter, D. H. (1993). Isolation of a Miller-Dieker lissencephaly gene containing G protein beta-subunit-like repeats. *Nature, 364*(6439), 717-721. doi:10.1038/364717a0

Ribbeck, K., & Mitchison, T. J. (2006). Meiotic spindle: sculpted by severing. *Curr Biol, 16*(21), R923-925. doi:10.1016/j.cub.2006.09.048

Ribchester, R. R. (1993). Co-existence and elimination of convergent motor nerve terminals in reinnervated and paralysed adult rat skeletal muscle. *J Physiol, 466*, 421-441.

Riccomagno, M. M., & Kolodkin, A. L. (2015). Sculpting neural circuits by axon and dendrite pruning. *Annu Rev Cell Dev Biol, 31*, 779-805. doi:10.1146/annurev-cellbio-100913-013038

Ridge, R. M., & Betz, W. J. (1984). The effect of selective, chronic stimulation on motor unit size in developing rat muscle. *J Neurosci, 4*(10), 2614-2620.

Riley, D. A. (1981). Ultrastructural evidence for axon retraction during the spontaneous elimination of polyneuronal innervation of the rat soleus muscle. *J Neurocytol, 10*(3), 425-440.

Roberts, A. J., Kon, T., Knight, P. J., Sutoh, K., & Burgess, S. A. (2013). Functions and mechanics of dynein motor proteins. *Nat Rev Mol Cell Biol, 14*(11), 713-726. doi:10.1038/nrm3667

Rogowski, K., van Dijk, J., Magiera, M. M., Bosc, C., Deloulme, J. C., Bosson, A., Peris, L., Gold, N. D., Lacroix, B., Bosch Grau, M., Bec, N., Larroque, C., Desagher, S., Holzer, M., Andrieux, A., Moutin, M. J., & Janke, C. (2010). A family of protein-deglutamylating enzymes associated with neurodegeneration. *Cell, 143*(4), 564-578. doi:10.1016/j.cell.2010.10.014

Roll-Mecak, A. (2018). How cells exploit tubulin diversity to build functional cellular microtubule mosaics. *Curr Opin Cell Biol, 56*, 102-108. doi:10.1016/j.ceb.2018.10.009

Roll-Mecak, A., & McNally, F. J. (2010). Microtubule-severing enzymes. *Curr Opin Cell Biol, 22*(1), 96-103. doi:10.1016/j.ceb.2009.11.001

Roll-Mecak, A., & Vale, R. D. (2005). The Drosophila homologue of the hereditary spastic paraplegia protein, spastin, severs and disassembles microtubules. *Curr Biol, 15*(7), 650-655. doi:10.1016/j.cub.2005.02.029

Roll-Mecak, A., & Vale, R. D. (2006). Making more microtubules by severing: a common theme of noncentrosomal microtubule arrays? *J Cell Biol, 175*(6), 849-851. doi:10.1083/jcb.200611149

Roll-Mecak, A., & Vale, R. D. (2008). Structural basis of microtubule severing by the hereditary spastic paraplegia protein spastin. *Nature, 451*(7176), 363-367. doi:10.1038/nature06482

Ross, J. L., Wallace, K., Shuman, H., Goldman, Y. E., & Holzbaur, E. L. (2006). Processive bidirectional motion of dynein-dynactin complexes in vitro. *Nat Cell Biol, 8*(6), 562-570. doi:10.1038/ncb1421

Rubenstein, J. L. R., & Rakic, P. (2013). *Comprehensive developmental neuroscience : patterning and cell type specification in the developing CNS and PNS* (First edition. ed.). Amsterdam: Elsevier/Academic Press.

Ruschel, J., Hellal, F., Flynn, K. C., Dupraz, S., Elliott, D. A., Tedeschi, A., Bates, M., Sliwinski, C., Brook, G., Dobrindt, K., Peitz, M., Brustle, O., Norenberg, M. D., Blesch, A., Weidner, N., Bunge, M. B., Bixby, J. L., & Bradke, F. (2015). Axonal regeneration. Systemic administration of epothilone B promotes axon regeneration after spinal cord injury. *Science, 348*(6232), 347-352. doi:10.1126/science.aaa2958

Sadleir, K. R., Kandalepas, P. C., Buggia-Prevot, V., Nicholson, D. A., Thinakaran, G., & Vassar, R. (2016). Presynaptic dystrophic neurites surrounding amyloid plaques are sites of microtubule disruption, BACE1 elevation, and increased Abeta generation in Alzheimer's disease. *Acta Neuropathol, 132*(2), 235-256. doi:10.1007/s00401-016-1558-9

Sajic, M., Mastrolia, V., Lee, C. Y., Trigo, D., Sadeghian, M., Mosley, A. J., Gregson, N. A., Duchen, M. R., & Smith, K. J. (2013). Impulse conduction increases mitochondrial transport in adult mammalian peripheral nerves in vivo. *PLoS Biol, 11*(12), e1001754. doi:10.1371/journal.pbio.1001754

Sandner, B., Puttagunta, R., Motsch, M., Bradke, F., Ruschel, J., Blesch, A., & Weidner, N. (2018). Systemic epothilone D improves hindlimb function after spinal cord contusion injury in rats. *Exp Neurol, 306*, 250-259. doi:10.1016/j.expneurol.2018.01.018

Sanes, J. R., & Lichtman, J. W. (1999). Development of the vertebrate neuromuscular junction. *Annu Rev Neurosci, 22*, 389-442. doi:10.1146/annurev.neuro.22.1.389

Sanes, J. R., & Lichtman, J. W. (2001). Induction, assembly, maturation and maintenance of a postsynaptic apparatus. *Nat Rev Neurosci, 2*(11), 791-805. doi:10.1038/35097557

Saotome, M., Safiulina, D., Szabadkai, G., Das, S., Fransson, A., Aspenstrom, P., Rizzuto, R., & Hajnoczky, G. (2008). Bidirectional Ca2+-dependent control of mitochondrial dynamics by the Miro GTPase. *Proc Natl Acad Sci U S A, 105*(52), 20728-20733. doi:10.1073/pnas.0808953105

Saxena, S., & Caroni, P. (2007). Mechanisms of axon degeneration: from development to disease. *Prog Neurobiol, 83*(3), 174-191. doi:10.1016/j.pneurobio.2007.07.007

Schindelin, J., Arganda-Carreras, I., Frise, E., Kaynig, V., Longair, M., Pietzsch, T., Preibisch, S., Rueden, C., Saalfeld, S., Schmid, B., Tinevez, J. Y., White, D. J., Hartenstein, V., Eliceiri, K., Tomancak, P., & Cardona, A. (2012). Fiji: an open-source platform for biological-image analysis. *Nat Methods, 9*(7), 676-682. doi:10.1038/nmeth.2019

Schnapp, B. J., Vale, R. D., Sheetz, M. P., & Reese, T. S. (1985). Single microtubules from squid axoplasm support bidirectional movement of organelles. *Cell, 40*(2), 455-462.

Schroer, T. A. (2004). Dynactin. *Annu Rev Cell Dev Biol, 20*, 759-779. doi:10.1146/annurev.cellbio.20.012103.094623

Schroer, T. A., Steuer, E. R., & Sheetz, M. P. (1989). Cytoplasmic dynein is a minus end-directed motor for membranous organelles. *Cell, 56*(6), 937-946.

Schuldiner, O., & Yaron, A. (2015). Mechanisms of developmental neurite pruning. *Cell Mol Life Sci, 72*(1), 101-119. doi:10.1007/s00018-014-1729-6

Schule, R., Wiethoff, S., Martus, P., Karle, K. N., Otto, S., Klebe, S., Klimpe, S., Gallenmuller, C., Kurzwelly, D., Henkel, D., Rimmele, F., Stolze, H., Kohl, Z., Kassubek, J., Klockgether, T., Vielhaber, S., Kamm, C., Klopstock, T., Bauer, P., Zuchner, S., Liepelt-Scarfone, I., & Schols, L. (2016). Hereditary spastic paraplegia: Clinicogenetic lessons from 608 patients. *Ann Neurol, 79*(4), 646-658. doi:10.1002/ana.24611

Sellgren, C. M., Gracias, J., Watmuff, B., Biag, J. D., Thanos, J. M., Whittredge, P. B., Fu, T., Worringer, K., Brown, H. E., Wang, J., Kaykas, A., Karmacharya, R., Goold, C. P., Sheridan, S. D., & Perlis, R. H. (2019). Increased synapse elimination by microglia in schizophrenia patient-derived models of synaptic pruning. *Nat Neurosci, 22*(3), 374-385. doi:10.1038/s41593-018-0334-7

Sheng, Z. H. (2014). Mitochondrial trafficking and anchoring in neurons: New insight and implications. *J Cell Biol, 204*(7), 1087-1098. doi:10.1083/jcb.201312123

Sheng, Z. H., & Cai, Q. (2012). Mitochondrial transport in neurons: impact on synaptic homeostasis and neurodegeneration. *Nat Rev Neurosci, 13*(2), 77-93. doi:10.1038/nrn3156

Sherwood, N. T., Sun, Q., Xue, M., Zhang, B., & Zinn, K. (2004). Drosophila spastin regulates synaptic microtubule networks and is required for normal motor function. *PLoS Biol, 2*(12), e429. doi:10.1371/journal.pbio.0020429

Shumyatsky, G. P., Malleret, G., Shin, R. M., Takizawa, S., Tully, K., Tsvetkov, E., Zakharenko, S. S., Joseph, J., Vronskaya, S., Yin, D., Schubart, U. K., Kandel, E. R., & Bolshakov, V. Y. (2005). stathmin, a gene enriched in the amygdala, controls both learned and innate fear. *Cell, 123*(4), 697-709. doi:10.1016/j.cell.2005.08.038

Singh, K. K., Park, K. J., Hong, E. J., Kramer, B. M., Greenberg, M. E., Kaplan, D. R., & Miller, F. D. (2008). Developmental axon pruning mediated by BDNF-p75NTR-dependent axon degeneration. *Nat Neurosci, 11*(6), 649-658. doi:10.1038/nn.2114

Sirajuddin, M., Rice, L. M., & Vale, R. D. (2014). Regulation of microtubule motors by tubulin isotypes and post-translational modifications. *Nat Cell Biol, 16*(4), 335-344. doi:10.1038/ncb2920

Smit-Rigter, L., Rajendran, R., Silva, C. A., Spierenburg, L., Groeneweg, F., Ruimschotel, E. M., van Versendaal, D., van der Togt, C., Eysel, U. T., Heimel, J. A., Lohmann, C., & Levelt, C. N. (2016). Mitochondrial Dynamics in Visual Cortex Are Limited In Vivo and Not Affected by Axonal Structural Plasticity. *Curr Biol, 26*(19), 2609-2616. doi:10.1016/j.cub.2016.07.033

Smith, B. N., Ticozzi, N., Fallini, C., Gkazi, A. S., Topp, S., Kenna, K. P., Scotter, E. L., Kost, J., Keagle, P., Miller, J. W., Calini, D., Vance, C., Danielson, E. W., Troakes, C., Tiloca, C., Al-Sarraj, S., Lewis, E. A., King, A., Colombrita, C., Pensato, V., Castellotti, B., de Belleroche, J., Baas, F., ten Asbroek, A. L., Sapp, P. C., McKenna-Yasek, D., McLaughlin, R. L., Polak, M., Asress, S., Esteban-Perez, J., Munoz-Blanco, J. L., Simpson, M., Consortium, S., van Rheenen, W., Diekstra, F. P., Lauria, G., Duga, S., Corti, S., Cereda, C., Corrado, L., Soraru, G., Morrison, K. E., Williams, K. L., Nicholson, G. A., Blair, I. P., Dion, P. A., Leblond, C. S., Rouleau, G. A., Hardiman, O., Veldink, J. H., van den Berg, L. H., Al-Chalabi, A., Pall, H., Shaw, P. J., Turner, M. R., Talbot, K., Taroni, F., Garcia-Redondo, A., Wu, Z., Glass, J. D., Gellera, C., Ratti, A., Brown, R. H., Jr., Silani, V., Shaw, C. E., & Landers, J. E. (2014). Exome-wide rare variant analysis identifies TUBA4A mutations associated with familial ALS. *Neuron, 84*(2), 324-331. doi:10.1016/j.neuron.2014.09.027

Song, Y., & Brady, S. T. (2014). Stabilization of neuronal connections and the axonal cytoskeleton. *Bioarchitecture, 4*(1), 22-24. doi:10.4161/bioa.28080

Song, Y., Kirkpatrick, L. L., Schilling, A. B., Helseth, D. L., Chabot, N., Keillor, J. W., Johnson, G. V., & Brady, S. T. (2013). Transglutaminase and polyamination of tubulin: posttranslational modification for stabilizing axonal microtubules. *Neuron, 78*(1), 109-123. doi:10.1016/j.neuron.2013.01.036

Soppina, V., Herbstman, J. F., Skiniotis, G., & Verhey, K. J. (2012). Luminal localization of alpha-tubulin K40 acetylation by cryo-EM analysis of fab-labeled microtubules. *PLoS One, 7*(10), e48204. doi:10.1371/journal.pone.0048204

Sorbara, C. D., Wagner, N. E., Ladwig, A., Nikic, I., Merkler, D., Kleele, T., Marinkovic, P., Naumann, R., Godinho, L., Bareyre, F. M., Bishop, D., Misgeld, T., & Kerschensteiner, M. (2014). Pervasive axonal transport deficits in multiple sclerosis models. *Neuron, 84*(6), 1183-1190. doi:10.1016/j.neuron.2014.11.006

Stepanova, T., Slemmer, J., Hoogenraad, C. C., Lansbergen, G., Dortland, B., De Zeeuw, C. I., Grosveld, F., van Cappellen, G., Akhmanova, A., & Galjart, N. (2003). Visualization of microtubule growth in cultured neurons via the use of EB3-GFP (end-binding protein 3-green fluorescent protein). *J Neurosci, 23*(7), 2655-2664.

Stewart, A., Tsubouchi, A., Rolls, M. M., Tracey, W. D., & Sherwood, N. T. (2012). Katanin p60-like1 promotes microtubule growth and terminal dendrite stability in the larval class IV sensory neurons of Drosophila. *J Neurosci, 32*(34), 11631-11642. doi:10.1523/JNEUROSCI.0729-12.2012

Stiess, M., & Bradke, F. (2011). Neuronal polarization: the cytoskeleton leads the way. *Dev Neurobiol, 71*(6), 430-444. doi:10.1002/dneu.20849

Stone, M. C., Roegiers, F., & Rolls, M. M. (2008). Microtubules have opposite orientation in axons and dendrites of Drosophila neurons. *Mol Biol Cell, 19*(10), 4122-4129. doi:10.1091/mbc.E07-10-1079

Stowers, R. S., Megeath, L. J., Gorska-Andrzejak, J., Meinertzhagen, I. A., & Schwarz, T. L. (2002). Axonal transport of mitochondria to synapses depends on milton, a novel Drosophila protein. *Neuron, 36*(6), 1063-1077.

Su, B., Ji, Y. S., Sun, X. L., Liu, X. H., & Chen, Z. Y. (2014). Brain-derived neurotrophic factor (BDNF)-induced mitochondrial motility arrest and presynaptic docking contribute to BDNF-enhanced synaptic transmission. *J Biol Chem, 289*(3), 1213-1226. doi:10.1074/jbc.M113.526129

Sudo, H., & Baas, P. W. (2011). Strategies for diminishing katanin-based loss of microtubules in tauopathic neurodegenerative diseases. *Hum Mol Genet, 20*(4), 763-778. doi:10.1093/hmg/ddq521

Sun, F., Zhu, C., Dixit, R., & Cavalli, V. (2011). Sunday Driver/JIP3 binds kinesin heavy chain directly and enhances its motility. *EMBO J, 30*(16), 3416-3429. doi:10.1038/emboj.2011.229

Svoboda, K., & Block, S. M. (1994). Force and velocity measured for single kinesin molecules. *Cell, 77*(5), 773-784.

Tanaka, Y., Kanai, Y., Okada, Y., Nonaka, S., Takeda, S., Harada, A., & Hirokawa, N. (1998). Targeted disruption of mouse conventional kinesin heavy chain, kif5B, results in abnormal perinuclear clustering of mitochondria. *Cell, 93*(7), 1147-1158.

Tang, Y., & Zucker, R. S. (1997). Mitochondrial involvement in post-tetanic potentiation of synaptic transmission. *Neuron, 18*(3), 483-491.

Tansey, E. M. (2006). Henry Dale and the discovery of acetylcholine. *C R Biol, 329*(5-6), 419-425. doi:10.1016/j.crvi.2006.03.012

Tapia, J. C., Wylie, J. D., Kasthuri, N., Hayworth, K. J., Schalek, R., Berger, D. R., Guatimosim, C., Seung, H. S., & Lichtman, J. W. (2012). Pervasive synaptic branch removal in the mammalian neuromuscular system at birth. *Neuron, 74*(5), 816-829. doi:10.1016/j.neuron.2012.04.017

Tarrade, A., Fassier, C., Courageot, S., Charvin, D., Vitte, J., Peris, L., Thorel, A., Mouisel, E., Fonknechten, N., Roblot, N., Seilhean, D., Dierich, A., Hauw, J. J., & Melki, J. (2006). A mutation of spastin is responsible for swellings and impairment of transport in a region of axon characterized by changes in microtubule composition. *Hum Mol Genet, 15*(24), 3544-3558. doi:10.1093/hmg/ddl431

Teriakidis, A., Willshaw, D. J., & Ribchester, R. R. (2012). Prevalence and elimination of sibling neurite convergence in motor units supplying neonatal and adult mouse skeletal muscle. *J Comp Neurol, 520*(14), 3203-3216. doi:10.1002/cne.23091

Theiss, C., & Meller, K. (2000). Taxol impairs anterograde axonal transport of microinjected horseradish peroxidase in dorsal root ganglia neurons in vitro. *Cell Tissue Res, 299*(2), 213-224. doi:10.1007/s004419900120

Thevenaz, P., Ruttimann, U. E., & Unser, M. (1998). A pyramid approach to subpixel registration based on intensity. *IEEE Trans Image Process, 7*(1), 27-41. doi:10.1109/83.650848

Thompson, W. (1983). Synapse elimination in neonatal rat muscle is sensitive to pattern of muscle use. *Nature, 302*(5909), 614-616.

Thompson, W., Kuffler, D. P., & Jansen, J. K. (1979). The effect of prolonged, reversible block of nerve impulses on the elimination of polyneuronal innervation of new-born rat skeletal muscle fibers. *Neuroscience, 4*(2), 271-281.

Trotta, N., Orso, G., Rossetto, M. G., Daga, A., & Broadie, K. (2004). The hereditary spastic paraplegia gene, spastin, regulates microtubule stability to modulate synaptic structure and function. *Curr Biol, 14*(13), 1135-1147. doi:10.1016/j.cub.2004.06.058

Turney, S. G., & Lichtman, J. W. (2012). Reversing the outcome of synapse elimination at developing neuromuscular junctions in vivo: evidence for synaptic competition and its mechanism. *PLoS Biol, 10*(6), e1001352. doi:10.1371/journal.pbio.1001352

Uchida, S., Martel, G., Pavlowsky, A., Takizawa, S., Hevi, C., Watanabe, Y., Kandel, E. R., Alarcon, J. M., & Shumyatsky, G. P. (2014). Learning-induced and stathmin-dependent changes in microtubule stability are critical for memory and disrupted in ageing. *Nat Commun, 5*, 4389. doi:10.1038/ncomms5389

Vale, R. D. (2003). The molecular motor toolbox for intracellular transport. *Cell, 112*(4), 467-480. doi:10.1016/s0092-8674(03)00111-9

Vale, R. D., Reese, T. S., & Sheetz, M. P. (1985). Identification of a novel force-generating protein, kinesin, involved in microtubule-based motility. *Cell, 42*(1), 39-50.

Vale, R. D., Schnapp, B. J., Mitchison, T., Steuer, E., Reese, T. S., & Sheetz, M. P. (1985). Different axoplasmic proteins generate movement in opposite directions along microtubules in vitro. *Cell, 43*(3 Pt 2), 623-632.

Valenstein, M. L., & Roll-Mecak, A. (2016). Graded Control of Microtubule Severing by Tubulin Glutamylation. *Cell, 164*(5), 911-921. doi:10.1016/j.cell.2016.01.019

van Dijk, J., Miro, J., Strub, J. M., Lacroix, B., van Dorsselaer, A., Edde, B., & Janke, C. (2008). Polyglutamylation is a post-translational modification with a broad range of substrates. *J Biol Chem, 283*(7), 3915-3922. doi:10.1074/jbc.M705813200

Varidaki, A., Hong, Y., & Coffey, E. T. (2018). Repositioning Microtubule Stabilizing Drugs for Brain Disorders. *Front Cell Neurosci, 12*, 226. doi:10.3389/fncel.2018.00226

Vemu, A., Atherton, J., Spector, J. O., Moores, C. A., & Roll-Mecak, A. (2017). Tubulin isoform composition tunes microtubule dynamics. *Mol Biol Cell, 28*(25), 3564-3572. doi:10.1091/mbc.E17-02-0124

Vemu, A., Szczesna, E., Zehr, E. A., Spector, J. O., Grigorieff, N., Deaconescu, A. M., & Roll-Mecak, A. (2018). Severing enzymes amplify microtubule arrays through lattice GTP-tubulin incorporation. *Science, 361*(6404). doi:10.1126/science.aau1504

Verdeny-Vilanova, I., Wehnekamp, F., Mohan, N., Sandoval Alvarez, A., Borbely, J. S., Otterstrom, J. J., Lamb, D. C., & Lakadamyali, M. (2017). 3D motion of vesicles along microtubules helps them to circumvent obstacles in cells. *J Cell Sci, 130*(11), 1904-1916. doi:10.1242/jcs.201178

Verstreken, P., Ly, C. V., Venken, K. J., Koh, T. W., Zhou, Y., & Bellen, H. J. (2005). Synaptic mitochondria are critical for mobilization of reserve pool vesicles at Drosophila neuromuscular junctions. *Neuron, 47*(3), 365-378. doi:10.1016/j.neuron.2005.06.018

Walczak, C. E., & Heald, R. (2008). Mechanisms of mitotic spindle assembly and function. *Int Rev Cytol, 265*, 111-158. doi:10.1016/S0074-7696(07)65003-7

Walsh, M. K., & Lichtman, J. W. (2003). In vivo time-lapse imaging of synaptic takeover associated with naturally occurring synapse elimination. *Neuron, 37*(1), 67-73.

Wang, H., Xiao, C., Dong, D., Lin, C., Xue, Y., Liu, J., Wu, M., He, J., Fu, T., Pan, H., Jiao, X., Lu, D., & Li, Z. (2018). Epothilone B Speeds Corneal Nerve Regrowth and Functional Recovery through Microtubule Stabilization and Increased Nerve Beading. *Sci Rep, 8*(1), 2647. doi:10.1038/s41598-018-20734-1

Wang, J. T., Medress, Z. A., & Barres, B. A. (2012). Axon degeneration: molecular mechanisms of a self-destruction pathway. *J Cell Biol, 196*(1), 7-18. doi:10.1083/jcb.201108111

Wehnekamp, F., Plucinska, G., Thong, R., Misgeld, T., & Lamb, D. C. (2019). Nanoresolution real-time 3D orbital tracking for studying mitochondrial trafficking in vertebrate axons in vivo. *Elife, 8*. doi:10.7554/eLife.46059

Weiss, P., & Hiscoe, H. B. (1948). Experiments on the mechanism of nerve growth. *J Exp Zool, 107*(3), 315-395.

Wharton, S. B., McDermott, C. J., Grierson, A. J., Wood, J. D., Gelsthorpe, C., Ince, P. G., & Shaw, P. J. (2003). The cellular and molecular pathology of the motor system in hereditary spastic paraparesis due to mutation of the spastin gene. *J Neuropathol Exp Neurol, 62*(11), 1166-1177.

Witte, H., & Bradke, F. (2008). The role of the cytoskeleton during neuronal polarization. *Curr Opin Neurobiol, 18*(5), 479-487. doi:10.1016/j.conb.2008.09.019

Wong-Riley, M., & Carroll, E. W. (1984). Effect of impulse blockage on cytochrome oxidase activity in monkey visual system. *Nature, 307*(5948), 262-264.

Wong-Riley, M. T., & Welt, C. (1980). Histochemical changes in cytochrome oxidase of cortical barrels after vibrissal removal in neonatal and adult mice. *Proc Natl Acad Sci U S A, 77*(4), 2333-2337. doi:10.1073/pnas.77.4.2333

Wood, J. D., Landers, J. A., Bingley, M., McDermott, C. J., Thomas-McArthur, V., Gleadall, L. J., Shaw, P. J., & Cunliffe, V. T. (2006). The microtubule-severing protein Spastin is essential for axon outgrowth in the zebrafish embryo. *Hum Mol Genet, 15*(18), 2763-2771. doi:10.1093/hmg/ddl212

www.genecards.org. (retrieved on 01. January 2020).

Wyatt, R. M., & Balice-Gordon, R. J. (2003). Activity-dependent elimination of neuromuscular synapses. *J Neurocytol, 32*(5-8), 777-794. doi:10.1023/B:NEUR.0000020623.62043.33

Xu, Z., Schaedel, L., Portran, D., Aguilar, A., Gaillard, J., Marinkovich, M. P., Thery, M., & Nachury, M. V. (2017). Microtubules acquire resistance from mechanical breakage through intralumenal acetylation. *Science, 356*(6335), 328-332. doi:10.1126/science.aai8764

Yang, F., Je, H. S., Ji, Y., Nagappan, G., Hempstead, B., & Lu, B. (2009). Pro-BDNF-induced synaptic depression and retraction at developing neuromuscular synapses. *J Cell Biol, 185*(4), 727-741. doi:10.1083/jcb.200811147

Yang, Y., Zhang, X., Ge, H., Liu, W., Sun, E., Ma, Y., Zhao, H., Li, R., Chen, W., Yuan, J., Chen, Q., Chen, Y., Liu, X., Zhang, J. H., Hu, R., Fan, X., & Feng, H. (2018). Epothilone B Benefits Nigrostriatal Pathway Recovery by Promoting Microtubule Stabilization After Intracerebral Hemorrhage. *J Am Heart Assoc, 7*(2). doi:10.1161/JAHA.117.007626

Yogev, S., Cooper, R., Fetter, R., Horowitz, M., & Shen, K. (2016). Microtubule Organization Determines Axonal Transport Dynamics. *Neuron, 92*(2), 449-460. doi:10.1016/j.neuron.2016.09.036

Yoshii, A., & Constantine-Paton, M. (2010). Postsynaptic BDNF-TrkB signaling in synapse maturation, plasticity, and disease. *Dev Neurobiol, 70*(5), 304-322. doi:10.1002/dneu.20765

Yu, I., Garnham, C. P., & Roll-Mecak, A. (2015). Writing and Reading the Tubulin Code. *J Biol Chem, 290*(28), 17163-17172. doi:10.1074/jbc.R115.637447

Yu, W., Qiang, L., Solowska, J. M., Karabay, A., Korulu, S., & Baas, P. W. (2008). The microtubule-severing proteins spastin and katanin participate differently in the formation of axonal branches. *Mol Biol Cell, 19*(4), 1485-1498. doi:10.1091/mbc.E07-09-0878

Zajac, A. L., Goldman, Y. E., Holzbaur, E. L., & Ostap, E. M. (2013). Local cytoskeletal and organelle interactions impact molecular-motor- driven early endosomal trafficking. *Curr Biol, 23*(13), 1173-1180. doi:10.1016/j.cub.2013.05.015

Zhai, Q., Wang, J., Kim, A., Liu, Q., Watts, R., Hoopfer, E., Mitchison, T., Luo, L., & He, Z. (2003). Involvement of the ubiquitin-proteasome system in the early stages of wallerian degeneration. *Neuron, 39*(2), 217-225.

Zhang, B., Carroll, J., Trojanowski, J. Q., Yao, Y., Iba, M., Potuzak, J. S., Hogan, A. M., Xie, S. X., Ballatore, C., Smith, A. B., 3rd, Lee, V. M., & Brunden, K. R. (2012). The microtubule-stabilizing agent, epothilone D, reduces axonal dysfunction, neurotoxicity, cognitive deficits, and Alzheimer-like pathology in an interventional study with aged tau transgenic mice. *J Neurosci, 32*(11), 3601-3611. doi:10.1523/JNEUROSCI.4922-11.2012

Zhang, C. L., Ho, P. L., Kintner, D. B., Sun, D., & Chiu, S. Y. (2010). Activity-dependent regulation of mitochondrial motility by calcium and Na/K-ATPase at nodes of Ranvier of myelinated nerves. *J Neurosci, 30*(10), 3555-3566. doi:10.1523/JNEUROSCI.4551-09.2010

Zhou, B., Yu, P., Lin, M. Y., Sun, T., Chen, Y., & Sheng, Z. H. (2016). Facilitation of axon regeneration by enhancing mitochondrial transport and rescuing energy deficits. *J Cell Biol, 214*(1), 103-119. doi:10.1083/jcb.201605101

Zott, B., Busche, M. A., Sperling, R. A., & Konnerth, A. (2018). What Happens with the Circuit in Alzheimer's Disease in Mice and Humans? *Annu Rev Neurosci, 41*, 277-297. doi:10.1146/annurev-neuro-080317-061725